**Collision Resolution in Wireless Networks**

A Thesis

Submitted to the Faculty

of

Drexel University

by

Xin Liu

in partial fulfillment of the

requirements for the degree

of

Doctor of Philosophy

in Electrical and Computer Engineering

January 2011

## Dedications

*To my parents*

## Acknowledgments

First of all, I would like to sincerely thank my advisors, Dr. Athina P. Petropulu and Dr. Youngmoo E. Kim. I am grateful to Dr. Petropulu for her tremendous time and efforts in leading, supporting and encouraging me during the past three years. If it is not her constant help and invaluable guidance throughout my Ph.D. study, it would be impossible for me to finish this work. I will always look up to her as an inspiration to my professional career. I would also like to thank Dr. Kim for his continuous support, especially in the last quarter. Without his support this dissertation would be impossible.

I am also deeply indebted to Professor H. Vincent Poor at Princeton University, Professor. Visa Koivunen at Aalto University, and Professor Saswati Sarkar at University of Pennsylvania for their guidance and suggestions during our collaborative research.

I would express my gratitude to the members of my Ph.D. thesis committee, Professors Steven Weber, John M. Walsh, and Kapil R. Dandekar for their precious time and their valuable suggestions.

Many thanks to my colleagues in the Communications and Signal Processing Laboratory (CSPL): Yao Yu, Yupeng Liu, Sagar Shah, Tingshan Huang and Shuangyu Luo for their many help and their friendship during the time we spent together. Finally, I would like to express my special thanks to my parents for their continuous understanding, supporting and encouraging in my research and life.

## Table of Contents

# List of Tables

## List of Figures

**Abstract**

Collision Resolution in Wireless Networks

Xin Liu

Advisor: Dr. Athina P. Petropulu and Dr. Youngmoo E. Kim, Ph.D.

In a wireless uplink, collisions occur when two or more wireless users transmit signals at the same time over the same channel. Traditionally, when this happens, the received packets are discarded and retransmissions are required, which is a waste of power and bandwidth. The main contributions of this dissertation include a study of approaches for collision resolution, i.e., recovery of collided packets, the design of pulse-shape functions that facilitate collision resolution and also the analysis of packet delays in a cellular wireless network whose base station has collision resolution capability.

In the first part of this dissertation a new scheme, namely ALOHA with Collision Resolution (ALOHA-CR), is proposed, which is a cross-layer approach for high throughput wireless communications in a cellular uplink scenario. Transmissions occur in a time-slotted ALOHA-type fashion but with an important difference: simultaneous transmissions of two users can be successful. When two users transmit, the collision is resolved by oversampling the collision signal and exploiting independent information about the users that is contained in the signal polyphase components. The performance of ALOHA-CR is demonstrated on the Wireless Open Access Research Platform (WARP) testbed containing five software defined radio (SDR) nodes. The testbed results indicate that ALOHA-CR leads to significant increase in throughput and reduction of service delays as compared to ALOHA. The second part of this dissertation focuses on optimal pulse-shape design for collision resolution. As mentioned above, the collided packets are separated by oversampling the collision signal.

Because of oversampling, high correlations can occur between the columns of the virtual multiple-input multiple-output(MIMO) system matrix, which can be detrimental to user separation. A novel pulse-shape waveform design is proposed, which results in low correlation between the columns of the system matrix, while it exploits all available bandwidth as dictated by a spectral mask. In the third part, we study the delay properties of random scheduling (RS) in a cellular wireless network, under the assumption that the base station (BS) has multi-packet reception (MPR) capability. We minimize the expected delay of RS by determining the scheduling probabilities of nodes that will transmit simultaneously. For the perfect reception case, (i.e., when the success probability of transmissions is 1), a lower bound of the delay performance for an arbitrary scheduling policy is provided. The imperfect reception case is also studied and a convex optimization formulation is proposed, which can minimize the upper bound on the expected delay of RS. An approximation and a lower bound on the expected delay of RS are also developed under the assumption that the base station can support simultaneous transmission of two users.

# 1. Introduction

In this chapter, we provide some background on how collisions in wireless networks occur and what their effects are. Then the contribution of this dissertation is described. Finally, we provide the outline of this dissertation.

## 1.1 Background Review

### 1.1.1 Collisions in wireless networks

In wireless networks, collisions occur when two or more users transmit at the same time over the same channel. Their transmitted signal will interfere with each other at the receiver; in the end none of them can be successfully received. In traditional networks, when a collision happens, the collided packets are discarded and re-transmissions are required. Thus, collisions lower throughput and waste power and bandwidth.

### 1.1.2 Collision avoidance

The first wireless network is known as ALOHA, which was developed at the University of Hawaii in 1968. The goal of ALOHA is to connect people on Hawaii islands by using low cost commercial radio [1]. ALOHA is a control free protocol; users can send data at any time. If there is a collision, the collided users will try to transmit again at a later time. Because of collisions, the maximum throughput of ALOHA is approximately 0.184 frames/frame-time. An improved version of ALOHA is slotted-ALOHA [2, 3], in which time is divided into discrete time slots and the transmission has to be initiated at the beginning of each time slot. In this way, the probability of collision is reduced, and the maximum throughput of slotted-ALOHA is 0.368

frames/frame-time.

Since collisions are harmful to wireless networks, carrier sensing multiple access (CSMA) was proposed [4] to avoid collisions. In CSMA the potential sender senses the medium. If the medium is busy, the potential sender has to wait until the medium is released; if the medium is idle, the potential sender can transmit immediately (1-persistent CSMA) or transmit with a probability $p$ ($p$-persistent CSMA). If a collision happens, the collided users wait for a random period of time and try to transmit again. This approach is effective if all the nodes can sense each other in the network. However this is not practical because coverage is limited due to power constraints. This leads to the hidden terminal problem [13] illustrated in Fig. 1.1. As node B is out of the coverage of node A, the two nodes cannot sense each other. The concurrently transmitted signals from node A and B will collide at the base station (BS). This hidden terminal problem makes CSMA work as poorly as ALOHA.

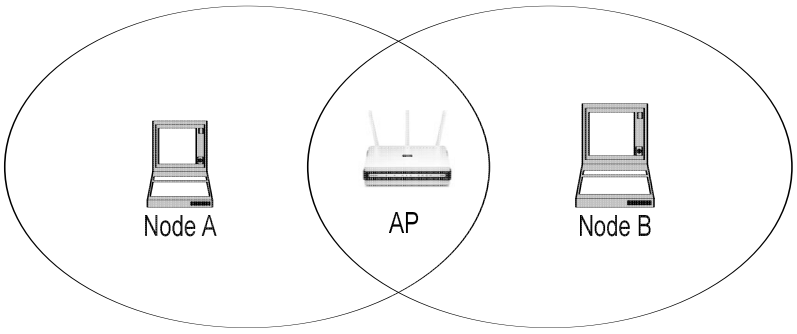


Figure 1.1: Hidden terminal

The protocol IEEE 802.11 [11] uses carrier sensing multiple access with collision avoidance (CSMA/CA)[5] together with request-to-send/clear-to-send (RTS-CTS) [6]

to counter this problem. CSMA/CA requires potential senders to sense the medium first. If the medium is occupied, the potential senders have to wait a random period of time and then sense the medium again. Compared to CSMA, CSMA/CA can reduce the probability of collision, because the users with this protocol are less "greedy". In addition to CSMA/CA, IEEE 802.11 uses Request-To-Send/Clear-To-Send (RTS/CTS) scheme to avoid collisions. Before transmission, the node wishing to transmit has to send a short RTS packet. If the channel is free, the intended receiver will respond with a CTS packet. Any other node who receives RTS or CTS will refrain from transmissions. By combining RTS/CTS protocol with CSMA/CA, the collision probability can be further reduced. However, collisions occur more frequently as the traffic load increases, in which case the RTS/CTS scheme becomes less effective due to collisions of the RTS reservation packets.

## 1.2 Motivation of the Dissertation

The previously mentioned MAC layer protocols (Slotted-ALOHA, CSMA/CA as well as RTS/CTS) can reduce the probability of collision, however, they do not eliminate the problem, as the large random topology and mobility in wireless networks strongly affect the performance of network protocols. In order to rule out collision, we might think of dividing the available channel into separate media and assigning different users to distinct media, like time division multiple access (TDMA)[7], frequency division multiple access (FDMA) [8], orthogonal frequency division multiple access (OFDMA) [9] or code division multiple access (CDMA)[10]. In TDMA, time is divided into separate time slots and different users are assigned to different time slots. Each user can only transmit in the assigned time slots. Hence the transmissions from different users will not collide. In FDMA, we assign different users to different frequency bands; in OFDMA we divide sub-carriers and in CDMA we use orthog-

onal codes. But these protocols are fixed source allocation, meaning that once the medium is assigned to a user, that user will occupy that medium even if the user has no data to transmit. Future wireless network will need to accommodate multimedia traffic which is bursty and has diverse quality of service (QoS) requirements, therefore fixed bandwidth allocation schemes such as TDMA, FDMA, OFDMA and CDMA are inefficient for such traffic.

By the use of multiple antennas at the receiver and/or at the transmitter, we can significantly increase the data throughput and improve channel reliability, and the simultaneous transmission of multiple users can be supported by exploiting the transmit and/or receive diversity. However the compatible mobile stations have physical size limitations. The use of multiple antennas might not be feasible for such systems.

In the signal processing literature, multiuser interference, which can be thought of as the equivalent of collision, can be successfully treated by using some form of diversity. By borrowing signal detection/seperation techniques, several network assisted diversity approaches were proposed for collision resolution. These approaches include the network-assisted diversity multiple access (NDMA) protocol [14, 15], ALLIANCES [16, 17] and ZigZag decoding [19]. In these schemes collisions can be resolved by combining collided packets and several retransmissions. If an order $K$ collision happens, the users involved in the collision have to retransmit their packets in the following $K-1$ slots. NDMA and ALLIANCES are proposed for the same problem. By combining the the original collided packets and the retransmissions, a MIMO problem is formulated, with the user data information as the input. In NDMA it is assumed that the channel coefficients between a node and the BS are independent at different time slots. This is not practical, as it only happens when the coherence time of the fading channel is in the order of a packet slot. Therefore NDMA will suffer from the linear dependency of the channel coefficients of adjacent

slots, which leads to high condition number of the channel matrix. However by asking the non-source nodes to transmit the received mixture of collided signal, ALLIANCES can work even for static channels. ZigZag decoding exploits the relative delay difference between users in different time slots to resolve collisions. Consider the hidden terminal problem illustrated in Fig. 1.1, where nodes A and B are unable to sense each other. Their simultaneous transmissions result in collision 1. When a collision happens, both node A and B retransmit their packets, causing collision 2. This is shown in Fig. 1.2, in which we use Pa and Pb to denote the packets from node A and B respectively. Because of the random transmission offset, there is a collision free

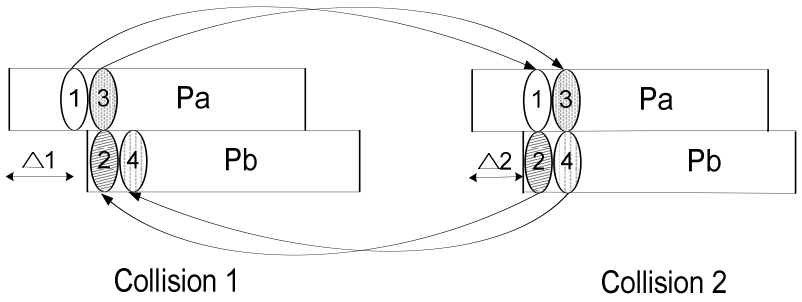


Figure 1.2: Zigzag decoding

stretch in the beginning of the two collisions (denoted as $\Delta 1$ and $\Delta 2$ respectively). Usually $\Delta 1 \neq \Delta 2$. For collision 1 it is decodable until chunk 3. Thus we can decode it and deflate it from collision 2. Then chunk 2 in collision 2 will be decodable. We can decode it and use it to decode chunk 3 in collision 1. Proceeding in a similar fashion we can decode these two collisions.

As stated before, the network assisted approach requires the retransmission of the

collided packets in order to resolve collisions. However the retransmissions of packets will consume additional bandwidth and power.

## 1.3 Contributions of the Dissertation

In this dissertation we consider a small scale network, where all nodes communicate with a BS. The transmitters and receiver are equipped with only one antenna. We assume that nodes transmit with the same power and that there is no significant power decrease due to propagation in small-scale networks. In cases where users can afford to transmit at different power levels, or due to propagation induced losses the signals are received at different powers, user separation is a relatively easier task and can be achieved via successive interference cancelation (SIC) [20]. Here, we propose a collision resolution approach that does not require retransmissions nor does it rely on power differences between the users. The effect of pulse shape on the performance of the collision separation algorithm is discussed. Also, by assuming that the BS has collision recovery capability, the delay property of a cellular wireless network is analyzed.

### 1.3.1 ALOHA with Collision Resolution (ALOHA-CR): Theory and Software Defined Radio Implementation

We consider a cellular uplink scenario where transmissions occur in a time-slotted ALOHA-type fashion, but with an important difference: simultaneous transmissions of two users can be successful. In the beginning of each slot, users with non-empty queues contend with some probability after experiencing an intentional random delay. If more than two users transmit in the same slot, no attempt is made by the based station to separate the collision; the packets are discarded and the users are asked to retransmit at a later time. If one or two users transmit, then, depending on

the state of the channel, the base station can recover the transmitted packets. The latter is achieved by oversampling the collision signal and by exploiting independent information about the users that is contained in the signal polyphase components. The properties of the user intentional random delays are determined to maximize the probability of a second order collision being separable. The throughput of ALOHA-CR under both infinite and finite backlog assumptions is derived. Under the former assumption, the optimal contention probability is calculated to maximize the system throughput, while under the latter assumption, the region of stabilizing contention probabilities is determined based on the packet arrival rate. Queuing delay analysis for network users is also conducted. The performance of ALOHA-CR is demonstrated on the WARP testbed containing five software defined radio nodes. The testbed results indicate that ALOHA-CR leads to significant increase in throughput and reduction of service delays as compared to ALOHA.

Novel points of this work include the following:

- ALOHA-CR does not require retransmissions nor does it rely on power differences between the users. The transmitters and the receiver are equipped with only one antenna.

- The statistics of the user delays, $\tau_k$'s, are determined to maximize the probability of a collision being separable.

- The analysis of MAC layer properties of ALOHA-CR is novel. Throughput and queuing delay expressions for any number of users are provided for the symmetric case, i.e., packet arrival rates, contention probability and probability of successfully receiving packets are the same for all nodes.

- The performance of ALOHA-CR is demonstrated via experiments conducted on a software defined radio (SDR) testbed.

This part of the work has appeared in:

- X. Liu, J. Kountouriotis, A.P. Petropulu, and K.R. Dandekar, "ALOHA with collision resolution (ALOHA-CR): Theory and software defined radio implementation," *IEEE Transactions on Signal Processing*, vol.58, no.8, pp.4396-4410, Aug. 2010 .

- X. Liu, J. Kountouriotis, A.P. Petropulu, and K.R. Dandekar, "ALOHA with Collision Resolution: Physical layer description and software defined radio implementation," *2010 IEEE International Conference on Acoustics Speech and Signal Processing (ICASSP)*, pp.3330-3333, 14-19 Mar. 2010 .

- J. Kountouriotis, X. Liu, A.P. Petropulu, and K.R. Dandekar,"ALOHA with Collision Resolution: MAC layer analysis and software defined radio implementation," *2010 44th Annual Conference on Sciences and Systems (CISS)*, pp.1-6, 17-19 Mar. 2010 .

### 1.3.2 Blind Separation Of Two Users Based on User Delays and Optimal Pulse-Shape Design

In order to resolve a second order collision, the collision signal has to be oversampled, and the polyphase components organized into a virtual MIMO system in which the user symbols information are the inputs. Because of the oversampling, high correlation will occur between the columns of the virtual MIMO system matrix, which is detrimental to the user separation. A novel pulse-shape waveform design is proposed that results in low correlation between the columns of the system matrix, while it exploits all available bandwidth as dictated by a spectral mask. Simulation results have confirmed that the proposed pulse design leads to SER performance better than of that conventional Pulse-shape waveforms.

The novel aspects of this work are the following:

- The introduction of an intentional half-symbol delay between the two users, which can improve the multi-user separation.
- Optimal design of the pulse shape waveform.
- The use of successive interference cancelation in combination with blind source separation to further improve the separation performance.

This part of work has appeared in:

- X. Liu, A.P. Petropulu, V. Poor, and V. Koivunen, "Blind Separation Of Two Users Based on User Delays and Optimal Pulse Shape Design," *EURASIP Journal on wireless communications and networking*, vol. 2010, Article ID 939340, 12 pages, 2010, doi:10.1155/2010/939340 .
- X. Liu, S. Oymak, A. P. Petropulu, and K. R. Dandekar, "Collision resolution based on pulse shape diversity," *IEEE International Workshop on Signal Processing Advances for Wireless Communications*, Perugia, Italy, Jun. 2009, pp. 409–413.

### 1.3.3 Delay Analysis for Random Scheduling in Centralized Wireless Networks

We study the delay properties of RS in a cellular network scheme, where all nodes communicate with a BS. The communication happens in a time slotted fashion and the BS has MPR capability (i.e. the BS can support the simultaneous transmissions of multiple users in a time slot). In each time slot nodes are scheduled according to predetermined probabilities and the scheduling decision is made independently at each node. Assuming the success probability of transmissions is always 1 (perfect reception), we provide a lower bound on the delay performance for an arbitrary scheduling

policy. We then study the imperfect reception case, in which the success probability of a node is not always 1 but varies depending on which nodes transmit along with that user. A convex optimization problem is proposed, which can minimize the upper bound on the expected delay of RS by determining scheduling probability of nodes that will transmit simultaneously. An approximation and a lower bound on the delay of RS are also developed for the case in which the BS can support simultaneous transmissions of two users.

Novel aspects of this work include:

- A lower bound of the delay performance of an arbitrary scheduling policy for the case of the probability of successful transmission equal to 1.
- Minimize the upper bound of the expected delay by determining the optimal scheduling probability of each node. The optimization formulation guarantees that RS can stabilize any packet arrival rate within the stability region.
- An approximation and a lower bound on the expected delay of RS for the case in which two users can transmit simultaneously.

This part of work is included in:

- X. Liu, A.P. Petropulu, and S. Sarkar, "Delay Analysis for Random Scheduling in Centralized Wireless Networks," in preparation, in 2010.

## 1.4 Outline of the Dissertation

This dissertation is organized as follows.

In chapter 2 a new scheme, namely ALOHA with Collision Resolution (ALOHA-CR) is proposed, which is a cross-layer approach for high throughput wireless communications in a cellular uplink scenario.

In chapter 3 we focus on the effects of pulse-shape on the performance of user separation algorithm proposed in chapter 2.

In chapter 4 we analyze delay property for RS, by assuming that BS is of multi-packet reception capability. An approximation and a lower bound on the delay are proposed.

Chapter 5 contains concluding remarks and possible directions for future work.

### 1.4.1 Notation

Bold capital letters denote matrices. Bold lower cases letters denote vectors. Superscript $H$ denotes conjugate transpose. Superscript $T$ denotes transpose. Superscript † denotes pseudo-inverse. $Diag\{\mathbf{v}\}$ denotes the diagonal matrix with diagonal elements $\mathbf{v}$. $Tr(\cdot)$ denotes the trace of its argument. $Arg\{\cdot\}$ denotes the phase of its argument.

# 2. ALOHA with Collision Resolution (ALOHA-CR): Theory and Software Defined Radio Implementation

## 2.1 Introduction

In a wireless uplink scenario, collisions occur when two or more users transmit at the same time over the same channel. Traditionally, once a collision occurs, retransmissions are requested. Retransmissions lower throughput and waste power and bandwidth. Well studied schemes for avoiding collisions include CSMA/CA (e.g., see IEEE 802.11 [11]). In order to overcome the hidden terminal problem, IEEE 802.11 incorporates a positive acknowledgment scheme, i.e., Request To Send (RTS) followed by Clear To Send (CTS). However, in most protocols, collisions occur more frequently as the traffic load increases, in which case the RTS/CTS scheme becomes less effective due to collisions of the RTS reservation packets.

Collision resolution can be viewed as multiuser separation. However, well known approaches that allow for multiuser separation, such as TDMA, FDMA, OFDMA, CDMA or use of multiple antennas might not be an ideal fit for wireless networks where traffic can be bursty, users operate on limited battery power, and in certain cases, wireless receivers have physical size limitations. TDMA, FDMA and OFDMA approaches are fixed resource allocation schemes and thus are not efficient for bursty traffic. The CDMA approach requires bandwidth expansion, which results in increased power consumption for each wireless network user. Finally, the use of multiple antennas, might not be feasible for compact wireless receivers. Wireless network-friendly approaches to achieve diversity include the NDMA protocol [12, 14], ALLIANCES [16, 18] and ZigZag decoding [19]. In these protocols, collisions are resolved by combining collided packets and several retransmissions of them. In the

aforementioned schemes it is assumed that nodes transmit with the same power, and that there is no significant power differences between users due to propagation, which is the case for propagation in small-scale networks. In cases where users can afford to transmit at different power levels, or due to propagation induced losses the signals are received at different powers, user separation is a relatively easier task, and can be achieved via successive interference cancelation (SIC) [20].

A potentially network-friendly approach that does not require retransmissions and does not rely on power differences between the users was recently proposed in [24, 25, 26]. According to [24, 25, 26], by upsampling the received signal and viewing its polyphase components as independent linear mixtures of the collided packets, under certain conditions, the collided packets can be recovered in a blind fashion based on a single collision. In [26], user separation was enabled by different carrier frequency offsets (CFO) and user delays. In [24, 25], pulse-shape diversity was investigated as source of additional diversity in case user delays and CFOs are small.

In this chapter, a novel cross-layer scheme, namely ALOHA-CR is proposed for high throughput wireless communications in a cellular uplink scenario. Transmissions occur in a time-slotted ALOHA-type fashion but with an important difference: simultaneous transmissions of two users can be successful. The wireless channel is assumed to be flat fading and constant over the duration of one time slot. A user $k$ with a non-empty queue transmits a packet with some probability $p$ in the beginning of each time slot, after waiting for a random time interval $\tau_k$. If a collision of more than two users occurs, the packets are discarded and the users are asked to retransmit at a later time. If there is only one user present, the user's packet is recovered with some probability, depending on the state of the channel. If a second order collision occurs, the BS can recover the transmitted packets via oversampling of the collision signal and exploiting independent information about the users that is contained in the

collision polyphase components. The statistics of the user delays, $\tau_k$'s, are determined to maximize the probability of a collision being separable. MAC layer properties of ALOHA-CR are also studied. Throughput and queuing delay expressions for any number of users are provided for the symmetric case, i.e., when packet arrival rates, contention probability and probability of successfully receiving packets are the same for all nodes. The performance of ALOHA-CR is demonstrated via simulations and also via experiments conducted on a SDR [27] testbed. This experimental wireless network consists of five nodes, i.e., one BS and four users, and was deployed in an indoor laboratory environment.

### 2.1.1 Relation to the literature

The collision separation approach of this chapter is based on the ideas of [26], where naturally occurring user delays and carrier frequency offsets are used as sources of diversity that enable blind user separation. However, in our experimental setup, we observed that the naturally occurring delays and CFOs are rather small to yield sufficient diversity. In this work, we ignore CFOs and introduce intentional random delays in addition to the naturally occurring ones. Further, the statistical characteristics of the intentional random delays are chosen to enhance the separability of the users. In order to keep the complexity low and the probability of user separation high, resolution of only second order collisions is considered here. The work of [26] was concerned with the physical layer only. Here, we propose a cross-layer approach, and study throughput and queuing performance as well as physical layer issues. Further, a host of physical layer issues motivated by the real implementation are studied.

Multiuser separation based on user delays was also considered in [28]. The approach of [28] considers transmission of isolated frames; it exploits the edges of a frame over which users do not overlap, and assumes knowledge of the channel. How-

ever, noise can be a problem when exploiting edge effects as samples are taken at points where the pulse is quite low.

In relation to the collision resolution approaches NDMA [12, 14], ALLIANCES [16, 18] and ZigZag decoding [19], the proposed approach resolves collisions of order two without retransmissions. Thus, no storage of the collision signals is needed, and network users not involved in the collision do not need to wait until the collision is resolved.

The analysis of ALOHA-CR falls under the general area of ALOHA with multipacket reception capability. The asymptotic stability region (infinite-user case) of slotted ALOHA with multipacket reception capability was established in [29, 30]. The exact expressions of stability region and delay of finite-user slotted ALOHA with multipacket reception can be found in [31, 32]. However, for the case of more than two users, the expression of the stability region becomes so complicated that, as stated in [32], "it is too difficult if not impossible to evaluate in practice in general". For the delay analysis, the work of [31, 32] focuses on the two-user symmetric case and assumes that at most one user has a successful packet transmission in a slot. Our analysis in this chapter is different and relies on the work of [33], where coupled queues are approximated by uncoupled queues. This approximation allows us to derive simple closed-form expressions for throughput and delay for any number of users, parametrized by the probability of a second order collision being separable. The validity of the proposed expression is tested via testbed measurements.

### 2.1.2 Organization

The rest of the chapter is organized as follows: The physical layer of ALOHA-CR is introduced in Section 2.2 and several implementation considerations are discussed in Section 2.3. Network performance quantities for ALOHA-CR, i.e., throughput and

packet delays are derived in Section 2.4. A brief description of the SDR platform used to implement ALOHA-CR is provided in Section 2.5.1, while specifics of the physical and MAC layers implementation on the SDR platform are given in Section 2.5.2. The obtained experimental results along with comparisons with analytical and simulation results are presented in Section 2.6. Finally, conclusions are drawn in Section 4.6.

## 2.2 ALOHA-CR: Physical Layer

The channel between transmitter and receiver is assumed to be flat fading. Moreover, the channel is assumed to remain constant over the duration of a packet.

If within a given time slot $K$ users transmit, the baseband signal received by the BS equals

$$y(t) = \sum_{k=1}^{K} a_k x_k(t - \tau_k) + w(t) \ , \tag{2.1}$$

where $a_k$ denotes the channel coefficient between the $k-th$ user and the BS; $\tau_k$ is a random delay associated with the user $k$; $w(t)$ represents noise; $x_k(t)$ is the $k$-th user signal, i.e.,

$$x_k(t) = \sum_{i} s_k(i) p(t - iT_s) \ , \tag{2.2}$$

where $s_k(i)$ is the $i-$th symbol of user $k$, which can be real or complex, $T_s$ is the symbol interval, and $p(t)$ is a pulse shaping function with support $[-\tilde{L}T_s, \tilde{L}T_s]$.

We should note that typically, in high-speed communication systems the main lobe of the pulse-shape functions overlap by 50% [41]. This extended time support, although it allows for better frequency concentration, or equivalently, less spectrum for the transmission of each symbol, it introduces intersymbol interference. When we sample at times $iT_s$, $i = 1, 2, ...$, the overlap does not play any role. However, when we obtain more than one samples during the symbol interval, the further away

from the aforementioned sampling instants the samples are taken, the stronger the ISI effects will be.

Suppose that the received signal is sampled at $M$ samples per symbol, and consider polyphase components of the received signal, spaced apart by $\Delta T = T_s/M$. The $m-$th polyphase component equals

$$y_m(i) = \sum_{k=1}^{K} a_k \left[ \sum_{l} s_k(l) p((i-l)T_s + m\Delta T - \tau_k) \right] + w_m(i) \tag{2.3}$$

$$= \sum_{k=1}^{K} h_{mk}(i) * s_k(i) + w_m(i) \tag{2.4}$$

where "$*$" denotes convolution, and $h_{mk}(i)$ is defined as

$$h_{mk}(i) = a_k p(iT_s + m\Delta T - \tau_k),\ i = ... -2, -1, 0, 1, 2, ... \ . \tag{2.5}$$

Polyphase component $y_m(i)$ can be expressed as

$$y_m(i) = [[h_{m1}(\tilde{L}) \dots h_{m1}(-\tilde{L})], \dots, [h_{mK}(\tilde{L}) \dots h_{mK}(-\tilde{L})]] \begin{bmatrix} \begin{bmatrix} s_1(i-\tilde{L}) \\ \vdots \\ s_1(i+\tilde{L}) \end{bmatrix} \\ \vdots \\ \begin{bmatrix} s_K(i-\tilde{L}) \\ \vdots \\ s_K(i+\tilde{L}) \end{bmatrix} \end{bmatrix} + w_m(i) \ . \tag{2.6}$$

Assuming that a pulse with low sidelobes is used, such as the Isotropic Orthogonal Transform Algorithm (IOTA) pulse [34] and $|\tau_k| \leq T_s/2$, the interference at the sampling points over the $i-$th symbol interval is mainly due to the $(i-1)$-th and $(i+1)$-th symbol. For such pulse, the channel $h_{mk}(i)$ can be approximated as of

length 3, which corresponds to $\tilde{L} = 1$.

Let us form the vector $\mathbf{y}(i)$ by appending $P$ $(P < M)$ polyphase components of the received signal, i.e., $y_m(i)$ for $m \in [m_1, m_2, ..., m_P]$ (see Fig. 2.1 for the two-user case).

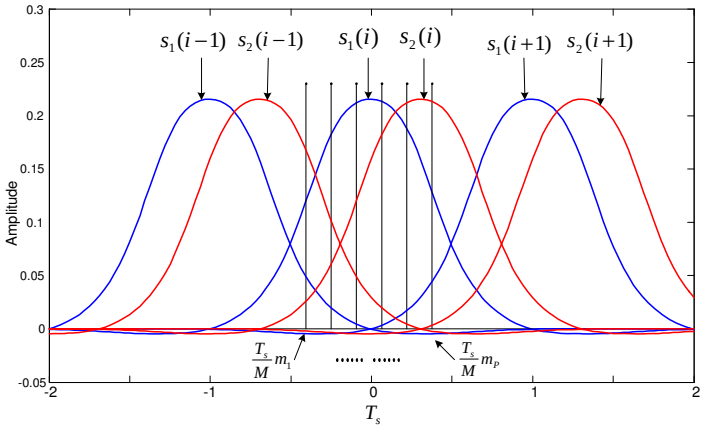


Figure 2.1: Illustration of sampling used in ALOHA-CR.

It holds

$$\mathbf{y}(i) = \mathbf{A}\mathbf{s}(i) + \mathbf{w}(i) \tag{2.7}$$

where $\mathbf{A}$ is a $P \times 3K$ matrix whose $r$-th row equals

$[[h_{m_r 1}(1), h_{m_r 1}(0), h_{m_r 1}(-1)], \ldots, [h_{m_r K}(1), h_{m_r K}(0), h_{m_r K}(-1)]]$;

$\mathbf{s}(i) = [s_1(i-1), s_1(i), s_1(i+1), \ldots, s_K(i-1), s_K(i), s_K(i+1)]^T$;

and $\mathbf{w}(i) = [w_{m_1}(i), \ldots, w_{m_P}(i)]^T$.

Matrix $\mathbf{A}$ can be estimated based on pilot symbols and then used for the recovery of the information bearing symbols. If no pilots are available, estimating $\mathbf{A}$ and then recovering $\mathbf{s}(i)$ is still possible by viewing (2.7) as a $P \times 3K$ instantaneous blind MIMO estimation problem. Assuming that $P \geq 3K$ and under certain conditions

on $\mathbf{A}$ the system is identifiable [26]. Any blind source separation algorithm (the JADE algorithm [35] is used in this chapter) can be applied to obtain an estimate of $\mathbf{A}$, i.e., $\hat{\mathbf{A}}$, within a column permutation ambiguity and a constant diagonal matrix representing phase ambiguity. These ambiguities are trivial, and are inherent in blind estimation problems [22]. Based on the estimate $\hat{\mathbf{A}}$ and using a least-squares equalizer we can get $\mathbf{s}(i)$ within permutation and phase ambiguities, i.e.,

$$\hat{\mathbf{s}}(i) = (\hat{\mathbf{A}}^H \hat{\mathbf{A}})^{-1} \hat{\mathbf{A}}^H \mathbf{y}(i) = e^{jArg\{-\mathbf{\Lambda}\}} |\mathbf{\Lambda}|^{-1} \mathbf{P}^T \mathbf{s}(i) \ , \tag{2.8}$$

where $\mathbf{\Lambda}$ is a diagonal matrix and $\mathbf{P}$ is a permutation matrix. Denoting by $\theta_k$ the $k-$th diagonal element of $Arg\{\mathbf{\Lambda}\}$, the $k-$th input signal can be recovered within a phase ambiguity as $\hat{s}_k(i) = s_k(i)e^{-j\theta_k}$.

For fixed sampling locations and a fixed pulse-shape function, the condition number of $\mathbf{A}$ can be controlled by the user delays $\tau_k$, where $k = 1, 2, ..., K$. If $\tau_k$'s are close to each other the columns of $\mathbf{A}$ are highly correlated, which results in high condition number for $\mathbf{A}$. Since naturally occurring delays might be too small to guarantee a well conditioned $\mathbf{A}$, we propose that, before transmission, each node introduces an intentional random delay. Let $\tau_k$ be the sum of the naturally occurring delay and the intentional random delay. Since in this work we only attempt to resolve second order collisions, let us express the delay difference between the two users as $\tau = \alpha + \delta$, where $\alpha$ is the difference between the intentional random delays between users $k_1$ and $k_2$, and $\delta$ is the difference between the naturally occurring delays. Let $f_\delta(x)$ be the pdf of the natural delays differences, and further assume that $f_\delta(x)$ is symmetric around the origin.

***Proposition 2.1***: *Let the intentional delays be uniformly distributed over some interval* $[0, T]$. *If* $T = T_s$, *the probability of the collision being non-resolvable achieves a local minimum, independent of the form of* $f_\delta(x)$.

The proof is given in Appendix I (in section 2.8).

## 2.3 Physical Layer Implementation

In the beginning of each slot, users with non-empty queues contend with some probability after experiencing an intentional random delay as described in the previous section. If more than two users transmit in the same slot, no attempt is made by the based station to separate the collision; the packets are discarded and the users are asked to retransmit at a later time. If one or two users transmit, the base station can recover the transmitted packets based on the method described on the previous section.

Several issues need to be addressed in a practical implementation of the proposed approach.

### 2.3.1 Frequency offsets and phase tracking

In a practical system the received signal contains CFOs, resulting from mismatch between transmitters and receiver oscillators, and also from Doppler shifts due to relative movement between transmitters and receiver. In this case the continuous-time base-band received signal $y(t)$ is of the form:

$$y(t) = \sum_{k=1}^{K} a_k x_k(t - \tau_k) e^{j2\pi F_k t} + w(t) \ , \tag{2.9}$$

where $F_k$ is the CFO for user $k$. In [26] the CFOs were used as source of diversity that enables user separation. In the implementation that we consider here the CFOs are too small to provide diversity, and thus are ignored in the problem formulation. However, the CFO effect is still present in the separated symbols, i.e., $\hat{s}_k(i) = s_k(i) e^{j(-\theta_k + 2\pi F_k T_s i)}$, from where it can be estimated and mitigated via a phase

locked loop (PLL) device [40], among other methods [44, 45]. The phase ambiguity, $\theta_k$ can be compensated for via use of pilot symbols, or by using differential phase offset keying.

### 2.3.2 About successive interference cancelation

SIC [20] applied on a mixture of signals treats one of the components of the mixture as the signal of interest and the rest as interference. The approach of Section 2.2 can be combined with SIC to further improve packet recovery performance. In particular, after blind source separation, the contribution of the strongest user signal can be reconstructed and deflated from the received signal. This usually provides a better estimate for the weak user. One way to determine who is the *strongest user* is to look among the blindly separated signals for the signal that has the smallest variance around the known constellation.

Let the strong user be user $k$, and let $\hat{s}_k(i)$ be the recovered symbols of that user. The user's contribution in the collision can be reconstructed based on knowledge of the pulse shape waveform, and estimates of the user's CFO ($\hat{F}_k$), channel coefficient ($\hat{a}_k$), and delay ($\hat{\tau}_k$). Assuming that the latter estimates are available, the reconstructed signal equals:

$$\hat{y}_k(t) = \hat{a}_k \sum_i \hat{s}_k(i) p(t - iT_s - \hat{\tau}_k) e^{j2\pi \hat{F}_k t}. \tag{2.10}$$

The user delays can be estimated at the synchronization step (see Section 2.3.3), and the CFOs can be estimated as described in Section 2.3.1. The channel coefficient estimates can be obtained by cross-correlating the received signal $y(t)$ with the signal: $\hat{y}'_k(t) = \sum_i \hat{s}_k(i) p(t - iT_s - \hat{\tau}_k) e^{j2\pi \hat{F}_k t}$.

Due to the delay between users, the peaks of different user pulses do not overlap (also see Fig. 2.1). One could naturally wonder whether applying SIC from the beginning would suffice for the recovery of the packets, instead of upsampling the

signal and performing packet separation along the lines of Section 2.2. As will be shown in Section 2.6 via both simulations and testbed measurements, using SIC directly results in inferior results.

### 2.3.3 Frame synchronization and collision order estimation

In order to determine the beginning of the packet, frame synchronization is required. For synchronization purposes, users are assigned distinct pseudo random sequences (pilots). The BS maintains a code book containing all pilot sequences in use in the network. When the packet arrives, the BS uses the beginning part of the received signal to perform correlation with every entry of the code book. A peak in the correlation of the received signal with code $k$ indicates the presence of user $k$. The peak location provides and estimate of the delay of user $k$, while the peak value provides the corresponding channel coefficient.

This can be repeated for all possible users, however, based on our experience with simulations and testbed data the following approach is more robust. We first identify the user that produces the largest peak in the correlation; let this be user $u_1$, and let $R_{u_1}$ be the correlation peak value occurring at location $\tau_{u_1}$. If $|R_{u_1}|$ is greater than some predetermined threshold, i.e., $T^*$, then we know that there is at least one user in the collision. Then, the $u_1$ user pilot sequence is reconstructed based on estimated channel coefficient and delay, respectively equal to $R_{u_1}$ and $\tau_{u_1}$, and is subsequently deflated from the pilot portion of the received signal along the lines of Section 2.3.2. The CFO effect is ignored here because of the short duration of the pilot segment.

Subsequently, the BS performs correlation of the residual header with every entry of the code book. Suppose that the $u_2$-th entry gives the largest correlation peak equal to $R_{u_2}$, with peak location $\tau_{u_2}$. If $|R_{u_2}| > T^*$ then user $u_2$ is also in the collision and the collision order should increase by one unless one the following happen: (i)

$u_2 = u_1$, which is obviously an error; (ii) $|\tau_{u_2} - \tau_{u_1}|$ is larger than the largest possible relative shift of any two users then, which is again an error. If $|R_{u_2}| > T^*$ then we reconstruct the pilot sequence of user $u_2$, based on the estimated channel coefficient and delay, respectively equal to $R_{u_2}$ and $\tau_{u_2}$, deflate it from the pilot portion of the first residual signal. At this point, the second residual signal contains either more users, or just noise. Which case it is can be determined again based on correlations with user pilots. If it turns out that there is another user in the second residual signal, then the collision order is at least equal to 3, in which case the entire signal is discarded and the users are asked to retransmit. Otherwise, the collision order is equal to 2, and we can proceed to separate the collision.

For synchronization purposes, the best pulse shaping waveform for the pilots is the raised root cosine (RRC) [37] function, as this function maximizes the signal-to-noise ratio (SNR) at the output of the matched filter [41] while it eliminates ISI at the sampling points.

We should note that the part of the packet containing the actual information will need to be oversampled in order for the method described in Section 2.2 to be applied. As explained in that section, a good choice of pulse shaping for the actual data is the IOTA pulse [34]. However, we cannot use the IOTA pulse for the pilots, because the convolution of IOTA with itself introduces ISI at $t = nT_s$, thus the matched filter would not work well.

### 2.3.4 Blind versus pilot-based user separation

Since a real communication system always uses pilots for synchronization purposes, one would think that these pilots could be used to estimate the matrix $\mathbf{A}$ in (2.7), which then could be used to recover the information bearing symbols. However, the fact that different pulse shape waveforms are used for pilots and information bear-

ing symbols renders that approach impossible; as it was mentioned in the previous section, RRC pulse shaping is best for the pilot symbols and IOTA pulse shaping is best for the payload symbols. Thus, since $\mathbf{A}$ depends on the pulse shape function (see (3.4) and (2.7)), the estimate of $\mathbf{A}$ based on the pilots would be different than that corresponding to the payload.

However, one can first estimate channel coefficient $a_k$ and user delay $\tau_k$ based on the pilot symbols, and subsequently combine them with the IOTA pulse shape function and sampling points (see (3.4) and (2.7)) to get an estimate of matrix $\hat{\mathbf{A}}$. Based on that estimate, the symbols can be recovered via least-squares. We term this approach as *training method*. In Section 2.6 we compare the training method to the blind approach, in which the matrix $\mathbf{A}$ is considered to be unknown. As it will be seen in that section, the estimation errors in channel coefficients and user delays, and the distortion of pulse shape introduced by the antennas render the training method inferior to the blind one.

### 2.3.5 Collision separation

Following the synchronization step, and once it has been decided that the collision order is 1 or 2, we take $P = 6$ polyphase components of the incoming packet in each symbol interval. Those components are taken around the center of the pulse of user $u_1$, whose header yielded the highest correlation peak during the collision order determination step. By applying the blind separation method of Section 2.2 on the 6 polyphase components we obtain 6 sequences. Each sequence is passed through a PLL to eliminate any carrier frequency offsets. Typically, the output of the PLL is scattered around the nominal constellation. Let the sequence with the smallest variance, i.e., the sequence corresponding to the strongest signal, be denoted by $s_u(.)$. Then, one of the following holds:

- If the received packet is a collision free packet, the strongest signal is $s_u(i)$.
- If the collision order is 2 and $u = u_1$, the strongest signal is $s_{u_1}(i)$. If $u \neq u_1$ and the relative shift between $u$ and $u_1$ satisfies $l'T_s \leq \tau_u - \tau_{u_1} \leq (l'+1)T_s$, the strongest signal should be $s_u(i - l')$ or $s_u(i - l' - 1)$.

Since we do not know which of the above holds, we have to test all shift possibilities. Based on previous experiments we may have some knowledge of the largest possible relative shift of any two users, i.e. $L'T_s$. Then, the possibilities for $s_u(\cdot)$ are $\{s_u(i - L'), \ldots, s_u(i + L')\}$. Deciding on the shift can be resolved using the user ID (i.e., the MAC address) (also see Section 2.5.2 and Fig. 2.2).

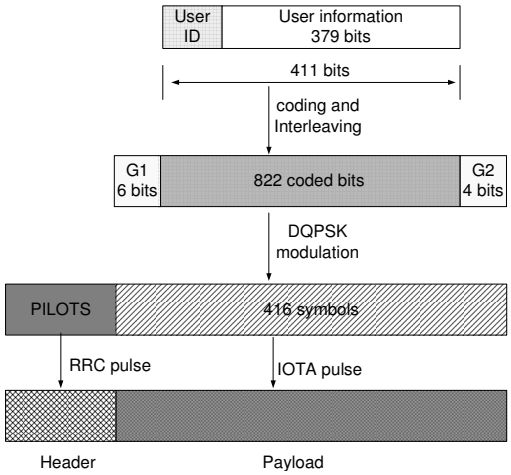


Figure 2.2: The transmitted packet structure.

Subsequently, if the detected collision order is 2, the strongest user will be deflated from the received signal as discussed in Section 2.3.2 to yield the symbols of the other user. Although at this step we have already found the channel coefficient of the strong user via pilot-based correlations as described in Section 2.3.3, we can obtain a better channel estimate by cross-correlating the received signal with the reconstructed

waveform obtained based on the recovered symbols and the IOTA pulse. This estimate will be better as it will be based on more symbols.

## 2.4 Throughput Analysis of ALOHA-CR

Consider a cellular network of $J$ users who communicate with a BS. Users transmit their packets in a time slotted fashion with probability $p$. Each packet contains multiple symbols, and the time slot duration is equal to the packet duration plus two symbols. The extended duration is to account for the intentional and naturally occurring shifts.

The proposed ALOHA-CR schemes follows the slotted ALOHA protocol, expect that second order collisions can be resolved. In this section we first analyze the throughput of ALOHA-CR for the simple case of a network with infinite backlog, i.e., the case in which the queues of the nodes are never empty, and each node always contends with some probability. Second, we consider the case in which the nodes have finite backlog and analyze the throughput and service delay of ALOHA-CR.

The throughput is defined here as the number of successfully delivered packets per slot. We consider a network of $J$ users with $J > 2$, where each user contends with probability $p$. The following possibilities exist for each slot.

- No transmissions are attempted (empty slot).
- A single transmission is attempted. In this case, let $P_0$ be the probability of successful reception.
- Two transmissions are attempted. Let the probability of receiving both transmissions correctly be $P_1$, and let the probability of successfully receiving only one of the two transmissions be $P_2$ (i.e., the probability of failing to receive any of the messages is $1 - P_1 - P_2$).

- More than two transmissions are attempted. In this case no attempt is made to recover the transmitted messages and users have to retransmit at some later time.

### 2.4.1 Network with infinite backlog and infinite number of users

For slotted ALOHA, the throughput is well established as $C(J) = Jp(1-p)^{J-1}$, which is maximized for contention probability $p^* = 1/J$, with maximum throughput $C(p^*) \to e^{-1}$ as $J \to \infty$.

For ALOHA-CR, the maximum throughput and optimum contention probability are given in the following proposition.

***Proposition 2.2***: *The maximum throughput of ALOHA-CR as $J \to \infty$ is:*

$$C = \frac{2P_0^2}{P_0 - 2P' + \sqrt{P_0^2 + 4P'^2}} \left(1 + \frac{2P'}{P_0 - 2P' + \sqrt{P_0^2 + 4P'^2}}\right) \times \exp\left(\frac{-2P_0}{P_0 - 2P' + \sqrt{P_0^2 + 4P'^2}}\right), \tag{2.11}$$

*where $P' = P_1 + \frac{P_2}{2}$, and is achieved for contention probability equal to*

$$p = \frac{2P_0}{2P_0 + a + \sqrt{a^2 + 4P_0 b}} \tag{2.12}$$

*where $a = (P_0 - 2P')(J-1)$ and $b = P'(J-1)(J-2)$.*

*Proof*: see Appendix II (in section 2.9).

### 2.4.2 Network with finite backlog and finite number of users

In this case the nodes with empty queues will not contend for medium access. Throughput analysis for this case is carried out by extending the approach of [33] to take into account the fact that the receiver can resolve second order collisions

with a certain probability. The method of [33] approximates the performance of $J$ coupled queues with $J$ uncoupled $geom/geom/1$ queues, an approximation that has been shown to hold very well and which simplifies the analysis greatly.

The assumptions in this section follow those in [33], i.e.,

- The arrival rate for each queue in the system is Bernoulli with rate $r$, i.e., the total arrival rate for a system with $J$ users is $rJ$.
- A queue $j$ is active in a time slot if it has one or more packets eligible for transmission, else it is inactive.
- Each active queue $j = 1, ..., J$ contends with the same contention probability $p$.

We further assume that there is an acknowledgment feedback loop, so that the transmitter knows whether the packet that was transmitted was successfully received, or has to be re-transmitted. Assuming that the probability that a queue is active in a typical time slot in steady state is $q$, the probability of success for an active queue becomes:

$$s(q) = P_0 p \left(1 - qp\right)^{J-1} + \left(P_1 + \frac{P_2}{2}\right)(J-1)\, qp^2 \left(1 - qp\right)^{J-2} \tag{2.13}$$

In the above equations it was assumed that in the case of two transmissions with only one successful reception, the successful packet could belong to any of the two users with equal probability, i.e., we assumed all the links to be equivalent.

### Active Probability $q$

Applying Little's Law to the server ($q$ is the average number of customers in service, $\frac{1}{s}$ is the average service delay, and $r$ is the arrival rate), we find that $q = \frac{r}{s}$, where $s$ is given by (2.13) [33].

Following the steps from [33], let us define

$$f(z) = P_0 z\,(1-z)^{J-1} + \left(P_1 + \frac{P_2}{2}\right)(J-1)\,z^2\,(1-z)^{J-2} \tag{2.14}$$

and $f^{max} = f(p^*)$, where $p^*$ is the maximizer for $f(z)$. Based on Appendix 2.8 $p^* = \frac{2P_0}{2P_0+a+\sqrt{a^2+4P_0 b}}$. The function $f(z)$ corresponds to the success probability of a queue in the system when the queues are unstable and thus always active. In other words, $f(z)$ corresponds to the maximum possible probability of success. Since a queue cannot output more packets than the ones that arrive in the queue, we can distinguish between two different modes of operation of the queue as a function of the arrival rate:

For $\underline{r : r \geq f^{max}}$ the arrival rate in the queue is larger than the maximum possible rate at which the packets can exit the queue. In this case the queue is always active (i.e., $q = 1$), and its success probability is simply $f(p)$, with $p$ being the contention probability.

For $\underline{r : r < f^{max}}$ the stability of the queue depends on the contention probability, since the physical layer can support a departure rate greater than the arrival rate. However, the queue is not stable for all possible contention probabilities. The equation $f(p) = r$ in this case has two real solutions; let these be $p^{min}$ and $p^{max}$. For $p \leq p^{min}$ (when $p = p^{min}$, the packet arrival rate is equal to the packet departure rate, however the active probability of the queue is equal to 1. See the active probability approximation (2.15).) and $p > p^{max}$, the queue is unstable and the active probability $q = 1$. This instability is due to either a very conservative choice of contention probability (for the $p \leq p^{min}$ case), or a very aggressive one (for the case of $p > p^{max}$). On the other hand, for $p \in (p^{min}, p^{max}]$, the queue becomes stable (active probability $q < 1$), as in this region of operation the physical layer can support a departure rate greater than $r$. Since a queue cannot output more packets than the ones arriving in

the queue, we conclude that the departure rate in this region equals the arrival rate in the queue. In order to calculate the active probability in this region of operation we can simply solve the equation $f(qp) = r$. The two solutions of that equation are $qp = p^{min}$ and $qp = p^{max}$. Solving for $q$, we get that $q = \frac{p^{min}}{p}$ and $q = \frac{p^{max}}{p}$. For the region under consideration, ($p \in (p^{min}, p^{max}]$ ), $q < 1$. Thus, since $p^{max}/p > 1$, $q = p^{max}/p$ cannot be a solution.

Summarizing, the active probability of each node equals

$$q = \begin{cases} \frac{p^{min}}{p}, & r < f^{max} \text{ and } p \in (p^{min}, p^{max}] \\ 1, & \text{otherwise} \end{cases} \tag{2.15}$$

The equations $f(p) = r$ and $f(qp) = r$ can efficiently be solved for $p$ and $q$ using any numerical method, for example Newton's method.

### Approximate Throughput

The throughput of $J$ independent queues, using $q$, $p^{min}$, $p^{max}$ and $f^{max}$ is

$$\tau = \begin{cases} Jr, & r < f^{max} \text{ and } p \in (p^{min}, p^{max}] \\ r', & \text{otherwise} \end{cases} \tag{2.16}$$

where $r' = JP_0p\left(1-p\right)^{J-1} + J\left(P_1 + \frac{P_2}{2}\right)\left(J-1\right)p^2\left(1-p\right)^{J-2}$. When the queues are stable, the system throughput (average number of successful transmissions per slot), is limited by the rate at which messages arrive at each of the queues. On the other hand, in the region where the queues are unstable ($q = 1$), the throughput is limited by the maximum achievable throughput of the physical layer, similarly to the case of infinite backlog.

**Average Total Delay (Queue+Service delays)**

For the regions of operation where the active probability $q$ is less than 1 and thus the queue is stable, we can further calculate the total delay that a packet will experience from the time it enters the queue until it is successfully transmitted. As shown in Section 2.4.2, the queue is stable when $r < f^{max}$ and $p \in (p^{min}, p^{max}]$. Using the well-known results from queuing theory for the geom/geom/1 queue, the total delay (queuing plus service delay) equals [42]

$$D_{tot} = \frac{1}{s\left(1 - \frac{r(1-s)}{s(1-r)}\right)},\ r < f^{max} \text{ and } p \in \left(p^{min}, p^{max}\right] \tag{2.17}$$

where $r\,(1-s)$ is the "birth probability", $s\,(1-r)$ is the "death probability" of the queue and $s$ is obtained from (2.13) after calculating the active probability $q$ from (2.15).

**Average Delay in Server**

Since for a geom/geom/1 queue with service rate $s$ the average service delay is $\delta = s^{-1}$ [42], the average service delay of the $J$ independent queues, using $q$, $p^{min}$, $p^{max}$ and $f^{max}$ is

$$\delta = \begin{cases} q/r, & r < f^{max} \text{ and } p \in (p^{min}, p^{max}] \\ \delta', & \text{otherwise} \end{cases} \tag{2.18}$$

where $\delta' = \left[P_0 p\,(1-p)^{J-1} + \left(P_1 + \frac{P_2}{2}\right)(J-1)\,p^2\,(1-p)^{J-2}\right]^{-1}$.

It is worthwhile to note that if $r < f^{max}$, the throughput of the network will be the same for any contention probability $p \in (p^{min}, p^{max}]$, however when $p = p^{max}$ the delay is the lowest for all contention probabilities. The proof is simple. When $p = p^{max}$, the active probability in (2.15) will achieve its minimum value, which leads

to the minimum service delay in (2.18).

## 2.5 Details on the SDR implementation

### 2.5.1 Testbed setting

The proposed approach was implemented on the WARP testbed [43, 27]. In this study we used the non-real time stage of the WARP testbed, which makes use of an application programming interface (API) called WARPLab. WARPLab allows all processing and modulation to be done in Matlab, turning the field-programmable gate array (FPGA) of WARP into a simple buffer. One can use Matlab to create a set of data, modulate it, apply the designed pulse shaping function, and transfer the data to the radio card. On the receive side, WARPLab allows for data to be processed in Matlab immediately after it has been downconverted by the Radio Frequency Integrated Circuit (RFIC) on the radio card.

Fig. 2.3 shows an experimental configuration where a single host computer controls five nodes. The host computer acts as the BS and controls all the nodes in order to provide correct synchronization between the transmitters and the receiver. The separation between nodes 1 and 2 is about 5 m, and the separation between nodes 3 and 4, and nodes 4 and 5 is also about 5 m. The separation between nodes 1 and 3, and nodes 2 and 5 is about 10 m.

### 2.5.2 SDR implementation

The user packet was structured as shown in Fig. 2.2. The SDR implementation was carried out in the following steps.

At the transmitter:

- *Payload* - The payload contained 411 bits (32 bits for the user ID and 379 random bits). Convolutional coding with rate 1/2 was applied to get 822 bits.

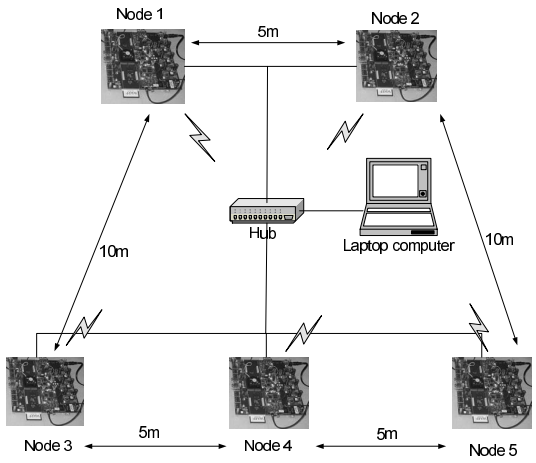


Figure 2.3: The experimental SDR setup consisting of 5 WARP nodes.

The coded bits were then interleaved. Specifically, the interleaver writes the input sequence in a matrix in row-wise fashion and then reads it in column-wise fashion. 6 bits and 4 bits were appended in the beginning and at the end of the packet, respectively, as guard bits. Differential quadrature phase shift keying (DQPSK) [21] was used to modulate the data. The IOTA pulse shape waveform with time support $[-2T_s, 2T_s]$ was used for transmission.

- *Pilots* - A 31 bit m-sequence [36] was added at the pilot portion of the packet (header). The pilot bits were BPSK modulated and an RRC pulse shape waveform was used for their transmission. A code book of four m-sequences was generated. The code book was kept at the BS and was linked to the user IDs.

- *Sampling rate* - The sampling rate of the board was 40 Msamples/second. The number of samples per symbol determines the symbol rate. We chose 32 samples/symbol, yielding data rate of 1.25 Msymbols/second. At that symbol rate we did not observe frequency selective fading.

- *Introducing user delays* - A random number of zero samples, chosen uniformly

in $[0, 32]$, was added in the beginning of the payload.

- *Transmission* - The signal was first up-converted to 5 MHz and sent to the transmission buffer. The board used channel 8 of the IEEE 802.11 standard to transmit the signal, i.e., the carrier frequency was 2.44GHz.

At the receiver:

- *Synchronization and collision order estimation* - The signal was read from the receiver buffer where it was already down-converted to 5 MHz. The sampling rate of the receiver was also 40 Msamples/second, with 32 samples/symbol. Subsequently it was down-converted to baseband. All entries of the code book were used to perform correlations with the header of the received signal. The entry which gave the largest correlation peak indicated who the corresponding user was. For the following discussion, suppose that this is user $u_1$ ($u_1$ could be any of the users present in the system).

  The delay and channel coefficient of user $u_1$ was estimated based on the location and value of the peak, respectively. The chosen m-sequence was deflated from the pilot portion of the received signal. All entries of the code book were used to perform correlation with the pilot portion of the deflated signal to detect the presence of another user as described in Section 2.3.3. The correlation threshold was taken to be $T^* = 0.75$. The largest possible relative shift of two user was observed to within $2T_s$, i.e. $L' = 2$. We introduced a random delay within $[0, T_s]$ for each user, and the natural delay differences of any two users was observed to be within $[-T_s, T_s]$.

- *Symbol recovery* - Symbol recovery was attempted only if the collision order was estimated to be 1 or 2. Otherwise, the received signal was discarded and users were asked to retransmit. As already mentioned, the received signal was

sampled with sampling rate $M = 32$ samples/symbol. Since the time support of the pulse is $[-2T_s, 2T_s]$, this corresponds to $M' = 4M + 1 = 129$ samples per pulse. We used only $P = 6$ polyphase components of the sampled signal, corresponding to samples $[52, 57, 62, 67, 72, 77]$ (see Fig. 2.1). These samples were taken around the peak of $u_1$. We should note that even if the detected collision order was 1, we still took $P = 6$ polyphase components and applied blind separation. This is to account errors in estimation of the collision order; if there are two users and we estimate the collision order to be one, by applying blind source separation we can still recover one of the users.

The 6 polyphase components were input to the JADE algorithm for source separation. The outputs of the JADE algorithm were passed through a PLL resulting in 6 sequences within phase and delay ambiguities. Let $s_u(.)$ be the strongest signal, i.e., the sequence that has the smallest variance around the known constellation. $s_u(.)$ could be either $s_{u_1}(.)$ or $s_{u_2}(.)$. Because the relative shift of any two users was within $2T_s$, i.e. $-2T_s \leq \tau_{u_1} - \tau_{u_2} \leq 2T_s$, $s_u(.)$ the possibilities for $s_{u_2}(.)$ were $[s_u(i-2), \ldots, s_u(i+2)]$ (see Section 2.3.5).

The symbols corresponding to $s_u(.)$ were demodulated. The use of DQPSK modulation allowed for removal of phase ambiguity. The demodulated output was passed through a de-interleaver and decoder, to get 411 decoded bits. If we misinterpreted $s_u(i-l_1)$ for $s_u(i-l_2)$, the de-interleaver would give a meaningless output. We used the user ID part in the beginning of the decoded output to do correlation with the corresponding entry of the user ID book in order to determine the shift and also whether the recorded signal corresponded to user $u_1$ or user $u_2$. If the strongest user was $s_u(i+2)$, the first 2 symbols would be lost. Since we used DQPSK, the first output symbol contained phase ambiguity. Therefore, we used 6 guard bits (3 symbols) in the beginning. Similarly, we used

4 guard bits at the end, to protect the integrity of $s_u(i-2)$.

Note that although we used correlation with the user IDs to determine the user, we cannot use this information to estimate the channel. This is because the received packet is interleaved and coded, thus the beginning part of the frame is a random sequence until decoding.

Subsequently, we performed SIC as described in section 2.3.2. As the output of PLL, $s_u(i)$, contained phase ambiguity, we first demodulated $s_u(i)$ to get estimates of the corresponding bits, and then applied DQPSK to get the estimated symbols $\hat{s}_u(i)$. The resulting $\hat{s}_u(i)$ contained no phase ambiguity. After that we used the estimated symbols $\hat{s}_u(i)$ to obtain the corresponding channel estimate by using cross-correlating the received signal with the reconstructed user waveform as described in section 2.3.2. Although we had obtained a channel estimate for that user during the synchronization step, the estimate obtained based on the recovered symbols is more robust, as it is based on 416 symbols as opposed to 32 pilot symbols. Finally, we deflated the corresponding signal from the received mixture.

## 2.6 Experimental results

### 2.6.1 Testbed measurements: A two-user system

In this experiments, nodes 3 and 5 were the two transmitters, and node 2 was the BS. For each time slot both nodes transmitted with probability 1. In this experiment the BS knew that the collision order was 2. All transmitters/receiver locations and antenna gains were fixed. By varying the amplitudes of the input signals we obtained throughput and BER performance of ALOHA-CR at different SNR levels. For each SNR level, 600 packets were transmitted. Since the indoor wireless channel was time

varying in both phase and amplitude, the received SNR of the two users varied between transmissions. The SNR difference of user 1 and user 2 was carefully controlled; 98.81% of the packets were within $3dB$ and 66.42% of them were within $1dB$.

**BER comparison**

This section shows the testbed performance of ALOHA-CR using blind source separation followed by SIC, described in Section 2.3.2 (denoted in the figures as *blind*), ALOHA-CR using training based source separation followed by SIC, described in Section 2.3.4, (denoted in the figures as *training*), and ALOHA-CR using SIC only, described in Section 2.3.2, (denoted in the figures as *SIC*). The BER shown here is raw BER, i.e., BER before decoding. The blind source separation algorithm used was the JADE method [35]; the code was downloaded from: http://perso.telecom-paristech.fr/∼cardoso/Algo/Jade/jade.m.

Intentional random delays in the interval $[0, T_s]$ were added to both users. Just for comparison purposes, for this BER evaluation we only included the cases corresponding to delay differences in the range $[T_s/2 - T_s/8, T_s/2 + T_s/8]$; when the delay differences are smaller, all methods yield high BER. The BER performance of the blind approach, as captured by the testbed is shown in Fig. 2.4. One can see that the proposed blind separation scheme works very well. The BER approaches $10^{-3}$ at an SNR of about $20dB$. Regarding the performance of the training method (also shown in Fig. 2.4) one can see that there is about $5dB$ performance loss as compared to the blind method when the SNR is higher than $15dB$. The inferior performance of the training method is due to the use of short pilot sequences for channel estimation. Moreover, in the testbed measurements there is distortion of the pulse shape due to the antennas, drifting of the sampling points, and errors in the channel coefficient estimates, all of which result in errors in estimating the channel matrix $\mathbf{A}$. The per-

formance of the SIC method is also included in Fig. 2.4. We can see that there is an error floor which does not decrease with increasing SNR. This is due to the fact that when we attempt to detect the first user, we treat the other user as interference.

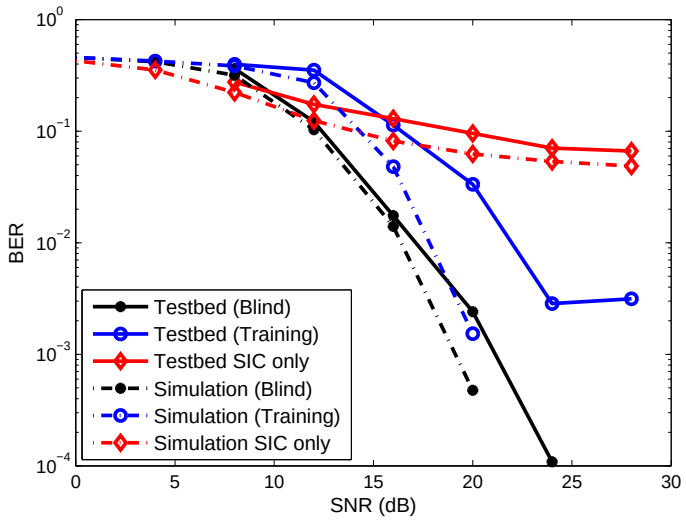


Figure 2.4: BER performance of three separation schemes.

Computer simulations were also conducted to produce the BER for the above described scenario. In the simulations, the amplitudes of the channel coefficients were given values obtained from testbed the measurements, while the phases of the channel coefficients were taken to be random. It was assumed that the channel remains the same within each block. The delays and CFOs were set equal to the values observed during the BER testbed experiments. The estimation results were averaged over 100 independent channels, and over 10 Monte-Carlo runs for each channel. Based on Fig. 2.4, one can see that for the blind method there is only $1dB$ gap between the testbed measurements and the computer simulations. For the training method, the gap is about 3 to 5 dB. The larger gap for the training method probably occurs because

the corresponding simulations rely on a non-realistic scenario where there is neither distortion of pulse shape nor drifting of sampling points.

### Throughput comparison

The throughput performance of the three methods is given in Fig. 2.5. In this figure all received packets were taken into account. We assume that any error in the decoding output results in failure of the transmission. The throughput was computed as the number of successfully delivered packets per time slot. We can see that, as expected, the blind separation method gives the highest throughput. The throughput of SIC is bounded by 0.4.

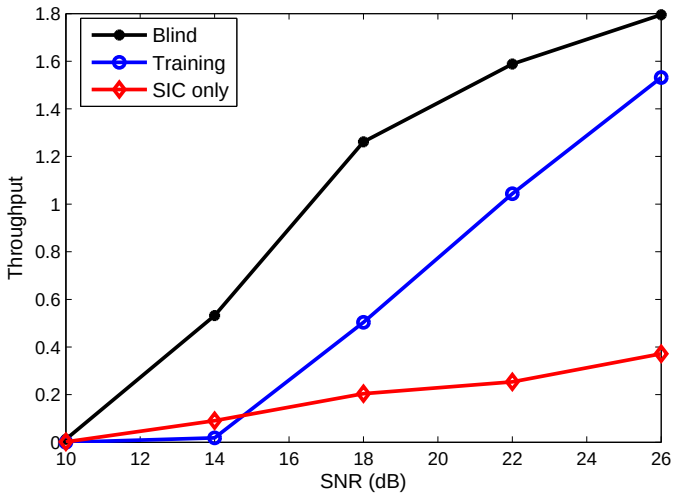


Figure 2.5: Throughput performance of three separation schemes.

Comparison of blind and training methods in terms of throughput fairness for the users is given in Fig. 2.6. We can see that in the throughput of the two users is almost the same, which indicates that the proposed ALOHA-CR is fair to both users.

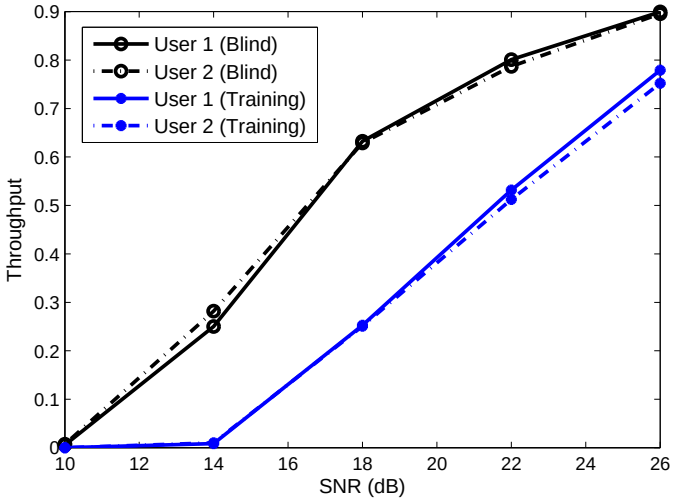


Figure 2.6: Throughput of individual users.

### Throughput versus different shift scenarios

In this experiment we verify *Proposition 2.1* in Section 2.2 by comparing throughput performance with and without intentional shifts. *Proposition 2.1* assumes that the pdf of natural delays differences $f_\delta(x)$ is symmetric around the origin, which represents the worst case scenario for the condition number of matrix $\mathbf{A}$. However in the measurements, for any two specific transmitters the center of $f_\delta(x)$ might not be at the origin due to the various factors, such as delays introduced by the hub, the time the transmitter takes to respond to the computer command, etc. In fact, in this experiment the natural delay differences were measured and found to be centered around 5 samples. The advantage of introducing intentional random delays is shown in Fig. 2.7. It is clear that without the intentional random delays the throughput is significantly lower. We should note that if the natural delay differences of two transmitters are around $T_s/2$, introducing random delay might lower the throughput. However, this would occur with a small probability.

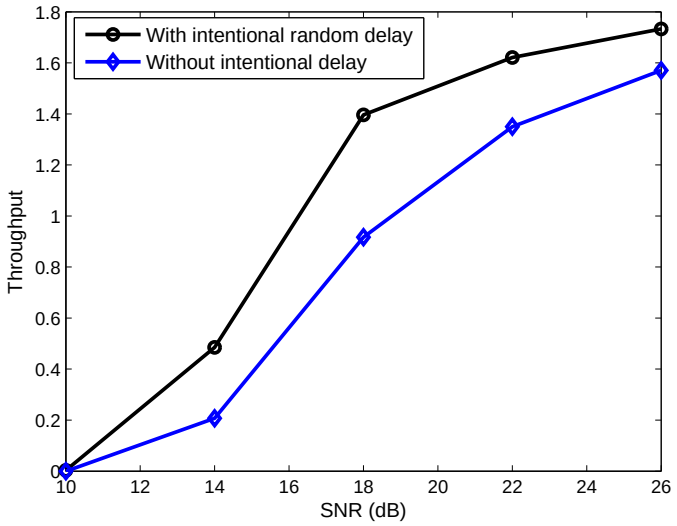


Figure 2.7: Throughput comparison for ALOHA-CR with and without intentional random delay.

### 2.6.2 Testbed measurements: Buffered Slotted ALOHA system

In this set of measurements we employed 5 SDR nodes, as depicted in Fig. 2.3. Node 4 played the role of the BS and all the other nodes were trying to communicate with it. The transmitted messages consisted of 411 random bits (before coding). Upon reception, the message was decoded and the transmission was considered successful if there were no bits in error. Each node had an independent Bernoulli arrival process of rate $r$, which resulted in a system arrival rate of $4r$. For the measurements, $r$ took the values of $\frac{1}{2}$, $\frac{1}{4}$, $\frac{1}{8}$, $\frac{1}{16}$ and $\frac{1}{32}$, so that we could measure the system performance at various loads. The contention probability for each of the above arrival rates took values in the range $[0.05, 0.95]$ with step 0.05.

In order to gather meaningful data, we had to make sure that the system was at steady state. Since the actual transmission and reception operations were time-consuming, the measurement process was performed in two steps, i.e., computer sim-

ulation and testbed measurements. In the computer simulation step, for each arrival rate and contention probability the system started at the empty state (all queues empty) and for the first $100,000$ slots we did not perform any actual transmissions but rather decided the outcome of each slot based on values for $P_0$, $P_1$ and $P_2$ that were measured off-line for this topology and the same number of contenting stations. For those off-line measurements, we first used the method described in Section 2.3.3 to detect the collision order, and then resolved the second order collisions when they occurred. The computed probabilities were $P_0 = 0.9964, P_1 = 0.9688$ and $P_2 = 0.0226$. During the process of reaching steady state, when there were no transmissions the slot was considered to be empty. When only one transmitter was trying to access the medium its queue would decrease by one with probability $P_0$. When two transmitters were contenting for the medium there was probability $P_1$ of both transmissions being successful, i.e., both of the queues would decrease their size by one with probability $P_1$, and with probability $P_2$ only one of the transmitters would decrease its queue. In the later case, where only one of the two nodes was successful, the successful transmission was assigned on either of the two contenting transmitters with equal probability of 0.5. If more than two transmitters were trying to access the medium, a collision was declared and no queue would decrease its size.

After the initial $100,000$ slots, $3,000$ additional slots were considered during which we used the testbed to perform on-line measurements and an attempt was made to resolve collisions of order two. The probability of correctly identifying the collision order was estimated to be 99.64% if one user transmitted, and 97.61% if two users transmitted. Data for service delay, total delay, throughput and active probability was gathered. For each slot, the outcome was determined by the receiver, depending on how many messages it was able to receive without any errors. Any message that was successfully received was removed from the corresponding queue. In case of errors the

message had to remain in the queue and be re-transmitted until successfully received.

The data that was gathered is plotted against the analytically calculated values determined as described in Section 2.4.2. The results for the active probability are given in Fig. 2.8. Figure 2.9 shows the measured and numerically calculated throughput, and Figs. 2.10 and 2.11 show the measured and analytical results, respectively, for the total service delays. From the plot of the total delay, the lines that correspond to arrival rate of 1/2 do not appear, since in this case the queues are unstable for all possible contention probabilities, thus the total delay goes to infinity. For the active probability and throughput, we see that there is almost a perfect match between measured and analytically predicted quantities, using the independent queues approach. For the delay the match is still pretty good, even though it is not as good as for throughput and active probability. Comparing the system with the conventional buffered slotted ALOHA, looking for example at the results of [33] where no collisions can be resolved, we can see that the achieved throughput for ALOHA-CR is more than double, the service and total delays are considerably smaller, and further, the system is stable for a much greater span of arrival rates and contention probabilities.

### 2.6.3 Comparison with ALOHA and TDMA

The throughput and service delay of ALOHA-CR are compared with that of ALOHA and TDMA in Fig. 2.12 and 2.13, respectively based on computer simulations. The number of users was 16. The packet arrival process of each node was an independent Bernoulli arrival process of rate $r$ taking the values $[1/512, 1/256, 1/128, 1/64, 1/32, 1/20, 1/16, 1/12]$. For ALOHA-CR and slotted ALOHA, we chose the contention probability that provides the highest throughput and the minimum service delay. If $r < f^{max}$ we chose contention probability $p = p^{max}$; if $r > f^{max}$, we chose $p = p^*$ so that $f(p^*) = f^{max}$. For ALOHA-CR, $f(z)$ is given in

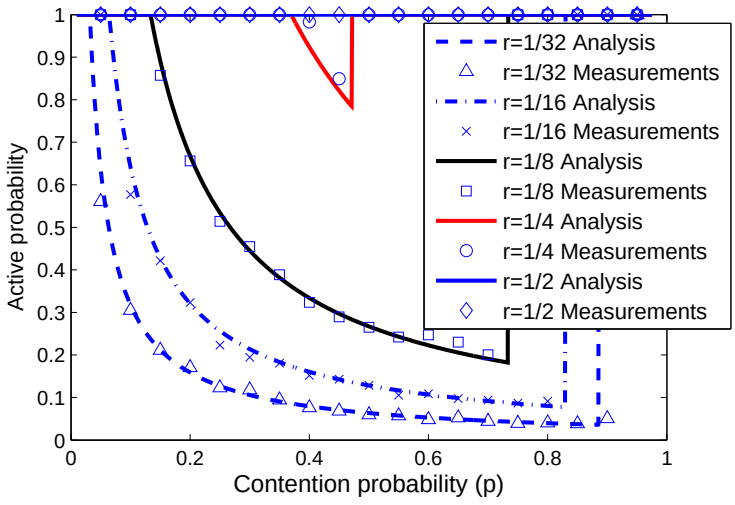


Figure 2.8: Active Probability vs contention probability of ALOHA-CR for different arrival rates (4 users).

eq. (2.14). For slotted ALOHA, the success probability of a queue is [33]

$$f_1(z) = P_0 z \left(1 - z\right)^{J-1} \quad . \tag{2.19}$$

We took $P_0 = 0.9964$, $P_1 = 0.9688$ and $P_2 = 0.0226$ as described in section 2.6.2.

The contention probability of ALOHA-CR for the considered packet arrival rates was calculated as $[0.402, 0.363, 0.319, 0.269, 0.205, 0.137, 0.102, 0.102]$. For ALOHA the corresponding contention probability was $[0.282, 0.239, 0.192, 0.132, 0.063, 0.063, 0.063, 0.063]$. For ALOHA and TDMA the probability of successful reception of a packet was set to 0.9964, which was indicated by prior testbed measurements, when only one user was transmitting. For ALOHA-CR the probabilities of successful packet reception were set to $P_0 = 0.9964$, $P_1 = 0.9688$ and $P_2 = 0.0226$. It is easy to observe from Figs. 2.12 and 2.13 that ALOHA-CR possesses the advantages of TDMA and ALOHA, i.e., when the packet arrival rate is low the service delay is low, while maintaining high

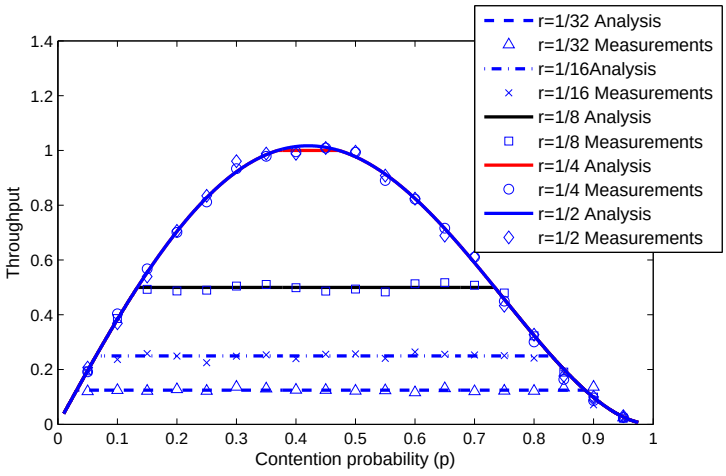


Figure 2.9: Throughput of ALOHA-CR vs contention probability for different arrival rates (4 users).

throughput when the packet arrival rate is high. The service delay of TDMA is higher than that of ALOHA-CR when the packet arrival rate is low; this is because the the active nodes have to remain silent until they are scheduled, even though the channel is free. We note that, unlike TDMA, ALOHA-CR does not require any scheduling.

In the same plot we also show the analytical results for comparison. We can observe that for both throughput and service delay there is almost a perfect match between the measured and the analytically predicted quantities.

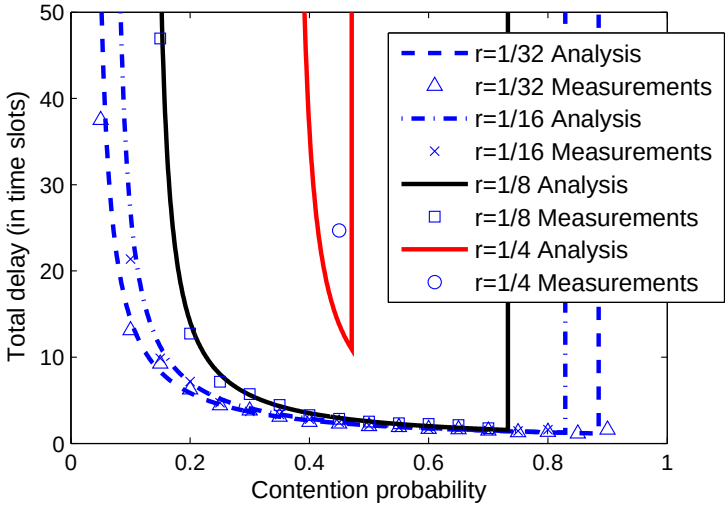


Figure 2.10: Total delay of ALOHA-CR vs contention probability for different arrival rates (4 users).

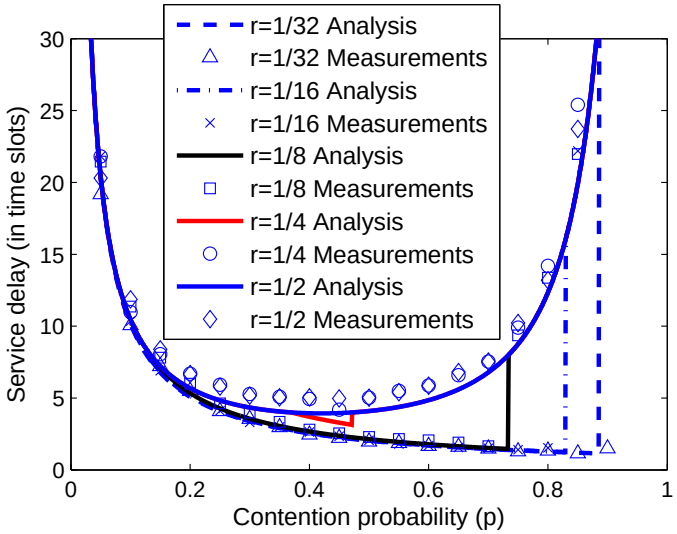


Figure 2.11: Service delay of ALOHA-CR vs contention probability for different arrival rates (4 users).

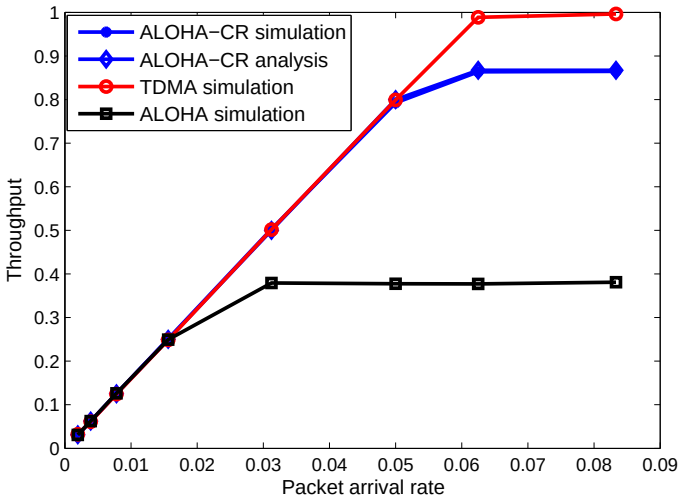


Figure 2.12: Throughput comparison (16 users).

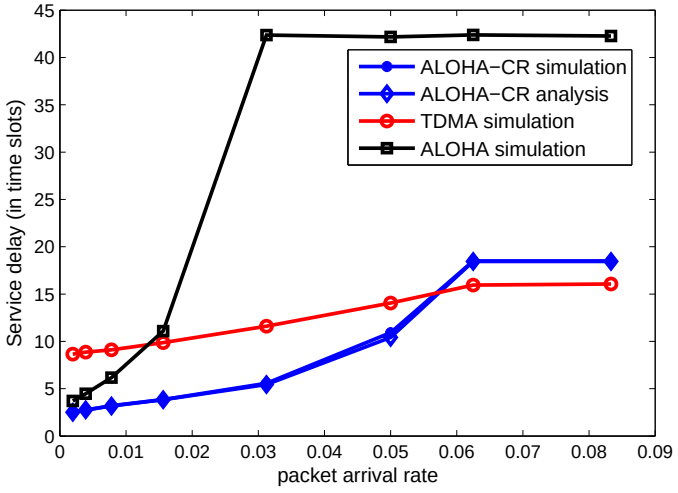


Figure 2.13: Service delay comparison (16 users).

## 2.7 Conclusion

In this chapter, we have proposed ALOHA-CR, which is a novel cross-layer scheme for high throughput wireless communications in a cellular scenario. This scheme can resolve second order collisions in the network without requiring retransmissions. We have described in detail the physical and MAC layers of the proposed scheme and derived analytical expressions to predict its performance. Further, the proposed scheme was implemented in a 5 node SDR system and its measured performance showed very good agreement with the analytical derived results. The conducted measurements show that ALOHA-CR can achieve more than twice the throughput of conventional slotted ALOHA, while maintaining stability for a much wider range of arrival rates and contention probabilities. This indicates that ALOHA-CR might be an excellent option for system deployments that can afford some extra complexity on the access point, while requiring low transmitter complexity (compared to other collision resolution schemes) to meet power or pricing requirements.

## 2.8 Appendix I: Proof of the Proposition 2.1

Let $f(x)$ be the pdf of the relative delay $\tau$ between the two users. The probability that the collision is not resolvable is:

$$P_c = \sum_{n=-\infty}^{\infty} \int_{-\Delta/2+nT_s}^{\Delta/2+nT_s} f(x)dx, \tag{2.20}$$

where $\Delta$ is some number smaller that $T$ representing the smallest distance between the peaks of the two users that still allows the users to be resolved.

In (2.20) $n$ runs from $-\infty$ to $\infty$, because when the relative delay $\tau$ is increased by by $nT_s$, $n \in \mathbb{Z}$, the channel channel matrix $\mathbf{A}$ remains the same.

Because the intentional delays are uniformly distributed in $[0, T]$, the pdf of $\alpha$ is :

$$f_\alpha(x) = \begin{cases} 1/T - |x|/T^2 & \text{if } |x| \leq T \\ 0 & \text{otherwise} \end{cases} \tag{2.21}$$

Since $\tau = \alpha + \delta$, the pdf of $\tau$ is:

$$\begin{aligned} f(x) &= \int_{-T}^{T} f_\alpha(v) f_\delta(x - v) dv \\ &= \int_0^T (\frac{1}{T} - \frac{v}{T^2}) f_\delta(x - v) dv + \int_{-T}^0 (\frac{1}{T} + \frac{v}{T^2}) f_\delta(x - v) dv \end{aligned} \tag{2.22}$$

Substituting (2.22) into (2.20), the probability of collision can be represented as:

$$P_c = \int_C \int_0^T (\frac{1}{T} - \frac{v}{T^2}) f_\delta(x - v) dv dx + \int_C \int_{-T}^0 (\frac{1}{T} + \frac{v}{T^2}) f_\delta(x - v) dv dx \tag{2.23}$$

where $\int_C dx = \sum_{n=-\infty}^{\infty} \int_{-\Delta/2+nT_s}^{\Delta/2+nT_s} dx$. Now $P_c$ is a function of $T$. Taking the first order derivative of $P_c$ with respect to $T$, we have

$$\frac{dP_c}{dT} = \underbrace{\frac{1}{T^2} \int_C \int_0^T (\frac{2v}{T} - 1) f_\delta(x - v) dv dx}_{\boldsymbol{\Xi_1}} + \underbrace{\frac{1}{T^2} \int_C \int_0^T (\frac{2v}{T} - 1) f_\delta(x + v) dv dx}_{\boldsymbol{\Xi_2}}. \tag{2.24}$$

Next we will show that $\frac{dP_c}{dT}|_{T=T_s} = 0$. Defining $\Phi(x) = \int_{-\infty}^x f_\delta(v) dv$ and $\int_a^b f_\delta(v) dv = \Phi(a) - \Phi(b)$, we get

$$\Xi_1|_{T=T_s} = \frac{1}{T_s^2}\int_0^{T_s}(\frac{2v}{T_s}-1)\sum_{n=-\infty}^{\infty}\Phi(\Delta/2+nT_s-v)-\Phi(-\Delta/2+nT_s-v)dv$$
$$= \frac{1}{T_s^2}\int_{-T_s/2}^{T_s/2}\frac{2u}{T_s}\underbrace{\sum_{n=-\infty}^{\infty}\Phi(\Delta/2+nT_s-u-T_s/2)-\Phi(-\Delta/2+nT_s-u-T_s/2)}_{\phi(\mathbf{u})}du \tag{2.25}$$

where $u = v - T_s/2$. As $2u/T_s$ is an odd function in $[-T_s/2, T_s/2]$, if $\phi(u)$ is an even function of $u$, then $\Xi_1|_{T=T_s} = 0$. Indeed, since $\Phi(x) = 1 - \Phi(-x)$, it can be easily seen that $\phi(-u) = \phi(u)$. Similarly we can show that $\Xi_2|_{T=T_s} = 0$. Thus $\frac{dP_c}{dT}|_{T=T_s} = 0$.

Next we show that $\frac{d^2P_c}{dT^2}|_{T=T_s} > 0$.

$$\frac{d^2P_c}{dT^2} = \frac{d\Xi_1}{dT} + \frac{d\Xi_2}{dT} \tag{2.26}$$

$$\frac{d\Xi_1}{dT} = \frac{-6}{T^4}\int_C\int_0^T vf_\delta(x-v)dvdx + \frac{2}{T^3}\int_C\int_0^T f_\delta(x-v)dvdx + \frac{1}{T^2}\int_C f_\delta(x-T)dx$$
$$= -\frac{2}{T}\Xi_1 + \frac{1}{T^2}\int_C f_\delta(x)dx - \frac{2}{T^4}\int_C\int_0^T vf_\delta(x-v)dvdx, \tag{2.27}$$

where $\int_C f_\delta(x)dx = \int_C f_\delta(x-T)dx$. Let us assume that $\int_C f_\delta(x)dx > \frac{1}{T_s}\int_0^{T_s}\int_C f_\delta(x-v)dxdv$. This means that the probability for non resolvable collisions when we do not introduce any intentional random delays to any user is larger that that when we only introduce an intentional random delay to one of the two users involved in the collision. The is intuitively correct, and was further confirmed in our testbed.

By applying $\Xi_1|_{T=T_s} = 0$, we get

$$\begin{aligned}\frac{d\Xi_1}{dT}|_{T=T_s} &> \frac{1}{T_s^3}\left[\int_0^{T_s}\int_C f_\delta(x-v)dxdv - \frac{2}{T_s}\int_C\int_0^{T_s} v f_\delta(x-v)dvdx\right] \\ &= -\frac{\Xi_1|_{T=T_s}}{T_s} = 0. \end{aligned} \tag{2.28}$$

Similarly, we can prove that $\frac{d\Xi_2}{dT}|_{T=T_s} > 0$, which leads to $\frac{d^2P_c}{dT^2}|_{T=T_s} > 0$. Thus we has shown that if we assign an intentional delay $\tilde{\tau}_k$ to each user that is uniformly distributed in $[0, T_s]$, the collision probability achieves a local minimum value.

## 2.9 Appendix II: Proof of the Proposition 2.2

Recall that for a single transmission the probability of successful reception is $P_0$. For order two collision the probability of receiving correctly both transmitted messages is $P_1$ and the probability of successfully receiving only one of the two transmitted messages is $P_2$. The corresponding throughput is :

$$\begin{aligned} C(p) &= P_0 Jp(1-p)^{J-1} + (2P_1 + P_2)\binom{J}{2}p^2(1-p)^{J-2} \\ &= P_0 Jp(1-p)^{J-1} + \underbrace{(P_1 + \frac{P_2}{2})}_{P'} J(J-1)p^2(1-p)^{J-2} \end{aligned} \tag{2.29}$$

To find the value of $p$ that maximizes throughput let us take the derivative of $C(p)$ with respect to $p$, i.e.,

$$\frac{dC(p)}{dp} = J(1-p)^{J-3}\left[P_0(1-p)^2 - \underbrace{(P_0 - 2P')(J-1)}_{a}p(1-p) - \underbrace{P'(J-1)(J-2)}_{b}p^2\right]. \tag{2.30}$$

Forcing $dC(p)/dp = 0$, besides a trivial solution at $p = 1$, we get two zeros at

$$\begin{cases} p_1^* = \frac{2P_0+a-\sqrt{a^2+4P_0b}}{2(P_0+a-b)} = \frac{2P_0}{2P_0+a+\sqrt{a^2+4P_0b}} \\ p_2^* = \frac{2P_0+a+\sqrt{a^2+4P_0b}}{2(P_0+a-b)} = \frac{2P_0}{2P_0+a-\sqrt{a^2+4P_0b}}. \end{cases} \tag{2.31}$$

Since $b > 0$, it holds that $a - \sqrt{a^2 + 4P_0b} < 0$. Thus, the possible range for $p_2^*$ is $(-\infty, 0)$ or $(1, \infty)$, both of which violate the requirement that $0 < p < 1$. Hence only $p_1^*$ is a valid solution. Moreover, it is easy to see that when $0 < p < p_1^*$, $dC(p)/dp > 0$, while when $p_1^* < p < 1$, $dC(p)/dp < 0$. Thus $C(p)$ is maximized when $p = p_1^*$. As $a$ and $b$ are related to $J$, defining $\eta(J) = 2P_0 + a + \sqrt{a^2 + 4P_0b}$, we get $p_1^* = 2P_0/\eta(J)$,

$$\lim_{J\to\infty} \frac{J}{\eta(J)} = \frac{1}{P_0 - 2P' + \sqrt{P_0^2 + 4P'^2}}, \tag{2.32}$$

and

$$\begin{aligned} \lim_{J\to\infty} \left(1 - \frac{2P_0}{\eta(J)}\right)^J &= \lim_{J\to\infty} \left(1 - \frac{2P_0}{\eta(J)}\right)^{\frac{\eta(J)}{2P_0} \lim_{J\to\infty} \frac{2P_0 J}{\eta(J)}} \\ &= \exp\left\{\frac{-2P_0}{P_0 - 2P' + \sqrt{P_0^2 + 4P'^2}}\right\} \end{aligned} \tag{2.33}$$

Substituting $p_1^* = 2P_0/\eta(J)$ into (2.29), and based on (2.32) and (2.33), we have

$$\begin{aligned} \lim_{J\to\infty} C(p_1^*) = &\frac{2P_0^2}{P_0 - 2P' + \sqrt{P_0^2 + 4P'^2}} \left(1 + \frac{2P'}{P_0 - 2P' + \sqrt{P_0^2 + 4P'^2}}\right) \\ &\times \exp\left\{\frac{-2P_0}{P_0 - 2P' + \sqrt{P_0^2 + 4P'^2}}\right\}, \end{aligned} \tag{2.34}$$

which gives us the asymptotical throughput as the number of users increases.

# 3. Blind Separation Of Two Users Based on User Delays and Optimal Pulse-Shape Design

## 3.1 Introduction

In chapter 2 we proposed ALOHA-CR, a cross-layer scheme that can resolve second order collisions in wireless networks. In order to resolve a second order collision, the collision signal has to be oversampled, and the polyphase components organized into a virtual MIMO system in which the user symbols information are the inputs. Because of the oversampling, high correlation will occur between the columns of the virtual MIMO system matrix, which is detrimental to the user separation. In this chapter a novel pulse-shape waveform design is proposed that results in low correlation between the columns of the system matrix, while it exploits all available bandwidth as dictated by a spectral mask. The CFO effects is also considered. We prove that the CFO difference between users can be exploited as a form of diversity. Introducing large intentional CFO differences among users could improve the separation performance, but that would increase the effective bandwidth.

At the physical layer, the collision resolution is a multi-user separation problem via approaches that do not use scheduling. This problem is of interest, for example, when traffic is generated in a bursty fashion, in which case fixed bandwidth allocation would result in poor bandwidth utilization. Lack of scheduling results in collisions, i.e., users overlapping in time and/or frequency. To separate the colliding users, one could enable multi-user separation via receive antenna diversity, or code diversity, as in CDMA systems. However, the former requires expensive hardware since multiple transceiver front ends involve significant cost. Further, the use of multiple antennas might not be possible on small size terminals or devices. CDMA systems require

bandwidth expansion, which requires greater spectral resources, and also introduces frequency selective fading. In the following, we narrow our field of interest to random access systems that for the aforementioned reasons cannot exploit antenna diversity, and that are inexpensive in terms of bandwidth. In such systems, the use of different power levels by the users can enable user separation by exploiting the capture effect [46], or successive interference cancellation (SIC) [20]. Different power levels can result from different distances between the users and the destination, or could be intentionally assigned to users in order to facilitate user separation. While the former case, when it arises, makes the separation problem much easier, the latter approach might not be efficient, as low-power users suffer from noise and channel effects. In the following, we focus on the most difficult scenario of separating a collision of equal power users. Almost equal powers would also result from power control. Power control is widely used, hence this scenarios is of practical interest.

A delay-division multiple access approach was proposed in [28], which exploits the random delays introduced by transmitters. The approach of [28] considers transmissions of isolated frames. It requires that users have distinct delays, and exploits the edges of a frame over which users do not overlap. The approach of [28] assumes full knowledge of the channel. Pulse-shape waveform diversity was considered in [47] to separate multiple users in a blind fashion. In [47], the received signal is oversampled and its polyphase components are viewed as independent mixtures of the user signals. User separation is achieved by solving a blind source separation problem. Although no specifics on waveform design are given in [47], the examples used in the simulations of [47] consider wideband waveforms for the users. However, if large bandwidth is available, then CDMA would probably be a better alternative to blind source separation. Pulse shape diversity is also employed in [24, 25], which treat situations in which the pulse-shape waveforms have bandwidth constraints.

In this chapter we follow the oversampling approach of [47], with the following differences. First, we introduce an intentional half-symbol delay between the two users. Second, both users use the same optimally designed pulse shape waveform. Third, we use successive interference cancelation in combination with blind source separation to further improve the separation performance.

The rest of the chapter is organized as follows. In Section 3.2 we describe the problem formulation. The proposed blind method is presented in Section 3.3. The pulse shape design is derived in Section 3.4. Simulation results validating the proposed methods are presented in Section 3.5, while concluding remarks are given in Section 3.6.

## 3.2 Problem formulation

We consider a distributed antenna system, in which $K$ users transmit simultaneously to a base station. Although much of this chapter studies the case $K = 2$, for reasons that will be explained later, we will keep the $K$ user notation throughout. Narrow-band transmission is assumed here, in which the channel between any user and the base station undergoes flat fading. In addition, quasi-static fading is assumed, i.e., the channel gains remain fixed during several symbols.

The transmitted signal of user $k$ is of the form given in eq. (2.2), and considering the CFO effects between transmitter and the receiver, the continuous-time base-band received signal $y(t)$ in eq. (2.1) can be expressed as:

$$y(t) = \sum_{k=1}^{K} a_k x_k(t - \tau_k) e^{j2\pi F_k t} + w(t) \ , \tag{3.1}$$

where $a_k$ denotes the complex channel gain between the $k-$th user and the base station; $\tau_k$ denotes the delay of the $k-$th user; $F_k$ is the CFO of the $k-$th user,

arising due relative motion or oscillator mismatch between receive and transmitter oscillators, and $w(t)$ represents noise.

Our objective is to obtain an estimate of each user sequence, $s_k(i), i = 0, 1, ...,$ up to a complex scalar multiple that is independent of $i$. The estimation will be based on the received signal only, while channel gains, CFOs and user delays are assumed to be unknown.

Sampling the received signal $y(t)$ at times $t = iT_s + mT_s/P$ we obtain

$$y_m(i) = \sum_{k=1}^{K} a_k \left[ \sum_l s_k(l) p\left( (i-l)T_s + \frac{mT_s}{P} - \tau_k \right) \right] e^{j2\pi f_k (iP+m)} + w_m(i) \tag{3.2}$$

$$= \sum_{k=1}^{K} h_{mk}(i) * \tilde{s}_k(i) + w_m(i), \ m = 1, ..., P \ , \tag{3.3}$$

where $f_k = F_k T_s/P$ ($|F_k T_s| \leq 0.5$) is the normalized CFO between the $k-$th user and the base station, $\tilde{s}_k(i) = s_k(i) e^{i2\pi f_k iP}$, "$*$" denotes convolution, and $h_{m,k}(i)$ is defined as

$$h_{m,k}(i) = a_k e^{j2\pi f_k (m+iP)} p\left( iT_s + \frac{mT_s}{P} - \tau_k \right), \ i = \ldots, -2, -1, 0, 1, 2, \ldots \ . \tag{3.4}$$

Assuming that user delay $\tau_k$ is within the interval $(0, T_s/P)$, the $m$-th polyphase

component, $y_m(i),\ m = 1, ..., P$, can be expressed as

$$y_m(i) = [[h_{m,1}(\tilde{L}-1)\dots h_{m,1}(-\tilde{L})],\dots,[h_{m,K}(\tilde{L}-1)\dots h_{m,K}(-\tilde{L})]] \times \begin{bmatrix} \begin{bmatrix} \tilde{s}_1(i-\tilde{L}+1) \\ \vdots \\ \tilde{s}_1(i+\tilde{L}) \end{bmatrix} \\ \vdots \\ \begin{bmatrix} \tilde{s}_K(i-\tilde{L}+1) \\ \vdots \\ \tilde{s}_K(i+\tilde{L}) \end{bmatrix} \end{bmatrix} + w_m(i)\ . \tag{3.5}$$

Let us form the vector $\mathbf{y}(i)$ as $\mathbf{y}(i) = [y_1(i), \dots, y_P(i)]^T$. It holds that

$$\mathbf{y}(i) = \mathbf{A}\mathbf{s}(i) + \mathbf{w}(i) \tag{3.6}$$

where $\mathbf{A}$ is a $P \times 2\tilde{L}K$ matrix whose $m$-th row equals
$[h_{m,1}(\tilde{L}-1), \dots, h_{m,1}(-\tilde{L}), \dots, h_{m,K}(\tilde{L}-1), \dots, h_{m,K}(-\tilde{L})]$;
$\mathbf{s}(i) = [\tilde{s}_1(i-\tilde{L}+1), \dots, \tilde{s}_1(i+\tilde{L}), \dots, \tilde{s}_K(i-\tilde{L}+1), \dots, \tilde{s}_K(i+\tilde{L})]^T$; and $\mathbf{w}(i) = [w_1(i), \dots, w_P(i)]^T$. This is a $P \times 2\tilde{L}K$ instantaneous multiple-input multiple-output (MIMO) problem. Under certain assumptions, to be provided in the following section, the channel matrix $\mathbf{A}$ is identifiable, and the vector $\mathbf{s}(i)$ can be recovered within certain ambiguities. In particular, for each $k$, we get $2\tilde{L}$ different versions of $s_k$, i.e., $s_k(i-\tilde{L}+1)e^{j2\pi f_k(i-\tilde{L}+1)P}, \dots, s_k(i+\tilde{L})e^{j2\pi f_k(i+\tilde{L})P}$ within a scalar ambiguity. The effects of the CFO on the separated signal can be mitigated by using any of the existing single CFO estimation techniques (e.g., [51], [44], [45], [52] [38], [39]), or a simple PLL device [40].

## 3.3 Blind user separation

### 3.3.1 Assumptions

The following assumptions are sufficient for user separation.

- **A1**) Each of the elements of $\mathbf{w}(i)$, as a function of $i$, is a zero-mean, complex Gaussian stationary random process with variance $\sigma_w^2$, and is independent of the inputs.

- **A2**) For each $k$, $s_k(\cdot)$ is independent and identically distributed (i.i.d.) with zero mean and nonzero kurtosis, i.e., $\gamma_{s_k}^4 = \text{Cumulant}[s_k(i), s_k^*(i), s_k(i), s_k^*(i)] \neq 0$. The $s_k$'s are mutually independent, and each user has unit transmission power.

- **A3**) The over-sampling factor $P$ satisfies $P \geq 2\tilde{L}K$.

- **A4**) The channel coefficients $a_k$ are non-zero.

- **A5**) The user delays, $\tau_k$, $k = 1, ..., K$, in eq. (3.2) are randomly distributed in the interval $(0, T_s/P)$.

- **A6**) Either the CFOs are distinct, or the user delays are distinct.

- **A7**) $p(t) > 0$ for $(-T_s, T_s)$; and $p(t) = 0$ only for $t = iT_s$ and $i = -\tilde{L}, \ldots, -1, 1, \ldots, \tilde{L}$.

Under assumption (**A2**), it is easy to verify that the rotated input signals $\tilde{s}_k(.)$ are also i.i.d. with zero mean and nonzero kurtosis[56]. Also, the $\tilde{s}_k$'s are mutually independent for different $k$'s. Assumptions (**A1**) and (**A2**) are needed for blind MIMO estimation based on (3.6). Assumptions (**A3**) $-$ (**A7**) guarantee that the virtual MIMO channel matrix $\mathbf{A}$ in (3.6) has full rank with high probability. Assumption (**A3**) can actually be relaxed. As will be discussed later, (see (4.3)), the contributions of low-value columns of $\mathbf{A}$ in (3.6) can be viewed as noise. This effectively reduces

the dimensionality of the problem. (**A5**) and (**A7**) guarantee that $p\left(iT_s + \frac{mT_s}{P} - \tau_k\right)$ will be nonzero for all allowable values of $i$, $m$ and $k$. To see the effect of (**A6**), let us write the channel matrix $\mathbf{A}$ as

$$\mathbf{A} = [\mathbf{h}_1(\tilde{L}-1), \ldots, \mathbf{h}_1(-\tilde{L}), \ldots, \mathbf{h}_K(\tilde{L}-1), \ldots, \mathbf{h}_K(-\tilde{L})] \tag{3.7}$$

where $\mathbf{h}_k(l)$ is formed by appending $h_{m,k}(l)$ in (3.4) for different $m$'s, i.e.

$$\begin{aligned}\mathbf{h}_k(l) = \Bigg[ & a_k e^{j2\pi f_k(1+lP)} p\left(lT_s + \frac{T_s}{P} - \tau_k\right), a_k e^{j2\pi f_k(2+lP)} p\left(lT_s + \frac{2T_s}{P} - \tau_k\right), \\ & \ldots, a_k e^{j2\pi f_k(1+l)P} p((1+l)T_s - \tau_k)\Big]^T \ .\end{aligned} \tag{3.8}$$

and consider the case in which all user have the same delays, i.e., $\tau_k = \tau,\ k = 1, ..., K$. If the CFOs are different, $\mathbf{A}$ has full column rank. Even if the CFOs are not distinct, the columns of the channel matrix can be viewed as having been drawn independently from an absolutely continuous distribution, and thus the channel matrix has full rank with probability one [58].

### 3.3.2 Channel estimation and user separation

One can apply to (3.6) any blind source separation algorithm (e.g., [35]) to obtain an estimate of the channel matrix, $\hat{\mathbf{A}}$, which is related to the true matrix as

$$\hat{\mathbf{A}} \stackrel{\triangle}{=} \mathbf{A}\mathbf{P}\mathbf{\Lambda} \ , \tag{3.9}$$

where $\mathbf{P}$ is a column permutation matrix and $\mathbf{\Lambda}$ is a complex diagonal matrix. The method of [35] requires fourth-order cumulants of $\mathbf{y}(i)$. And accordingly the estimate of the de-coupled signals $\tilde{\mathbf{s}}(i)$ within permutation and diagonal complex scalar

ambiguities is

$$\hat{\tilde{\mathbf{s}}}(i) = e^{jArg\{-\mathbf{\Lambda}\}}|\mathbf{\Lambda}|^{-1}\mathbf{P}^T\tilde{\mathbf{s}}(i) \ . \tag{3.10}$$

Denoting by $\theta_{k,l}$ the diagonal element of $Arg\{\mathbf{\Lambda}\}$, which corresponds to the phase ambiguity of user $k$ with delay $l$, the separated signal can be expressed as

$$\hat{\tilde{s}}_k(i-l) = s_k(i-l)e^{j(-\theta_{k,l}+2\pi f_k(i-l)P)} \ . \tag{3.11}$$

At this point, the users' signals have been decoupled, and all that is left is to mitigate the CFO in each recovered signal. This can be achieved with any of the existing single CFO estimation methods, such as [51], [44], [45], [52] [38], or [39]. Alternatively, if the CFO is very small we can estimate it and at the same time mitigate its effect using a PLL. We should note here that even a very small CFO needs to be mitigated in order to have good symbol recovery. For example, for 4-ary quadrature amplitude modulation (4QAM) [49] signals and without CFO compensation, even if the normalized CFO $Pf_k = F_kT_s$ is only 0.001, the constellation will be rotated to a wrong position after $0.25/0.001 = 250$ samples.

If the CFO is large, then a PLL does not suffice. In this case, the phase of the estimated channel matrix $\hat{\mathbf{A}}$ can be used to obtain a CFO estimate. If $p(t) > 0$ for all $t$, it can be easily seen that $Arg\{\hat{A}\} = \mathbf{\Psi P}$ with

$$\mathbf{\Psi} = \begin{pmatrix} 2\pi f_1\mathbf{1}_{2\tilde{L}}^T + \mathbf{r}_1^T & \dots & 2\pi f_K\mathbf{1}_{2\tilde{L}}^T + \mathbf{r}_K^T \\ \vdots & \ddots & \vdots \\ 2\pi f_1P\mathbf{1}_{2\tilde{L}}^T + \mathbf{r}_1^T & \dots & 2\pi f_KP\mathbf{1}_{2\tilde{L}}^T + \mathbf{r}_K^T \end{pmatrix} \ , \tag{3.12}$$

where $\mathbf{1}_N$ is a $(1\times N)$ vector with all elements equal to one, and $\mathbf{r}_k^T = [Arg\{a_ke^{j2\pi f_k(\tilde{L}-1)P}\}+ \theta_{k,\tilde{L}-1}, ..., Arg\{a_ke^{j2\pi f_k(-\tilde{L})P}\} + \theta_{k,-\tilde{L}}]$. The least-squares [57] estimates of the CFO

can be obtained as

$$\hat{f}_{k'} = \frac{1}{2\pi} \frac{P\left(\sum_{p=1}^{P} p\Psi_{p,k'}\right) - \left(\sum_{p=1}^{P} p\right)\left(\sum_{p=1}^{P} \Psi_{p,k'}\right)}{P\left(\sum_{p=1}^{P} p^2\right) - \left(\sum_{p=1}^{P} p\right)^2}, \tag{3.13}$$

where $\Psi_{p,k'}$ is the $(p,k')$-th element of $\mathbf{\Psi}$.

On noting that the de-coupled signals $\hat{\tilde{s}}_k(i-l)$ in (3.11) are permuted (see eq. (3.10)) in the same manner as the estimated CFOs in (3.13), we can use the $\hat{f}_{k'}$'s to compensate for the effect of CFO in the decoupled signals in (3.11) and obtain estimates of the input signals as

$$\hat{\mathbf{s}}(i) \triangleq e^{-j2\pi\hat{\mathbf{F}}\mathbf{P}Pi}\hat{\tilde{\mathbf{s}}}(i) = e^{jArg\{-\mathbf{\Lambda}\}}\mathbf{P}^T\mathbf{s}(i) \tag{3.14}$$

where $\hat{\mathbf{F}} \triangleq \text{diag}\left\{\hat{\mathbf{f}}_1^T, \ldots, \hat{\mathbf{f}}_K^T\right\}$ with $\hat{\mathbf{f}}_k = \left[\hat{f}_{2\tilde{L}(k-1)+1}, \ldots, \hat{f}_{2\tilde{L}k}\right]^T$. In order to resolve user permutation and shift ambiguities one can use user IDs embedded in the data [48].

Although in theory, under the above stated conditions, the matrix $\mathbf{A}$ has full rank for any number of users, $K$, the matrix condition number may become too high when CFOs or delay differences between users become small. As $K$ increases, the latter problem will escalate. Further, for large $K$, the oversampling factor, $P$, must be large. However, as $P$ increases, neighboring pulse-shape function samples will be close to each other, and the condition number of $\mathbf{A}$ will increase. Therefore, the shape of the pulse shape function sets a limit on the oversampling factor one can use and thus on the number of users one can separate. Recognizing that the above are difficult issues to deal with, we next focus on the two user case. Further, we propose to introduce an intentional delay of $T_s/2$ between the two users, in addition to any small random delays there exist in the system.

The performance of user separation depends on the pulse-shape function and also

on the location of the samples. Although uniform sampling was described above, non-uniform sampling can also be used, in which case the expressions would require some straightforward modifications. If the samples correspond to a low-value region of the pulse, the corresponding polyphase components will suffer from low signal-to-noise ratio. Also, if the sampling points are close to each other the condition number of $\mathbf{A}$ will increase. Therefore, one should select the sampling points so that the corresponding samples are all above some threshold and the sampling points are as separated as possible. The effect of pulse shape and optimal shape design will be discussed in the following section.

### 3.4 Pulse shape design

In this section we first investigate the effects of pulse shape on the condition number of $\mathbf{A}$. Since the condition number of a matrix increases as the column correlation increase, we next look at the correlation between the columns of $\mathbf{A}$.

Let us partition the channel matrix $\mathbf{A}$ into two sub-matrices $\mathbf{A}_P$ and $\mathbf{A}_I$, containing respectively the columns of $\mathbf{A}$ corresponding to the main lobe and those corresponding to the side lobes of the pulse. We can rewrite (3.6) as follows:

$$\mathbf{y}(i) = [\mathbf{A}_P \;\; \mathbf{A}_I] \begin{bmatrix} \mathbf{s}_P(i) \\ \mathbf{s}_I(i) \end{bmatrix} + \mathbf{w}(i) = \mathbf{A}_P \mathbf{s}_P(i) + \mathbf{A}_I \mathbf{s}_I(i) + \mathbf{w}(i) \; . \tag{3.15}$$

where

$$\begin{aligned} \mathbf{A}_P &= [\mathbf{h}_1(0)\ \mathbf{h}_1(-1)\ \ldots\ \mathbf{h}_K(0)\ \mathbf{h}_K(-1)] \\ \mathbf{A}_I &= \Big[[\mathbf{h}_1(\tilde{L}-1), \ldots, \mathbf{h}_1(1), \mathbf{h}_1(-2), \ldots, \mathbf{h}_1(-\tilde{L})], \ldots, \\ &\quad [\mathbf{h}_K(\tilde{L}-1), \ldots, \mathbf{h}_K(1), \mathbf{h}_K(-2), \ldots, \mathbf{h}_K(-\tilde{L})]\Big] , \end{aligned} \tag{3.16}$$

with $\mathbf{h}_k(l)$ as defined in (3.8). Correspondingly, $\mathbf{s}_P = [\tilde{s}_1(i), \tilde{s}_1(i+1), \ldots, \tilde{s}_K(i), \tilde{s}_K(i+1)]^T$ and $\mathbf{s}_I = [\tilde{s}_1(i-\tilde{L}+1), \ldots, \tilde{s}_1(i-1), \tilde{s}_1(i+2)\ldots, \tilde{s}_1(i+\tilde{L}), \ldots, \tilde{s}_K(i-\tilde{L}+1), \ldots, \tilde{s}_K(i-1), \tilde{s}_K(i+2)\ldots, \tilde{s}_K(i+\tilde{L})]^T$. If the sidelobes of the pulse are very low, $\mathbf{A}_I\mathbf{s}_I(i)$ can be treated as noise and (3.15) can be written as

$$\mathbf{y}(i) = \mathbf{A}_P\mathbf{s}_P(i) + \tilde{\mathbf{w}}(i) \ . \tag{3.17}$$

### 3.4.1 Pulse effects

In order to maintain a well conditioned $\mathbf{A}_P$ the correlation coefficient between its columns should be low. Let us further divide the matrix $\mathbf{A}_P$ into $\mathbf{A}_0 = [\mathbf{h}_1(0), \ldots, \mathbf{h}_K(0)]$ and $\mathbf{A}_{-1} = [\mathbf{h}_1(-1), \ldots, \mathbf{h}_K(-1)]$. The elements of $\mathbf{h}_k(0)$ are samples from the decreasing part of the main-lobe of the pulse. On the other hand, the elements of $\mathbf{h}_k(-1)$ are from the increasing part of the main-lobe of the pulse. Thus, the correlation coefficient of $\mathbf{h}_k(0)$ and $\mathbf{h}_m(-1)$ is smaller than the correlation coefficient of $\mathbf{h}_k(0)$ and $\mathbf{h}_m(0)$, or that of $\mathbf{h}_k(-1)$ and $\mathbf{h}_m(-1)$. Thus, we focus on the effects of the pulse on the column correlations within $\mathbf{A}_0$ and $\mathbf{A}_{-1}$.

***Proposition 3.1***: Let $p(t)$ be a Nyquist pulse that is positive within its mainlobe, i.e. $p(t) > 0$ for $t \in (-T_s, T_s)$. We further assume $p(t)$ is an even function with very low sidelobes. For $\tau_{k_1}$ and $\tau_{k_2}$ $(\tau_{k_1} \neq \tau_{k_2})$ in $(0, T_s/P)$, the absolute value of the correlation coefficient between $\mathbf{h}_{k_1}(0)$ and $\mathbf{h}_{k_2}(0)$ is upper bounded as follows:

$$|\mathbf{h}_{k_1}(0), \mathbf{h}_{k_2}(0)\rangle| \leq \frac{E_P + (\tau_{k_2} - \tau_{k_1})p^2(0)}{\sqrt{E_P[E_P + 2(\tau_{k_2} - \tau_{k_1})p^2(0) + 2\Delta t(\tau_{k_2} - \tau_{k_1})^2\|\mathbf{h}'_{k_1}(0)\|_2^2]}} \tag{3.18}$$

where $E_p = \int_{-\infty}^{\infty} p^2(t)dt$, $\Delta t$ is the sampling interval, i.e., $\Delta t = T_s/P$, and $\mathbf{h}'_k(0)$ is

given by

$$\mathbf{h}'_{k_1}(0) = \left[ p'\left(\frac{T_s}{P} - \tau_{k_1}\right), \ldots, p'\left(T_s - \tau_{k_1}\right) \right]^T \ , \tag{3.19}$$

where $p'(t)$ denotes the first order derivative of $p(t)$.

*Proof*: See Appendix III (in section 3.7).

When $P$ is large, the following approximation holds:

$$\|\mathbf{h}'_{k_1}(0)\|_2^2 \Delta t \approx \int_0^{T_s} [p'(t)]^2 dt \ . \tag{3.20}$$

Thus, for fixed $E_p$ and $p(0)$, the correlation coefficient between $\mathbf{h}_{k_1}(0)$ and $\mathbf{h}_{k_2}(0)$ decreases with increasing $\int_0^{T_s} p'^2(t)dt$. It can be shown that the same holds for the correlation coefficient between $\mathbf{h}_{k_1}(-1)$ and $\mathbf{h}_{k_2}(-1)$.

Because $p(t)$ should be a Nyquist pulse with small sidelobes and $p(t) > 0$ for $t \in (-T_s, T_s)$, it should hold that

$$\begin{aligned} &\int_{T_s}^{\tilde{L}T_s} p^2(t)dt + \int_{-\tilde{L}T_s}^{-T_s} p^2(t)dt \leq \epsilon \ , \\ &p(iT_s) = 0 \ , \quad \text{for } i = -\tilde{L}, \ldots, -1, 1, \ldots, \tilde{L} \ , \quad \text{and} \\ &p(t) > 0 \ , \quad \text{for } t \in (-T_s, T_s), \end{aligned} \tag{3.21}$$

where $\epsilon$ is small.

There are additional constraints that the pulse should satisfy, the most important of which is a bandwidth constraint. Most commercial systems, e.g., the IEEE 802.11a, IEEE 802.11b and IEEE 802.11g wireless local area networks (WLANs) [11], are equipped with a spectral mask that dictates the maximum allowable spectrum, or

equivalently, the maximum symbol rate. This leads to a constraint of the form

$$|P(f)|^2 \leq M(f) \qquad \text{for all } f \ , \tag{3.22}$$

where $P(f)$ is the Fourier transform of $p(t)$, and $M(f)$ denotes the spectral mask.

### 3.4.2 Optimum Pulse Design

Based on the above constraints and assuming that $p(t)$ satisfies the conditions of *Proposition 3.1*, the pulse design problem can be expressed as

$$\max \int_0^{T_s} [p'(t)]^2 dt \tag{3.23a}$$

$$\text{subject to} \quad |P(f)|^2 \leq M(f) \ , \quad \text{for all } f \ , \tag{3.23b}$$

$$\int_{T_s}^{\tilde{L}T_s} p^2(t)dt \leq \frac{\epsilon}{2} \ , \tag{3.23c}$$

$$p(iT_s) = 0 \ , \quad \text{for } i = 1, \ldots, \tilde{L} \quad \text{and} \tag{3.23d}$$

$$p(t) > 0 \ , \quad \text{for } t \in [0, T_s) \ . \tag{3.23e}$$

The problem (3.23) is not easy to solve. Next we will take steps towards reformulating it into a convex optimization problem. Let $\mathbf{p} = [p(0), p(T_s/\xi), \ldots, p((L-1)T_s/\xi)]^T$ be a vector containing samples of $p(t)$ taken in $[0, \ \tilde{L}T_s]$, with sampling interval $\Delta\bar{t} = T_s/\xi$, in which case $L = \tilde{L}\xi + 1$ ($\xi$ is the number of samples in each symbol interval). The objective function (3.23a) is equivalent to

$$\max \quad \|\mathbf{\Gamma p}\|_2^2 \ , \tag{3.24}$$

where $\mathbf{\Gamma}$ is of the form

$$\mathbf{\Gamma} = \begin{bmatrix} -1 & 1 & 0 & 0 & 0 & 0 & \dots & 0 \\ 0 & -1 & 1 & 0 & 0 & 0 & \dots & 0 \\ \vdots & \vdots & \ddots & \ddots & \vdots & \vdots & \vdots & \vdots \\ 0 & \dots & 0 & -1 & 1 & 0 & \dots & 0 \end{bmatrix}_{\xi \times L} . \tag{3.25}$$

As $p(t)$ is an even symmetric function, the Fourier transform of $\mathbf{p}$ can be represented as $P(f) = \mathbf{v}^T(f)\mathbf{p}$, where $\mathbf{v}(f) = [1, 2\cos(2\pi f \Delta\bar{t}), \dots, 2\cos(2\pi f(L-1)\Delta\bar{t})]^T$, with power spectral density (PSD) [55] equal to $|\mathbf{v}^T(f)\mathbf{p}|_2^2$. Hence the constraint (3.23b) is equivalent to

$$|\mathbf{v}^T(f)\mathbf{p}|_2^2 \leq M(f) \qquad \text{for all } f \ . \tag{3.26}$$

Because (3.26) involves an infinite number of constraints, we sample $|\mathbf{v}^T(f)\mathbf{p}|_2^2$ in the frequency domain:

$$|\mathbf{v}^T(f_n)\mathbf{p}|_2^2 \leq M(f_n) \quad \text{for all} \quad f_n \in \mathcal{F}^N = \left\{ \frac{n}{2N\Delta\bar{t}} \right\}_{n=0}^{N-1}, \tag{3.27}$$

where $N$ is the number of samples in $[0, 1/(2\Delta\bar{t})]$. In order for (3.27) to be a good approximation of (3.26), $N$ should be on the order of $15L$ [53].

In the discrete-time domain, (3.23c) is equivalent to

$$\mathbf{p}^T Diag\{\mathbf{a_1}\}\mathbf{p} \leq \tilde{\epsilon} \ , \tag{3.28}$$

where $\tilde{\epsilon}$ is small and $\mathbf{a_1} = [0, \dots, 0, 1, \dots, 1]$ with $\xi + 1$ leading zeros.

Define $\mathbf{l}_j = [0, \dots, 0, 1, 0, \dots, 0, ]^T$, with the $j$-th element equal to 1. (3.23d) is

equivalent to

$$\mathbf{l}_j^T \mathbf{p} = 0 \ , \tag{3.29}$$

with the $j = i\xi + 1$. Hence the problem (3.23) can be reformulated as

$$\max_{\mathbf{p}} \quad \|\mathbf{\Gamma p}\|_2^2 \tag{3.30a}$$

$$\text{subject to} \quad |\mathbf{v}^T(f_n)\mathbf{p}|_2^2 \leq M(f_n) \quad \text{for all} \ \ f_n \in \mathcal{F}^N \ , \tag{3.30b}$$

$$\mathbf{p}^T Diag\{\mathbf{a_1}\}\mathbf{p} \leq \tilde{\epsilon} \quad , \tag{3.30c}$$

$$\mathbf{l}_j^T \mathbf{p} = 0 \quad , \quad \text{for } j = i\xi + 1 \ , \ i = 1, \ldots, \tilde{L} \quad \text{and} \tag{3.30d}$$

$$\mathbf{l}_u^T \mathbf{p} > 0 \quad , \quad \text{for } u = 1, \ldots, \xi \ . \tag{3.30e}$$

Since it involves *maximization* of a convex function, (3.30a) is not a convex optimization problem. Letting $\mathbf{G} = \mathbf{p}\mathbf{p}^T$, $\mathbf{G}$ should be a positive semidefinite matrix of rank 1. Problem (3.30) is equivalent to

$$\min_{\mathbf{G}} \quad -Tr\left(\mathbf{G}\mathbf{\Gamma}^T\mathbf{\Gamma}\right) \tag{3.31a}$$

$$\text{subject to} \quad Tr\left(\mathbf{G}\mathbf{v}(f_n)\mathbf{v}^T(f_n)\right) \leq M(f_n) \quad \text{for all} \ \ f_n \in \mathcal{F}^N \ , \tag{3.31b}$$

$$Tr\left(\mathbf{G}Diag\{\mathbf{a_1}\}\right) \leq \tilde{\epsilon} \ , \tag{3.31c}$$

$$Tr\left(\mathbf{G}\mathbf{l}_j\mathbf{l}_j^T\right) = 0 \quad , \quad \text{for } j = i\xi + 1 \ , \ i = 1, \ldots, \tilde{L} \ , \tag{3.31d}$$

$$Tr\left(\mathbf{G}\mathbf{l}_u\mathbf{l}_v^T\right) > 0 \quad , \quad \text{for } u = 1, \ldots, \xi \ , \ v = 1, \ldots, \xi \ , \tag{3.31e}$$

$$\mathbf{G} \succeq 0 \ \ \text{and} \tag{3.31f}$$

$$rank(\mathbf{G}) = 1 \ . \tag{3.31g}$$

However the constraint of (3.31g) is not a convex constraint. By dropping it, we obtain a semidefinite relaxation of the primal problem [54]. The resulting convex optimization problem is

$$\min_{\mathbf{G}} \quad -Tr\left(\mathbf{G}\mathbf{\Gamma}^T\mathbf{\Gamma}\right) \tag{3.32a}$$

$$\text{subject to} \quad Tr\left(\mathbf{G}\mathbf{v}(f_n)\mathbf{v}^T(f_n)\right) \leq M(f_n) \qquad \text{for all} \ \ f_n \in \mathcal{F}^N \ , \tag{3.32b}$$

$$Tr(\mathbf{G}Diag\{\mathbf{a_1}\}) \leq \tilde{\epsilon} \ , \tag{3.32c}$$

$$Tr\left(\mathbf{G}\mathbf{l}_j\mathbf{l}_j^T\right) = 0 \ \ , \quad \text{for } j = i\xi + 1 \ , \ i = 1, \ldots, \tilde{L} \ , \tag{3.32d}$$

$$Tr\left(\mathbf{G}\mathbf{l}_u\mathbf{l}_v^T\right) > 0 \ \ , \quad \text{for } u = 1, \ldots, \xi \ , \ v = 1, \ldots, \xi \text{ and} \tag{3.32e}$$

$$\mathbf{G} \succeq 0 \ . \tag{3.32f}$$

As we drop the constraint $rank(\mathbf{G}) = 1$, the resulting $\mathbf{G}^*$ might not be of unit rank. In this case we apply eigen-decomposition to $\mathbf{G}^*$. Let

$$\mathbf{p}^* = \sqrt{\lambda_1}\mathbf{u}_1 \ , \tag{3.33}$$

where $\lambda_1$ is the largest eigenvalue of $\mathbf{G}^*$ and $\mathbf{u}_1$ is the corresponding eigenvector. As $\mathbf{G}^* \succeq 0$, its eigenvalues $\lambda_\mu \geq 0$ for $\mu \in \{1, \ldots, L\}$. If

$$\lambda_1 \gg \sum_{\mu=2}^{L} \lambda_\mu \ , \tag{3.34}$$

then $\mathbf{p}^*$ can result in a good pulse shape. If $\lambda_1 \gg \sum_{\mu=2}^{L} \lambda_\mu$, then it holds that

$$\|\mathbf{\Gamma}\mathbf{p}^*\|_2^2 \approx Tr\left(\mathbf{G}\mathbf{\Gamma}^T\mathbf{\Gamma}\right) \ , \tag{3.35}$$

which indicates that $\int_0^{T_s}[p'(t)]^2dt$ in problem (3.23) is maximized. Moreover $\mathbf{p}^*$ can guarantee the validity of (3.30b) and (3.30c). Also, if $\lambda_1 \gg \sum_{\mu=2}^{L}\lambda_\mu$ and $\lambda_\mu \geq 0$, then

$$|\mathbf{v}^T(f_n)\mathbf{p}^*|_2^2 \leq \sum_{\mu=1}^{L}\lambda_\mu Tr\left(\mathbf{u}_\mu\mathbf{u}_\mu^T\mathbf{v}(f_n)\mathbf{v}^T(f_n)\right) = Tr\left(\mathbf{G}\mathbf{v}(f_n)\mathbf{v}^T(f_n)\right) \leq M(f_n)\ . \tag{3.36}$$

This indicates that the PSD of $\mathbf{p}^*$ will be under the IEEE 802.11 mask. In the same way, we can prove that

$$\mathbf{p}^{*T}Diag\{\mathbf{a_1}\}\mathbf{p}^* \leq \tilde{\epsilon}\ , \tag{3.37}$$

which further indicates that $\mathbf{p}^*$ has small sidelobes. Moreover $\tilde{\epsilon}$ is small and the validity of (3.37) implies

$$\mathbf{l}_j^T\mathbf{p}^* \approx 0\ , \quad \text{for } j = i\xi + 1\ ,\ i = 1,\ldots,\tilde{L}\ , \tag{3.38}$$

which indicates that, if we sample at intervals $T_s$, the interference from neighboring symbols can be neglected.

If $\lambda_1 \gg \sum_{i=2}^{L}\lambda_i$, then it holds that $\mathbf{G} \approx \mathbf{p}^*\mathbf{p}^{*T}$. Also, (3.32e) requires that the $(u,v)$-th element of $\mathbf{G}$ be greater than zero for $u,v \in 1,\ldots,\xi$. Hence, $\mathbf{p}^*(u) > 0$ or $\mathbf{p}^*(u) \approx 0$ for $u = 1,\ldots,\xi$. Thus, within its mainlobe, $p(t)$ is greater than zero or its amplitude becomes very small.

## 3.5 Simulation Results

### 3.5.1 Pulse design examples

In this section we demonstrate the performance of a pulse designed as described in Section 3.4.2. We take 16 samples per symbol, i.e., $\xi = 16$, and set $\tilde{L} = 4$. Then we obtain $L = \tilde{L}\xi + 1 = 65$ and $N = 15L = 975$ samples in the time and frequency domains, respectively. We take $\tilde{\epsilon}$ to be $3 \times 10^{-5}$. In Fig. 3.1, we show the ratio $\eta = \lambda_1 / \sum_{\mu=2}^{L} \lambda_\mu$ of the resulting matrix $\mathbf{G}^*$ at different symbol rates, where $\lambda_1$ is the largest eigenvalue of $\mathbf{G}^*$. One can see that the smallest $\eta$ is above $10^2$, which means that the condition of (3.34) is satisfied. Therefore, $\mathbf{p}^* = \sqrt{\lambda_1}\mathbf{u}_1$ is a good choice of pulse shape.

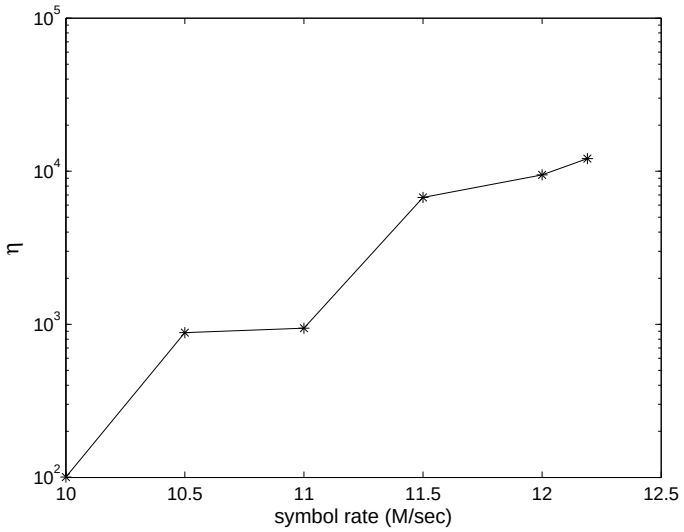


Figure 3.1: Comparison of $\eta$ for different symbol rates.

For symbol rate $10M/sec$, or equivalently, $T_s = 10^{-7} sec$, the designed time domain pulse is shown in Fig. 3.2. For comparison, the IOTA pulse [34] is also shown in the

same figure. The corresponding PSDs, along with the IEEE 802.11 spectral mask are given in Fig. 3.3. From the figures we can see that the proposed pulse decreases faster than the IOTA pulse within $[0, T_s]$. The larger the value of $|p'(t)|$, the faster $p(t)$ decreases. In Fig. 3.3, one can see that the PSD of the proposed pulse is under the 802.11 mask, while the PSD of the IOTA pulse violates the mask at $f = 22$MHz.

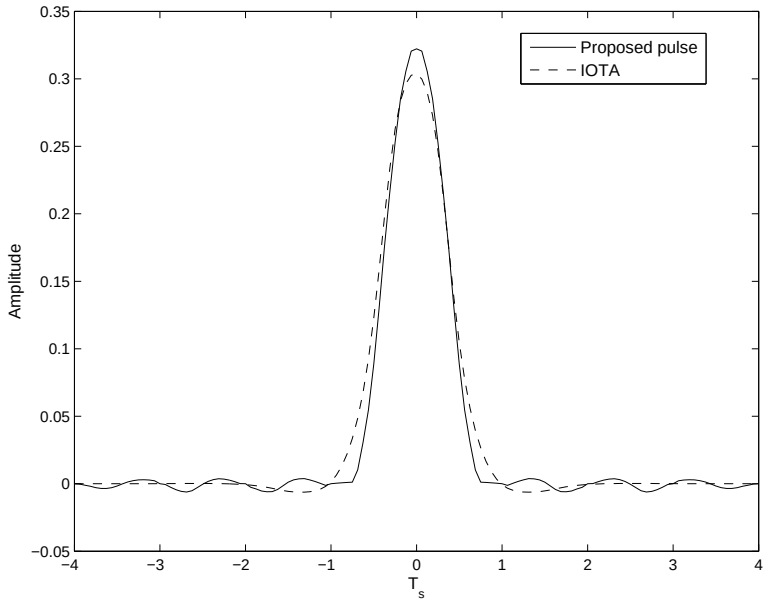


Figure 3.2: Pulse shapes in the time domain for symbol rate 10M/sec.

For symbol rate $12.19M/sec$, or, $T_s = 0.82 \times 10^{-7} sec$, the obtained pulse is given in Figs. 3.4 and 3.5. We also plot the raised cosine pulse with roll off factor equal to 1. One can see that, in the frequency domain, the proposed pulse is under the 802.11 mask, while in the time domain the proposed pulse is narrower. Note that at this symbol rate, the IOTA pulse cannot meet the mask constraint.

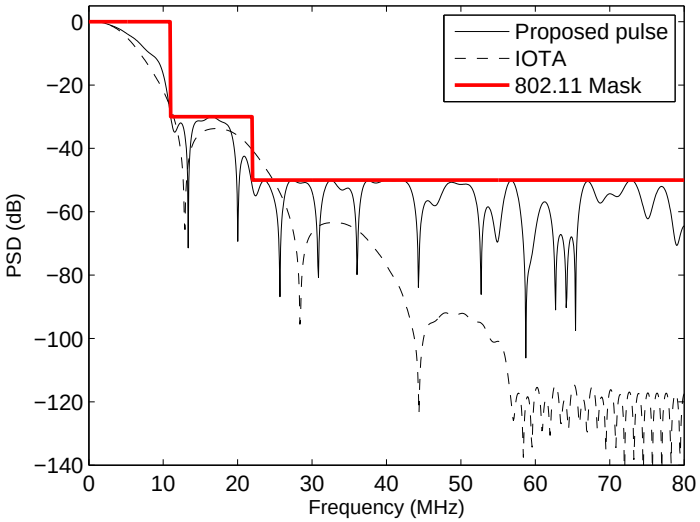


Figure 3.3: Pulse shapes in the frequency domain for symbol rate 10M/sec.

### 3.5.2 SER performance

In this section, we demonstrate the performance of the proposed user separation approach via simulations. We consider a two user system. The channel coefficients $a_1$ and $a_2$ are taken to be zero-mean complex with unit amplitude and phase that is randomly distributed in $[0, 2\pi]$. The CFOs are chosen randomly in the range $\left[0, \frac{0.001}{T_s}\right]$. The input signals are 4-QAM containing 1024 symbols. The estimation results are averaged over 100 independent channels, and 10 Monte-Carlo runs for each channel. One user is intentionally delayed by half a symbol and in addition, small delays, taken randomly from the interval $[-T_s/8, T_s/8]$, are introduced to each user.

In our simulations we combine blind source separation method with SIC [20]. For blind source separation the Joint Approximate Diagonalization of Eigenmatrices (JADE) algorithm was used, which was downloaded from http://perso.telecom-paristech.fr/∼cardoso/Algo/Jade/jade.m. We first apply JADE to decouple the users, and then correct the decoupled users' CFOs. Subsequently, the strongest user, i.e.,

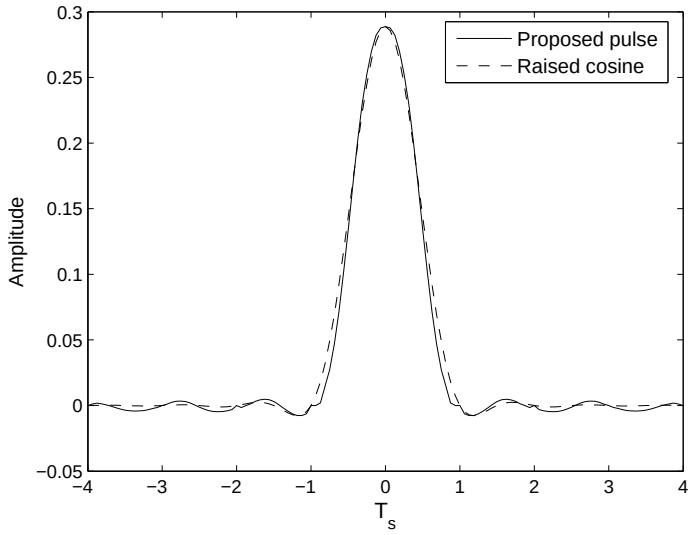


Figure 3.4: Pulse shapes in the time domain for symbol rate 12.19M/sec.

the one which shows the best concentration around the nominal constellation is deflated from the received polyphase components to detect the other user. SIC requires that the first user should be detected very well. To achieve this, the sampling points are chosen around the peak of one user signal, so that ISI and inter-user interference effects are minimized.

Eliminating CFO effects from the decoupled users can be done via a PLL, if the CFO is small, or a PLL initialized with a good CFO estimate, if the CFO is large as the PLL by itself would not converge in this case. For the latter case, since we sample around the peak of one user, the CFO estimation formula of (3.13) requires a small modification before it is applied. Let the $P$ sampling points occur at $\delta_1, \delta_2, \ldots, \delta_P$ and $\mathbf{\Psi}'$ be the phase of the channel matrix corresponding to these sampling points.

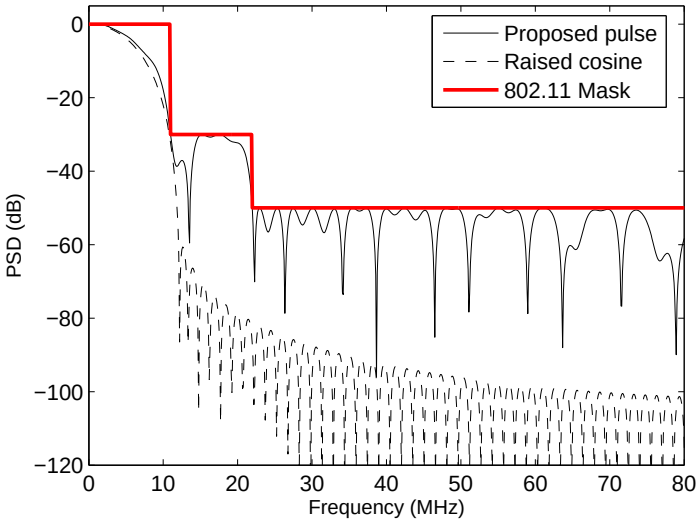


Figure 3.5: Pulse shapes in the frequency domain for symbol rate 12.19M/sec.

The least squares estimate of the CFO $f_{k'}$ can be obtained as

$$\hat{f}_{k'} = \frac{T_s}{2\pi P} \frac{P\left(\sum_{p=1}^{P} \delta_p \Psi'_{p,k'}\right) - \left(\sum_{p=1}^{P} \delta_p\right)\left(\sum_{p=1}^{P} \Psi'_{p,k'}\right)}{P\left(\sum_{p=1}^{P} \delta_p^2\right) - \left(\sum_{p=1}^{P} \delta_p\right)^2}\,, \tag{3.39}$$

where $\Psi'_{p,k'}$ is the $(p,k')$-th element of $\mathbf{\Psi}'$.

In this experiment the pulse has time support $[-4T_s, 4T_s]$. We take $P = 7$ polyphase components of the received symbols, each consisting of samples taken evenly over the interval $[-3T_s/8, 3T_s/8]$, with sampling period $T_s/8$. In order to sample around the peak of one user, we used the true shift values. However, in a realistic scenario this information would be obtained via synchronization pilots [48].

The symbol error rate (SER) performance at $T_s = 10^{-7}$sec, i.e. symbol rate 10 M/sec, and using the waveform of Fig. 3.2, is shown in Fig. 3.6 along with the performance corresponding to the IOTA pulse. We can see that the performance of the proposed pulse is better; there is an approximate 4 dB SNR advantage over the

IOTA result.

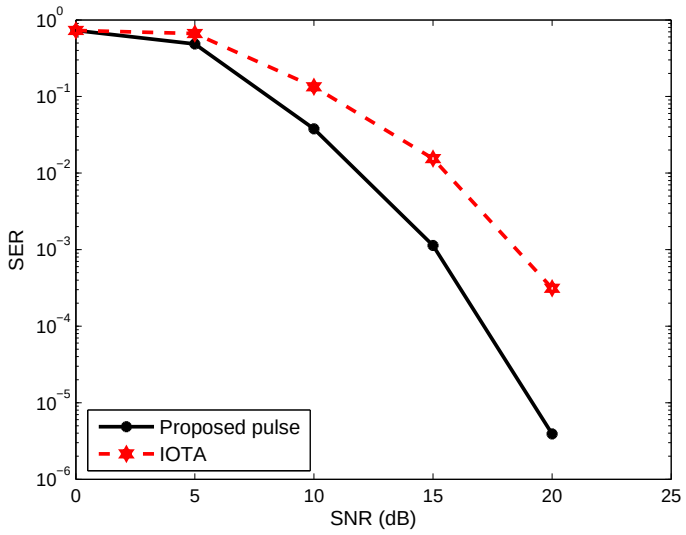


Figure 3.6: SER performance for different pulse shapes for symbol rate 10M/sec, with CFOs randomly chosen within the range $\left[0, \frac{0.001}{T_s}\right]$.

In Fig. 3.7 we show the SER vs. SNR at different symbol rates. First, by taking $T_s = 0.82 \times 10^{-7} sec$, or equivalently symbol rate 12.19 M/sec, we compare the SER performance of the proposed pulses and the raised cosine pulse with roll off factor 1. As we can see, the performance of the proposed pulse is better. For example, the proposed pulse can achieve SER=0.01 at 25 dB SNR, while the raised cosine pulse needs 30dB SNR to achieve the same SER. In the same figure we show the SER performance of the proposed pulse at symbol rate 11M/sec. At this rate, the proposed pulse can achieve an SER of 0.01 at 15dB SNR.

In Fig. 3.8 we show SER performance for different values of the oversampling factor, $P$, at different symbol rates. For $P = 4$, the sampling occurs evenly within the interval $[-3T_s/10, 3T_s/10]$ of each received symbol with sampling period $T_s/5$.

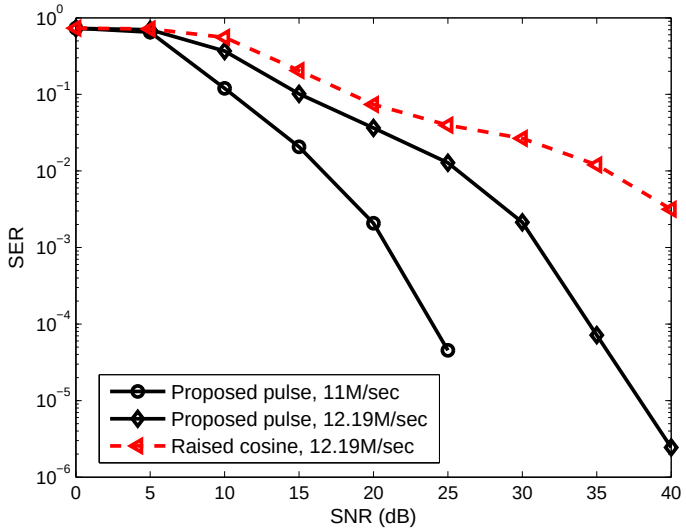


Figure 3.7: SER performance for different pulse shapes and different symbol rates, with CFOs randomly chosen within the range $\left[0, \frac{0.001}{T_s}\right]$.

One can see that for symbol rate 12.19M/sec, when the SNR is higher than 25 dB the SER performance improves by increasing $P$ from 4 to 7. For symbol rates equal to 10M/sec and 11M/sec the SER performance remains almost the same with increasing $P$.

In order to demonstrate the effect of the proposed pulse on the condition number of the system matrix, we show in Fig. 3.9 the condition number of $\mathbf{A}_P$ corresponding to the proposed and IOTA pulses, averaged over 100 random channels realizations and with $P = 4$. In order to make a fair comparison, the CFOs and random delays were set to be the same for both pulses. No noise was added in the data. The estimated $\mathbf{A}_P$'s were collected from the JADE output, and their condition numbers were calculated. One can see that the proposed pulse results consistently in lower condition number than the IOTA pulse.

Next, we show the effect of user delays on performance. As before, one user is

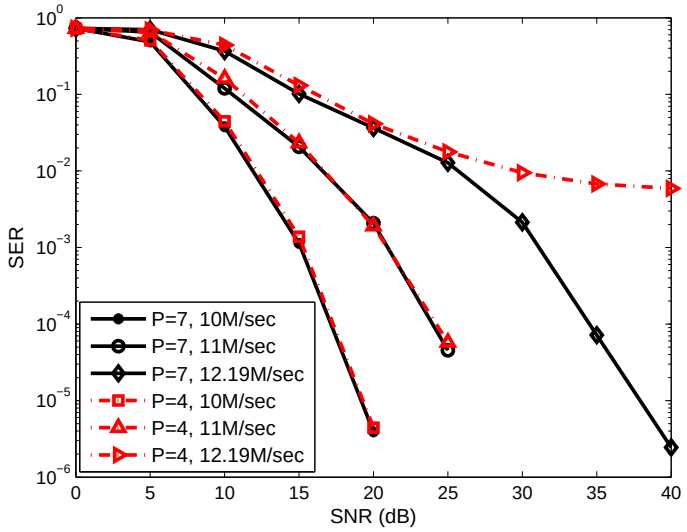


Figure 3.8: SER performance comparison for different oversampling factors $P$, with CFOs randomly chosen within the range $\left[0, \frac{0.001}{T_s}\right]$.

delayed by a half symbol interval, and in addition, a random delay $\tau$ is added to both users to model random delays introduced at the transmitter. In this experiment, the range for the random delay $\tau$ is increased from $[-T_s/8, T_s/8]$ to $[-T_s/5, T_s/5]$. For random delays within $[-T_s/5, T_s/5]$, in order to prevent the delay difference of two users from being too small, we select the delays so that their difference is no less than a threshold $\tau_d = T_s/5$. The resulting SER performance is shown in Fig. 3.10. When the range of $\tau$ increases from $[-T_s/8, T_s/8]$ to $[-T_s/5, T_s/5]$ the performance becomes worse. This is because by increasing the range for the random delay, the signals of the two users overlap by a larger amount, which results in high condition number for the channel matrix $\mathbf{A}$. The best performance would be obtained with just the half symbol delay and no random delays, however, this is not a realistic case.

Next, to show the advantage of the intentional half symbol delay, we consider a case without intentional delay, with random user delays only. The random delays of both

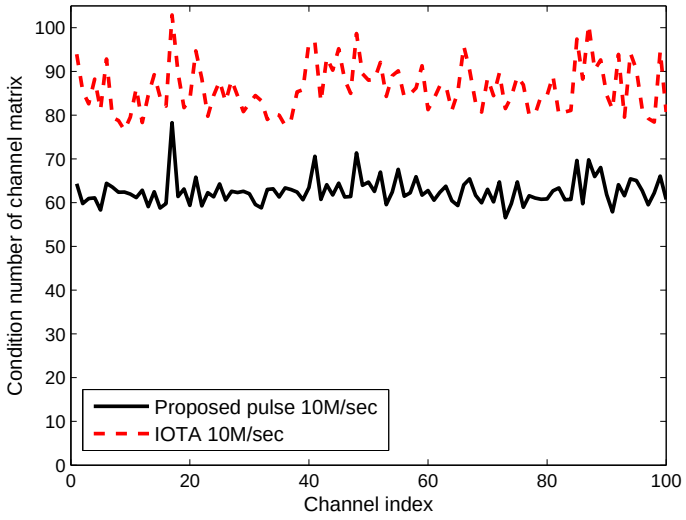


Figure 3.9: Condition number comparison for different pulses, with CFOs randomly chosen within the range $\left[0, \frac{0.001}{T_s}\right]$.

users are taken within $[-T_s/8, T_s/8]$. In order to prevent worsening of performance we restricted the smallest delay difference between two users to be no less than $\tau_d = T_s/5$. In Fig. 3.11 we compare the SER performance of the proposed pulse with IOTA and raised cosine pulses at different symbol rates. Firstly, comparing the corresponding curves in Fig. 3.10 one can first see that without the intentional delay the SER performance decreases. In particular, for the proposed pulse in order to achieve SER 0.01, we need an SNR of 17dB and 30dB for symbol rates 10M/sec and 12.19M/sec respectively. Secondly, the SER performance of the proposed pulse is still better than that of IOTA and raised cosine pulses at the corresponding symbol rate.

Finally, we show the effect of CFOs on performance (see Fig. 3.12). In order to highlight the effect of the CFOs, SER results were obtained without intentional delay, with random delays taken in the interval $[-T_s/8, T_s/8]$ and by setting the delay difference of the two users to be no less than $\tau_d = T_s/5$. The normalized CFOs were

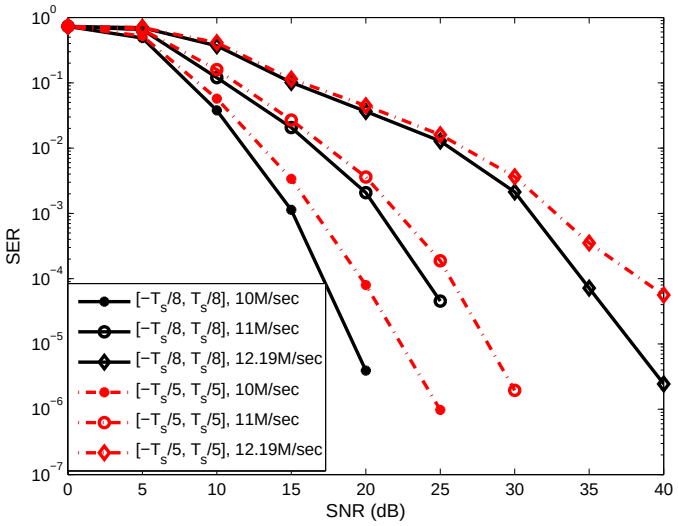


Figure 3.10: SER performance comparison for different amounts of random delays, with CFOs randomly chosen within the range $\left[0, \frac{0.001}{T_s}\right]$.

chosen randomly within the range $[0, CFO_r]$ for $CFO_r = 0.3$ and $CFO_r = 0.001$. For $CFO_r = 0.3$ we restricted the smallest difference between two CFOs to be no less than $CFO_d = 0.1$, and for $CFO_r = 0.001$ we set no threshold on the CFO difference of two users. For $CFO_r = 0.3$, the CFO is quite large, and the PLL by itself is not enough to remove the CFO in the decoupled users. Therefore, we first used the method described in Section 3.3.2 to estimate the CFOs, and then used the PLL to compensate for the residual CFO.

The quality of the CFO estimates depends on the accuracy of the channel matrix estimate. Since low magnitude elements of the channel matrix correspond to low values of the pulse, and as such are susceptible to errors, we set a threshold, $\varphi$, defined as $\varphi = \alpha\|\mathbf{h}_k(l)\|_\infty$, and for CFOs estimation we only use elements of $\mathbf{h}_k(l)$ whose amplitudes are greater than $\varphi$. In this experiment, we took $\alpha = 0.2$. The CFO effects were eliminated via a PLL initialized with the CFO estimate of (3.39). One can

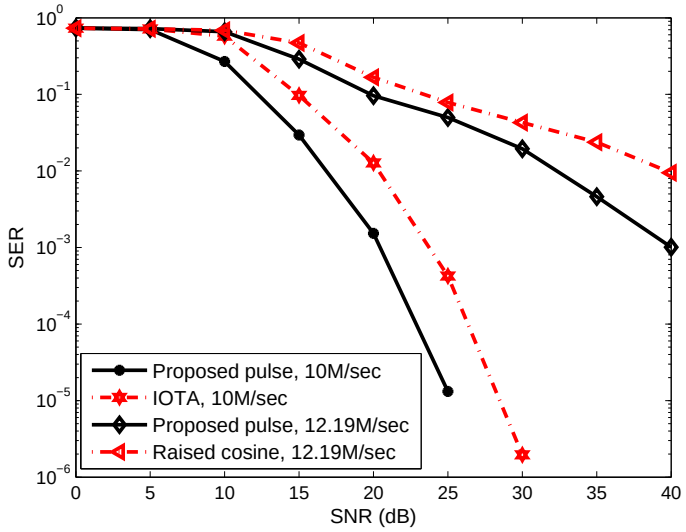


Figure 3.11: SER performance comparison for random delay only at different symbol rates, with CFOs randomly chosen within the range $\left[0, \frac{0.001}{T_s}\right]$.

see that the larger $CFO_r$ gives better performance. It is important to note that the large CFOs involve bandwidth expansion. The percentage of bandwidth expansion can be calculated as $CFO_r/(T_sW)$, where $W = 11$MHz is the bandwidth of the pulse. For $CFO_r = 0.3$ and $T_s = 1/(\text{symbol rate})$, the percentages of bandwidth expansion for symbol rate 10M/sec, 11M/sec and 12.19M/sec are respectively 27.27%, 30% and 33.25%.

## 3.6 Conclusions

A blind two-user separation scheme has been proposed that relies on intentional user delays, optimal pulse shape waveforms design, and also combines blind user separation with SIC. The proposed approach achieves low SER at a reasonable SNR level. Simulation results have confirmed that the proposed pulse design leads to better SER performance than conventional pulse shape waveforms. The intentional

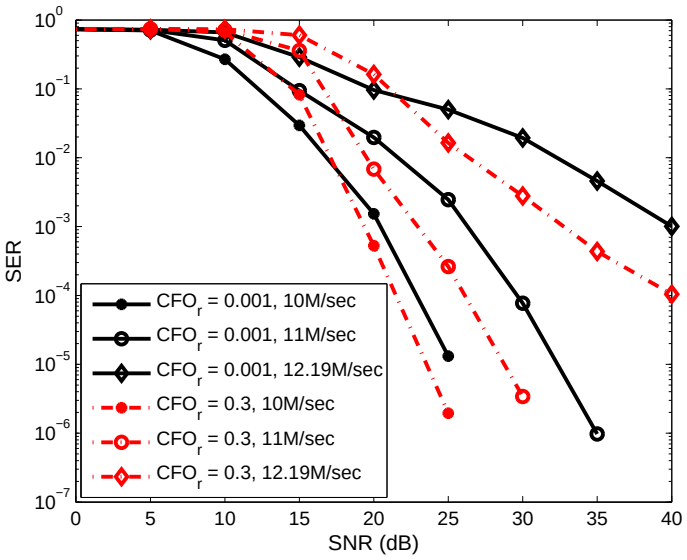


Figure 3.12: SER performance comparison for random delay only and different amounts of CFO.

delay was equal to half a symbol interval, which means that the users still overlap significantly during their transmissions. The use of intentional delay was necessitated by the fact that, although small user delay and CFO differences help preserve the identifiability of the problem, in practice, they may not suffice to separate the users. Also, although the proposed approach can work for any number of users, as the number of users increases, the CFO and delay differences become smaller, which would make the separation more difficult. Based on our experiments, small CFO differences did not affect performance. Although introducing large intentional CFO differences among users could help, that would increase the effective bandwidth. A new ALOHA-type protocol that separates second-order collision based on the ideas described in this chapter, along with a software-defined radio implementation can be found in [48].

## 3.7 Appendix III: Proof of the Proposition 3.1

We have

$$\begin{aligned}\mathbf{h}_{k_1}(0) &= a_{k_1}\left[e^{j2\pi f_{k_1}}p\left(\frac{T_s}{P}-\tau_{k_1}\right),\ldots,e^{j2\pi P f_{k_1}}p(T_s-\tau_{k_1})\right]^T \\ \text{and}\quad \mathbf{h}_{k_2}(0) &= a_{k_2}\left[e^{j2\pi f_{k_2}}p\left(\frac{T_s}{P}-\tau_{k_2}\right),\ldots,e^{j2\pi P f_{k_2}}p(T_s-\tau_{k_2})\right]^T .\end{aligned} \tag{3.40}$$

On letting $2\pi f_{k_1} = w_{k_1}$ and $2\pi f_{k_2} = w_{k_2}$, the correlation between $\mathbf{h}_{k_1}(0)$ and $\mathbf{h}_{k_2}(0)$ is equal to

$$\langle \mathbf{h}_{k_1}(0), \mathbf{h}_{k_2}(0)\rangle = \frac{a_{k_1}a_{k_2}^* \sum_{m=1}^{P} e^{jm(w_{k_1}-w_{k_2})} p\left(\frac{mT_s}{P}-\tau_{k_1}\right) p\left(\frac{mT_s}{P}-\tau_{k_2}\right)}{\|\mathbf{h}_{k_1}(0)\|_2 \|\mathbf{h}_{k_2}(0)\|_2} . \tag{3.41}$$

Taking the absolute value of (3.41) we have

$$|\langle \mathbf{h}_{k_1}(0), \mathbf{h}_{k_2}(0)\rangle| = \frac{|\sum_{m=1}^{P} e^{jm(w_{k_1}-w_{k_2})} p\left(\frac{mT_s}{P}-\tau_{k_1}\right) p\left(\frac{mT_s}{P}-\tau_{k_2}\right)|}{\sqrt{\sum_{m=1}^{P} p^2\left(\frac{mT_s}{P}-\tau_{k_1}\right)\sum_{m=1}^{P} p^2\left(\frac{mT_s}{P}-\tau_{k_2}\right)}} \tag{3.42}$$

$$\leq \frac{\sum_{m=1}^{P} |p\left(\frac{mT_s}{P}-\tau_{k_1}\right) p\left(\frac{mT_s}{P}-\tau_{k_2}\right)|}{\sqrt{\sum_{m=1}^{P} p^2\left(\frac{mT_s}{P}-\tau_{k_1}\right)\sum_{m=1}^{P} p^2\left(\frac{mT_s}{P}-\tau_{k_2}\right)}} \tag{3.43}$$

$$= \frac{\tilde{\mathbf{h}}_{k_1}(0)^T \tilde{\mathbf{h}}_{k_2}(0)}{\|\tilde{\mathbf{h}}_{k_1}(0)\|_2 \|\tilde{\mathbf{h}}_{k_2}(0)\|_2} . \tag{3.44}$$

The last step is due to the fact that $p(t) > 0$ for $t$ within the mainlobe, and that both $\tau_{k_1}$ and $\tau_{k_2}$ are within the interval $(0, T_s/P)$. We also have

$$\begin{aligned}\tilde{\mathbf{h}}_{k_1}(0) &= \left[p\left(\frac{T_s}{P}-\tau_{k_1}\right),\ldots,p\left(T_s-\tau_{k_1}\right)\right]^T \\ \text{and}\quad \tilde{\mathbf{h}}_{k_2}(0) &= \left[p\left(\frac{T_s}{P}-\tau_{k_2}\right),\ldots,p\left(T_s-\tau_{k_2}\right)\right]^T .\end{aligned} \tag{3.45}$$

When the number of samples $P$ is large, $\tau_{k_1}$ and $\tau_{k_2}$ are close. Applying first order

Taylor series expansion to each component of $\tilde{\mathbf{h}}_{k_2}(0)$ we have

$$\begin{aligned} p\left(\frac{T_s}{P}-\tau_{k_2}\right) &= p\left(\frac{T_s}{P}-\tau_{k_1}\right)+p'\left(\frac{T_s}{P}-\tau_{k_1}\right)(\tau_{k_1}-\tau_{k_2})+O(\tau_{k_1}-\tau_{k_2}) \\ &\vdots \\ p\left(T_s-\tau_{k_2}\right) &= p\left(T_s-\tau_{k_1}\right)+p'\left(T_s-\tau_{k_1}\right)(\tau_{k_1}-\tau_{k_2})+O(\tau_{k_1}-\tau_{k_2})\ . \end{aligned} \tag{3.46}$$

On writing

$$\Delta\mathbf{h}=\left[p'\left(\frac{T_s}{P}-\tau_{k_1}\right),\ldots,p'\left(T_s-\tau_{k_1}\right)\right]^T(\tau_{k_1}-\tau_{k_2})\ , \tag{3.47}$$

we can approximate $\tilde{\mathbf{h}}_{k_2}(0)$ by

$$\tilde{\mathbf{h}}_{k_2}(0)\approx\tilde{\mathbf{h}}_{k_1}(0)+\Delta\mathbf{h}\ . \tag{3.48}$$

The correlation between $\mathbf{h}_{k_1}(0)$ and $\mathbf{h}_{k_2}(0)$ is bounded by

$$|\langle\mathbf{h}_{k_1}(0),\mathbf{h}_{k_2}(0)\rangle|\leq\frac{\tilde{\mathbf{h}}_{k_1}(0)^T\tilde{\mathbf{h}}_{k_1}(0)+\tilde{\mathbf{h}}_{k_1}(0)^T\Delta\mathbf{h}}{\|\tilde{\mathbf{h}}_{k_1}(0)\|_2\sqrt{\tilde{\mathbf{h}}_{k_1}(0)^T\tilde{\mathbf{h}}_{k_1}(0)+2\tilde{\mathbf{h}}_{k_1}(0)^T\Delta\mathbf{h}+\Delta\mathbf{h}^T\Delta\mathbf{h}}}\ . \tag{3.49}$$

$\tilde{\mathbf{h}}_{k_1}(0)^T\Delta\mathbf{h}$ can be approximated by

$$\tilde{\mathbf{h}}_{k_1}(0)^T\Delta\mathbf{h}\approx\frac{\tau_{k_1}-\tau_{k_2}}{\Delta t}\int_{\frac{T_s}{P}-\tau_{k_1}}^{T_s-\tau_{k_1}}p(t)p'(t)dt\ , \tag{3.50}$$

where $\Delta t=T_s/P$. Since

$$\begin{aligned} \int_{\frac{T_s}{P}-\tau_{k_1}}^{T_s-\tau_{k_1}}p(t)p'(t)dt &= \int_{\frac{T_s}{P}-\tau_{k_1}}^{T_s-\tau_{k_1}}p(t)dp(t) \\ &= p^2(t)|_{\frac{T_s}{P}-\tau_{k_1}}^{T_s-\tau_{k_1}}-\int_{\frac{T_s}{P}-\tau_{k_1}}^{T_s-\tau_{k_1}}p(t)p'(t)dt\ , \end{aligned} \tag{3.51}$$

we obtain

$$\int_{\frac{T_s}{P}-\tau_{k_1}}^{T_s-\tau_{k_1}} p(t)p'(t)dt = \frac{1}{2}\left[p^2\left(T_s-\tau_{k_1}\right) - p^2\left(\frac{T_s}{P}-\tau_{k_1}\right)\right]. \tag{3.52}$$

On substituting (4.5) into (3.50), we have

$$\begin{aligned}\mathbf{h}_{k_1}(0)^T\Delta\mathbf{h} &\approx \frac{\tau_{k_1}-\tau_{k_2}}{2\Delta t}\left[p^2\left(T_s-\tau_{k_1}\right) - p^2\left(\frac{T_s}{P}-\tau_{k_1}\right)\right] \\ &\approx \frac{\tau_{k_2}-\tau_{k_1}}{2\Delta t}p^2(0)\ .\end{aligned} \tag{3.53}$$

In the last step of (4.6), we assumed that $P$ is large and $\tau_k$ and $\tau_l$ are small, and also that $p(T_s) = 0$.

In the same way $\tilde{\mathbf{h}}_{k_1}(0)^T\tilde{\mathbf{h}}_{k_1}(0)$ can be approximated as

$$\tilde{\mathbf{h}}_{k_1}(0)^T\tilde{\mathbf{h}}_{k_1}(0) \approx \frac{1}{\Delta t}\int_0^{T_s} p^2(t)dt\ . \tag{3.54}$$

Because $p(t)$ is an even function and also has very low sidelobes, (3.54) can be further simplified as

$$\tilde{\mathbf{h}}_{k_1}(0)^T\tilde{\mathbf{h}}_{k_1}(0) \approx \frac{1}{2\Delta t}\int_{-\infty}^{\infty} p^2(t)dt = \frac{E_p}{2\Delta t}\ . \tag{3.55}$$

Substituting (4.6) and (3.54) into (3.49), we have

$$\begin{aligned}|\mathbf{h}_{k_1}(0), \mathbf{h}_{k_2}(0)\rangle| &\le \frac{E_P + (\tau_{k_2}-\tau_{k_1})p^2(0)}{\sqrt{E_P[E_P + 2(\tau_{k_2}-\tau_{k_1})p^2(0) + 2\Delta t\|\Delta\mathbf{h}\|_2^2]}} \\ &= \frac{E_P + (\tau_{k_2}-\tau_{k_1})p^2(0)}{\sqrt{E_P[E_P + 2(\tau_{k_2}-\tau_{k_1})p^2(0) + 2\Delta t(\tau_{k_2}-\tau_{k_1})^2\|\mathbf{h}'_{k_1}(0)\|_2^2]}}\ .\end{aligned} \tag{3.56}$$

In this last step we let

$$\mathbf{h}'_{k_1}(0) = \left[ p'\left(\frac{T_s}{P} - \tau_{k_1}\right), \ldots, p'(T_s - \tau_{k_1}) \right]^T . \tag{3.57}$$

# 4. Delay Analysis for Random Scheduling in Centralized Wireless Networks

## 4.1 Introduction

We consider a centralized network scheme, in which all nodes communicate with a BS and the communication occurs in a time slotted fashion. The BS can resolve simultaneous transmissions of multiple users. We consider the general multi-packet reception case, i.e. the success probability of a node varies depending on which nodes transmit along with that node. The same scenario operating under the ALOHA protocol, i.e., each node transmitting with a fixed probability and the BS having multi-packet reception capability, was employed in [31], where the stability region and delay were analyzed. In this chapter we consider the problem of scheduling of nodes that will transmit simultaneously. In particular, we consider an RS scheme. In RS, once the scheduling probability is calculated by the BS, for each time slot the scheduling decision is made independently at each node. Thus, unlike maximum weigh scheduling (MWS) [60, 61], there is no need to exchange scheduling information between BS and the mobile nodes in each slot, nor is global knowledge of the queueing length in the entire network required.

### 4.1.1 Main contribution

The main contributions of this chapter are:

- Assuming the success probability of transmissions is always 1, we provide a lower bound on the delay performance for an arbitrary scheduling policy.
- For the cases in which the success probability of transmissions is not always 1, we propose a convex optimization formulation that can minimize an upper bound

of the expected delay by determining the optimal scheduling probability of each node. Also the optimization formulation guarantees that RS can stabilize any packet arrival rate within the stability region.

- We develop an approximate expression and a lower bound for the expected delay of RS for the case in which two users can transmit simultaneously.

### 4.1.2 Related work

The MWS approach [60] has received a lot of attention. In any given time slot, MWS schedules a set of links that can be scheduled simultaneously with the longest accumulated queuing length. The scheduling should satisfy the interference and conflict requirements and the weighted sum of the queueing length of the chosen set should be the largest among all such sets. MWS is throughput optimal and can achieve the stability region of a system. The delay property of MWS is studied in [59, 61]. To combat the high computational complexity of MWS, approximations were proposed in [62]. MWS and its approximations require knowledge of queueing length of the entire network, which is hard to expect in a real implementation.

The fundamental lower bounds on the delay for single hop networks can be found in [59, 61]. In [61], the delay lower bound is based on the concept of exclusive sets, i.e., sets of links in which no more than one link can be scheduled at any given slot. This is realistic in single hop networks, e.g. a node cannot both transmit and receive in a single time slot. However in a centralized network we do not have such constraints. In the perfect reception case, we assume any $n$ nodes can transmit simultaneously and the transmitted messages can be received with probability 1. The delay lower bound for arbitrary policy derived in [59] is independent of the pack arrival rate.

The throughput analysis of RS with multi-packet reception capability can be found in [63, 64]. It is shown in [63, 64] that RS can achieve the stability region of a gen-

eralized wireless network with multi-packet reception capability. However, the delay property was not considered in [63, 64]. Moreover, in the application section of [63, 64], the authors analyzed the capacity of the Manhattan network and ring topology network by assuming that either the success probability of a node depends only on the cardinality of the transmission set, or the success probability of a node, when it transmit along with different nodes, is either 1 or 0. Throughput maximization with delay constraints was proposed in [67]; that work did not consider any multi-packet reception capability. The stability region and delay of ALOHA with multi-packet reception can be found in [31]. However, an ALOHA network cannot achieve the stability region of the centralized network when the total number of users is more than 2. The delay analysis in [31] was restricted to the two user case only.

### 4.1.3 Organization

The rest of this chapter is organized as follows. The system model is introduced in Section 4.2. In Section 4.3 a convex formulation of the delay minimization for RS is proposed and a fundamental lower bound on the delay performance of arbitrary policy is proved for the case in which the success probability of each node is always 1. In Section 4.4 we extend this delay minimization problem to the more realistic case in which the success probability of a node varies when the nodes transmits together with other nodes (general multi-packet reception case). An approximation and a lower bound on the delay performance of RS are developed by assuming that two users can transmit simultaneously. Some numerical examples are given in Section 4.5 and conclusions are drawn in Section 4.6.

## 4.2 System model

Suppose there are $N$ users in a centralized wireless network, and let $S_m$, $m = 1, \ldots, M$ denote independent sets of those users which can transmit simultaneously with high success probability. In each time slot, the nodes with non-empty transmission queue within $S_m$ will be selected to transmit, while other nodes remain silent. This can be achieved in a non-centralized fashion as follows [64, 66]. All nodes have the same random number generator "seed". At the beginning of a time slot, each node generates a random number, i.e., $u$. Note that this number will be the same for all nodes since all nodes are using the same seed. Assume that the probability of selecting $S_m$ is $p_m$ (the way to determine $p_m$ will be described later). If $u < p_1$, the nodes in $S_1$ will transmit; if $\sum_{l=1}^{m-1} p_l \leq u < \sum_{l=1}^{m} p_l$, $m > 1$, the nodes in $S_m$ will transmit. After that all the nodes update their seed simultaneously.

In this chapter we make following assumptions:

- **A1**) The packet will arrive at the beginning of time slot and leave and the end of time slot. There is at most one arrival or departure per time slot for each node.

- **A2**) The queue size at slot $t$ is measured after the arrival and before the departure.

- **A3**) Packets are eligible for transmission in the same time slot in which they arrive.

- **A4**) Both the arrivals and the departures are Bernoulli distributed.

- **A5**) The success probability of a node varies depending on which other nodes transmit at the same time.

- **A6**) For the simultaneous transmission of multiple users, the success of a user's transmission is independent of the transmission outcome of other users.

## 4.3 Delay minimization with perfect reception

In this section we will determine the scheduling probability of $S_m$ to minimize the expected delay of the packets. We start with the simplest possible case in which the BS can support simultaneous transmission of two users and in which the packets can be correctly received with probability 1 (perfect packet reception). The imperfect reception case will be discussed in Section 4.4.

Let $r_i$ denote the packet arrival rate of node $i$, and $q_i$ the probability of departure (i.e. successful transmission) of node $i$ when node $i$ is active. The network can support simultaneous transmission of $n \geq 2$ users, where $n$ is the maximum number of simultaneous transmissions allowed. The success probability for the $n$ users is 1. In this case the number of independent sets is $M = \binom{N}{n}$. Let $\mathbf{p} = [p_1, \ldots, p_M]^T$, where $p_m$ denotes the probability of choosing the set $S_m$, and $\mathbf{c}_m$ the indicator vector of $S_m$, i.e. if $i \in S_m$, the $i$-th component of $\mathbf{c}_m$ is 1; otherwise it is 0. There are exactly $n$ components equal to 1 in each $\mathbf{c}_m$. The delay optimization problem can be expressed as

$$\min_{\mathbf{p},\mathbf{q}} f(\mathbf{q}) = \frac{1}{\sum_{i=1}^{N} r_i} \sum_{i=1}^{N} \frac{r_i(1-r_i)}{q_i - r_i} \tag{4.1a}$$

$$\text{subject to} \quad q_i > r_i \quad , \quad \text{for } i = 1, 2, \ldots, N \ , \tag{4.1b}$$

$$\mathbf{q} = \sum_{m=1}^{M} p_m \mathbf{c_m} \ , \tag{4.1c}$$

$$\mathbf{1}^T \mathbf{p} = 1 \ , \tag{4.1d}$$

$$0 \leq p_m \leq 1 \quad , \quad \text{for } m = 1, 2, \ldots, M \ . \tag{4.1e}$$

The stability region discussion of a generalized wireless network with multi-packet

reception can be found in [64]. From the discussion of [64] we can see that the feasible region of the this convex optimization method given by (4.1b)-(4.1e) guarantees that RS can stabilize any packet arrival rate within the stability region.

### 4.3.1 Lower bound for any policy

***Proposition 4.1***: In a centralized network of $N$ users, in which the BS can support simultaneous transmissions of $n$ users, the expected delay of an arbitrary policy is lower bounded as follows:

$$\frac{\sum_{i=1}^{N} r_i - r_i^2}{2\sum_{i=1}^{N} r_i \left(n - \sum_{i=1}^{N} r_i\right)} \ . \tag{4.2}$$

*Proof*: See Appendix IV (in section 4.7).

Please note that this lower bound for an arbitrary policy is different from that proposed in [59, 61]. Here, we consider a centralized network and any $n$ users can transmit simultaneously. Unlike [61], for each link $l$ we do not have a exclusive set $\chi_l$ in which no more than one link can be scheduled at any given slot. The above lower bound depends on the packet arrival rate $r_i$, whereas the bound of [59] does not.

## 4.4 Delay minimization with imperfect reception

Next, we consider a more realistic case, in which the success probability of the simultaneously transmissions is not always 1. We assume that the BS can support simultaneous transmissions of $n = 2$ users. Let $P_{i,j}$ be the probability of scheduling nodes $i$ and $j$, and $P_{i,i}$ the probability of scheduling node $i$ only. Let $B_{i,j}$ be the $(i, j)$-th element of $\mathbf{B}$, denoting the success probability of node $i$ when node $i$ and $j$ transmit simultaneously and $B_{i,i}$ be the success probability of node $i$, when only node $i$ transmits. We assume $B_{i,i} > B_{i,j}$, since without interference from node $j$ the

success probability of node $i$ should be higher. The probability of success of node $i$ can be approximated as:

$$q_i \approx \sum_{j=1}^{N} B_{i,j} P_{i,j} \tag{4.3}$$

which is an underestimate of the actual success probability. To see why, suppose that in some slot, nodes $i$ and $j$ were selected to transmit, but the transmission queue of node $j$ is empty. In that case, node $j$ would remain silent and only node $i$ would transmit. Then, the success probability of node $i$ would $B_{i,i}$ instead of $B_{i,j}$. Hence (4.3) is an underestimate of the success probability of node $i$.

The delay minimization problem can be formulated as

$$\min_{\mathbf{P},\mathbf{q}} f(\mathbf{q}) = \frac{1}{\sum_{i=1}^{N} r_i} \sum_{i=1}^{N} \frac{r_i(1-r_i)}{q_i - r_i} \tag{4.4a}$$

$$\text{subject to} \quad q_i > r_i \quad , \quad \text{for } i = 1, 2, \ldots, N \ , \tag{4.4b}$$

$$q_i \leq 1 \quad , \quad \text{for } i = 1, 2, \ldots, N \ , \tag{4.4c}$$

$$\sum_{j=1}^{N} B_{i,j} P_{i,j} = q_i \quad \text{for } i = 1, 2, \ldots, N \ , \tag{4.4d}$$

$$\sum_{i=1}^{N} \sum_{j=i}^{N} P_{i,j} = 1 \ , \tag{4.4e}$$

$$0 \leq P_{i,j} \leq 1 \quad , \quad \text{for } i = 1, 2, \ldots, N \ , j = 1, 2, \ldots, N \tag{4.4f}$$

$$P_{i,j} = P_{j,i} \quad , \quad \text{for } i = 1, 2, \ldots, N \ , j = 1, 2, \ldots, N \tag{4.4g}$$

By solving this problem we can get the optimal scheduling probability of each independent set, which can minimize the delay of packets in the network. It is worthwhile to note that although the BS can support simultaneous transmission of two users,

it is not necessary that we have to schedule two users for every slot. If the success probability of simultaneous transmissions of two users is low, we should schedule only one user in each slot.

### 4.4.1 Approximation for the delay

In this section we introduce an approximation for the packet delay of RS. Eq. (4.3) gives a lower bound of the success probability of node $i$ by assuming that the nodes are always active. Let $k_i$ be the active probability of node $i$. The success probability of node $i$ can be approximated as

$$q_i \approx \left( \sum_{j=1, j\neq i}^{N} B_{i,j} P_{i,j} k_j + B_{i,i} P_{i,j} (1 - k_j) \right) + B_{i,i} P_{i,i} \ . \tag{4.5}$$

At the same time, if the queues are stable, we have $r_i = k_i q_i$. Let

$$g_i = k_i \left( \left( \sum_{j=1, j\neq i}^{N} B_{i,j} P_{i,j} k_j + B_{i,i} P_{i,j} (1 - k_j) \right) + B_{i,i} P_{i,i} \right) - r_i \ , \tag{4.6}$$

By solving $g_i = 0$ for $i = 1, \ldots, N$ we can calculate the active probability $k_i$. The schedule probability $P_{i,j}$ and $P_{i,i}$ are obtained by solving the optimization problem (4.4). After calculating the active probability $k_i$, we can obtain $q_i$ based on $q_i = r_i/k_i$. The packet delay equals $D = \sum_i^N r_i D_i / \left( \sum_i^N r_i \right)$, where $D_i = (1 - r_i)/(q_i - r_i)$.

For $N = 2$, we can prove that there is only one solution for $k_i$ within the region $[0, 1]$ (see appendix 4.8). For $N > 2$, it is hard to prove theoretically that there is only one solution for $k_i$ within the region $[0, 1]$. We can use numerical methods such as trust-region methods [65] to solve the equation. It is interesting to note that we will always get the same solution if the initial values for $k_i$ is chosen within the region $[0, 1]$. In section 4.5 from simulation results we can observe that the approximated delay is very close to the expected delay.

### 4.4.2 The delay lower bound of RS for the imperfect reception case

In this section we will derive a lower bound for the expected delay of RS by assuming that two users can transmit simultaneously.

Let $\mathbf{b}_m = [b_{1|m}, \ldots, b_{N|m}]^T$, where $b_{i|m}$ is the success probability of node $i$ if $i \in S_m$, when the nodes within $S_m$ transmit simultaneously. If $i \notin S_m$, $b_{i|m} = 0$. Let $p_m$ be the probability that we schedule the independent set $S_m$; and define $p_{\{\cdot\}} = p_m|_{S_m=\{\cdot\}}$ and $\mathbf{b}_{\{\cdot\}} = \mathbf{b}_m|_{S_m=\{\cdot\}}$. According to this definition $p_{\{i,j\}}$ is the probability that we schedule nodes $i$ and $j$; $\left\|\mathbf{b}_{\{i\}}\right\|_1$ is the success probability of node $i$ when only node $i$ transmits and $\left\|\mathbf{b}_{\{i,j\}}\right\|_1$ is the sum of the success probability of node $i$ and $j$, when these two nodes transmit simultaneously. We further assume that the success probabilities for the simultaneous transmission of two nodes are high, i.e.,

- **A7**) $\left\|\mathbf{b}_{\{i\}}\right\|_1 < \left\|\mathbf{b}_{\{i,j\}}\right\|_1$ for $i, j = 1, \ldots, N$ and $i \neq j$.

The assumption (**A7**) indicates that success probability of node $i$ when only node $i$ transmits is smaller than the sum of the success probability of node $i$ and $j$ when these two nodes transmit simultaneously.

Before we start to derive the lower bound, we introduced three basic constraints that have to be satisfied by a stable queue.

$$r_i \leq \sum_{i \in S_m} p_m \left\|\mathbf{b}_{\{i\}}\right\|_1 \text{ for } i = 1 \ldots N \tag{4.7}$$

$$r_i + r_j \leq p_{\{i,j\}} \left\|\mathbf{b}_{\{i,j\}}\right\|_1 + \left(\sum_{i \in S_m} p_m - p_{\{i,j\}}\right) \left\|\mathbf{b}_{\{i\}}\right\|_1 + \left(\sum_{j \in S_m} p_m - p_{\{i,j\}}\right) \left\|\mathbf{b}_{\{j\}}\right\|_1 \text{for } i, j = 1 \ldots N \text{ and } i \neq j \ . \tag{4.8}$$

$$\sum_{i=1}^{N} r_i \leq \sum_{m=1}^{M} p_m \left\|\mathbf{b}_m\right\|_1 \tag{4.9}$$

(4.7) is the requirement for the packet arrival rate of node $i$. The success prob-

ability of node $i$ when only node $i$ transmits is $\left\|\mathbf{b}_{\{i\}}\right\|_1$. The success probability of node $i$ will decrease if node $i$ and $j$ transmit simultaneously. Therefore if queue $i$ is stable, (4.7) has to be satisfied.

(4.8) is the sum rate requirement for node $i$ and $j$. Because of assumption (**A7**), if we schedule node $i$ and $j$, the sum of the departure rates of nodes $i$ and $j$ cannot be greater than $\left\|\mathbf{b}_{\{i,j\}}\right\|_1$; if either node $i$ or $j$ does not transmit, the sum of the departure rates will only decrease. If we schedule node $i$ and $l$, $l \neq j$, the "best" case for node $i$ is for $l$ to keep silent and only node $i$ to transmit. In this case, the success probability of node $i$ is $\left\|\mathbf{b}_{\{i\}}\right\|_1$.

(4.9) is the sum rate requirement. Because of assumption (**A7**), if we schedule nodes within $S_m$, the largest possible expected sum of delivered rate is $\|\mathbf{b}_m\|_1$. Given that $p_m$ is the probability of scheduling $S_m$, the total throughput of this system cannot exceed $\sum_{m=1}^{M} p_m \|\mathbf{b}_m\|_1$. In order to maintain the stability of the system, (4.7), (4.8) and (4.9) are necessary but not sufficient.

With these two restrictions we derived the lower bound of expected delay for RS, which is given in *proposition 2*.

***Proposition 4.2***: In a centralized network of totally $N$ users, if we allow two users to transmit simultaneously, the expected delay of RS is no smaller than $max(f_1^*, f_2^*)$. $f_1^*$ is the the optimal value of the problem

$$\min_{\mathbf{p},\mathbf{q}} f_1(\mathbf{q}) = \frac{1}{\sum_{i=1}^{N} r_i} \sum_{i=1}^{N} \frac{r_i(1-r_i)}{q_i - r_i} \tag{4.10a}$$

$$\text{subject to} \quad q_i \geq r_i \quad , \quad \text{for } i = 1, 2, \ldots, N \ , \tag{4.10b}$$

$$q_i = \sum_{i \in S_m} p_m \left\|\mathbf{b}_{\{i\}}\right\|_1 , \ \text{for } i = 1, 2, \ldots, N \ , \tag{4.10c}$$

$$r_i + r_j \leq p_{\{i,j\}} \left\|\mathbf{b}_{\{i,j\}}\right\|_1 + \left(\sum_{i \in S_m} p_m - p_{\{i,j\}}\right) \left\|\mathbf{b}_{\{i\}}\right\|_1 + \left(\sum_{j \in S_m} p_m - p_{\{i,j\}}\right) \left\|\mathbf{b}_{\{j\}}\right\|_1 \text{for } i,j = 1 \ldots N \text{ and } i \neq j \ , \tag{4.10d}$$

$$\sum_{i=1}^{N} r_i \leq \sum_{m=1}^{M} p_m \left\|\mathbf{b}_m\right\|_1 \tag{4.10e}$$

$$\mathbf{1}^T \mathbf{p} = 1 \ , \tag{4.10f}$$

$$0 \leq p_m \leq 1 \quad , \quad \text{for } m = 1, 2, \ldots, M \ . \tag{4.10g}$$

$$f_2^* = \frac{\sum_{i=1}^{N} r_i - r_i^2}{2 \sum_{i=1}^{N} r_i \left(U^* - \sum_{i=1}^{N} r_i\right)} \ , \tag{4.11}$$

where $U^*$ is the optimal value of the optimization problem

$$\max_{\mathbf{p},\mathbf{q}} U = \sum_{m=1}^{M} p_m \left\|\mathbf{b}_m\right\|_1 \tag{4.12a}$$

$$\text{subject to} \quad q_i \geq r_i \quad , \quad \text{for } i = 1, 2, \ldots, N \ , \tag{4.12b}$$

$$q_i = \sum_{i \in S_m} p_m \left\|\mathbf{b}_{\{i\}}\right\|_1 , \ \text{for } i = 1, 2, \ldots, N \ , \tag{4.12c}$$

$$r_i + r_j \leq p_{\{i,j\}} \left\|\mathbf{b}_{\{i,j\}}\right\|_1 + \left(\sum_{i \in S_m} p_m - p_{\{i,j\}}\right) \left\|\mathbf{b}_{\{i\}}\right\|_1 + \left(\sum_{j \in S_m} p_m - p_{\{i,j\}}\right) \left\|\mathbf{b}_{\{j\}}\right\|_1 \text{for } i,j = 1 \ldots N \text{ and } i \neq j \ , \tag{4.12d}$$

$$\sum_{i=1}^{N} r_i \leq \sum_{m=1}^{M} p_m \left\|\mathbf{b}_m\right\|_1 \tag{4.12e}$$

$$\mathbf{1}^T\mathbf{p} = 1 \ , \tag{4.12f}$$

$$0 \leq p_m \leq 1 \quad , \quad \text{for } m = 1, 2, \ldots, M \ . \tag{4.12g}$$

*Proof*: See Appendix VI (in section 4.9).

### 4.4.3 Extension to the general multi-packet reception with imperfect reception

In this section we will expand our discussion to the cases in which the BS can resolve $n > 2$ simultaneous transmissions, where $n$ is the maximum number of simultaneous transmissions that the BS can support. We use $S_m$ to denote the independent set $m$, where $m = 1, \ldots, M$ and $M = \sum_{l=1}^{n} \binom{N}{l}$. $M$ is the total number of independent sets. $\mathbf{b}_m = [b_{1|m}, \ldots, b_{N|m}]^T$, is the success probability vector defined in Section 4.4.2. Moreover, if $S_{m'} \subset S_m$ and $S_{m'} \neq \emptyset$, for any $j \in S_{m'}$ it holds that $b_{j|m'} \geq b_{j|m}$. $S_{m'} \subset S_m$ means there are fewer nodes in set $S_{m'}$ than in $S_m$. Therefore, if the nodes in $S_{m'}$ transmit simultaneously, for each node the mutual interference is smaller than that in $S_m$, which leads to the higher success probability of the nodes in $S_{m'}$.

The delay minimization problem is formulated as

$$\min_{\mathbf{p},\mathbf{q}} f(\mathbf{q}) = \frac{1}{\sum_{i=1}^{N} r_i} \sum_{i=1}^{N} \frac{r_i(1 - r_i)}{q_i - r_i} \tag{4.13a}$$

$$\text{subject to} \quad q_i > r_i \quad , \quad \text{for } i = 1, 2, \ldots, N \ , \tag{4.13b}$$

$$\mathbf{q} = \sum_{m=1}^{M} p_m \mathbf{b}_m \ , \tag{4.13c}$$

$$\mathbf{1}^T\mathbf{p} = 1 \ , \tag{4.13d}$$

$$0 \leq p_m \leq 1 \quad , \quad \text{for } m = 1, 2, \ldots, M \ . \tag{4.13e}$$

It is worthwhile to note that $\mathbf{q} = \sum_{m=1}^{M} p_m \mathbf{b}_m$ is an underestimate of the success probability of the nodes. As explained before, when $S_m$ is scheduled, the nodes $i \in S_m$ might be inactive, therefore node $i$ will not transmit. In this case the success probability of an active node $j \in S_m$ should be higher than $b_{j|m}$. Hence (4.13) minimizes the upper bound of the packet delay.

From the stability region analysis of [64], we can see that the feasible set of this convex optimization given by (4.13b)-(4.13e) guarantees that the proposed RS can stabilize any packet arrival rate in the stability region. Therefore the proposed RS achieves the stability region of the centralized system.

## 4.5 Simulation

### 4.5.1 Perfect reception

First we show the performance of the lower bound on the delay of any policy proposed in *proposition 1* by comparing it with the simulation results of MWS and RS. The number of users in the network was set to $N = 5$ and the BS can support simultaneous transmissions of $n = 2$ users. The lower bound for the delay performance of any policy proposed in *proposition 1* is given in Fig. 4.1. In the same figure we plot the delay performance of RS and MWS for comparison. We observe that the lower bound of the arbitrary policy is tight and the delay performance of MWS is close to that bound. We can see a similar trend by increasing the total number of users $N$ to 12 and the allowable simultaneous transmission $n$ to 3. We should note that MWS requires the queueing length of every node in the network; moreover the BS and the nodes need to exchange scheduling information in every slot.

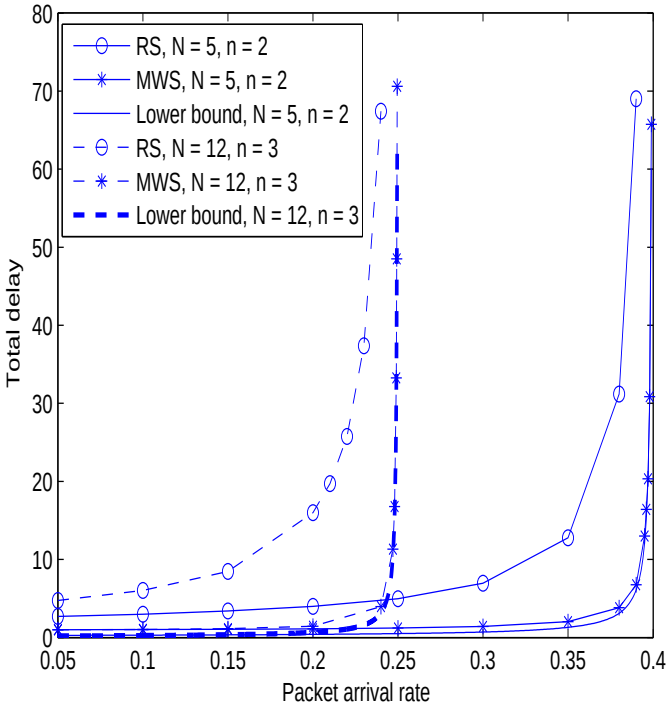


Figure 4.1: The lower bound performance of any policy.

### 4.5.2 Imperfect reception

#### Symmetric case

In this section we demonstrate the validity of the approximation of Section 4.4.1 and the lower bound of RS in Section 4.4.2 via computer simulations. The number of users in the network was set to $N = 5$ and the BS can successfully receive the simultaneous transmissions of $n = 2$ users. In this symmetric case, we assume that the success probability of a node is 1 when no other node transmits at the same time and the success probability of a node is 0.8 when another node transmit simultaneously. For the simultaneous transmission of two users, we assume that whether the transmission of a user is successful or not is independent to the transmission outcome of the other user. The packet arrival process of each node is an independent Bernoulli

arrival process of rate $r$, taking the values $[0.05, 0.1, 0.15, 0.2, 0.25, 0.28, 0.3, 0.31]$. The expected delay performance of RS and the approximation proposed in Section 4.4.1 is given in Fig. 4.2. It is easy to observe that there is almost a perfect match between the approximation and the computer simulation.

Moreover, we plot the upper bound of the delay, i.e., the optimal value of (4.4a) for comparison. The upper bound is close to the simulation when the packet arrival rate is low, while the gap is relatively larger when the packet arrival rate is high. The delay lower bound proposed in *proposition 2* is also plotted. We observe that when the packet arrival rate is low, the lower bound is tight, while when the packet arrival rate is high, the lower bound becomes loose. The reason is that (4.7), (4.8) and (4.9) are necessary but not sufficient conditions for maintaining the stability of the system. When the packet arrival rate approaches the boundary of the stability region, the lower bound does not increase fast.

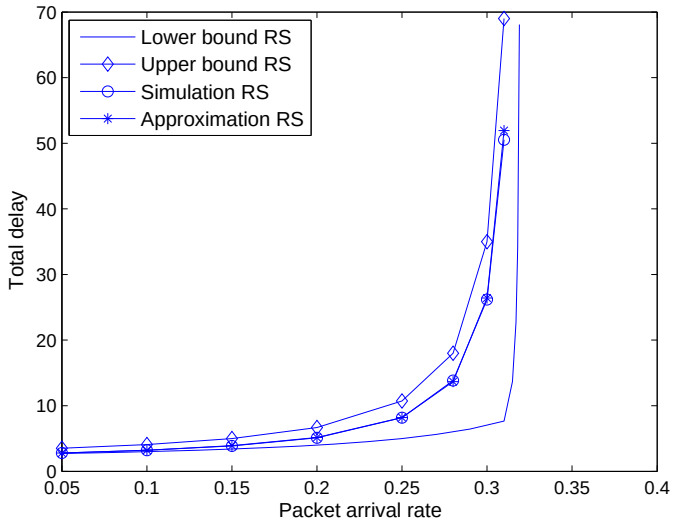


Figure 4.2: Total delay performance comparison for the symmetric case, $N = 5$ and $n = 2$.

Next we increase the total number of users $N$ to 10. By assuming a success probability of simultaneous transmissions of 2 users as 0.8, we compare the performance of the lower bound, upper bound and approximation in Fig. 4.3. We observe a similar trend as in the previous case. The performance of the approximation is still good. When the packet arrival rate is low and medium low, the lower bound is tight; when the packet arrival rate is high, the lower bound becomes loose. The reason is addressed before. In the same figure we plot the delay performance by allowing the simultaneous transmission of $n = 3$ users with success probability 0.7 for each user. It is easy to see that by allowing 3 users to transmit simultaneously, the delay of packet is reduced considerably. For $n = 3$, the upper bound is the optimal value of (4.13a).

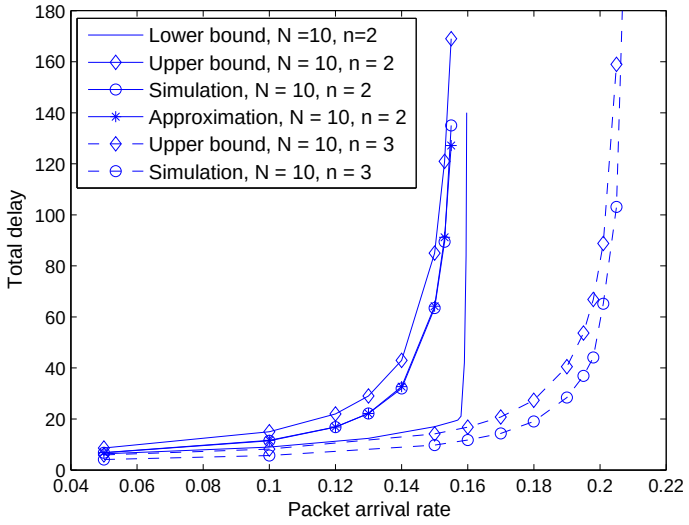


Figure 4.3: Total delay performance comparison for the symmetric case, $N = 10$.

**Asymmetric case**

In this asymmetric case, we set the total number of users $N = 10$. The success probability of a node is 1, when only one node transmits; while the success probability of a node is set as a random number within the range $[0.7, 0.95]$ when 2 nodes transmit simultaneously. For simultaneous transmission of 2 users, whether the transmission of a user is successful or not is independent of the outcome of the transmission of the other user. The expected delay performance of RS and the approximation are given in Fig. 4.4. The match between the proposed approximation and the simulation is still pretty close. As for the lower bound, we observe a similar trend as that in the symmetric case, i.e., when when the packet arrival rate is low and medium low, the lower bound is tight, while when the packet arrival rate is high, the lower bound becomes loose.

In the same figure, we plot the delay performance of uniform scheduling (i.e. we schedule each pair of nodes with the same probability.) for comparison. We can observe that the delay performance of uniform scheduling is higher than the proposed method. Because the proposed scheduling method tends to schedule the sets of nodes for which the success probabilities of simultaneous transmissions are high.

Finally we assume the base station can successfully receive the simultaneous transmissions of $n = 3$ nodes. When 3 nodes transmit simultaneously the success probability of each node is randomly chosen within $[0.6, 0.8]$; when 2 nodes transmit simultaneously, the success probability of each node is randomly chosen within the range $[0.8, 0.9]$; and the success probability of a single transmission is 1. The scheduling probability of each independent set is calculated by solving the optimization problem (4.13), and the delay performance is plotted in Fig. 4.5. In the same figure, the delay performance of uniform scheduling (i.e. we schedule each set of three nodes with the same probability.) is shown for comparison. We observe that by using the

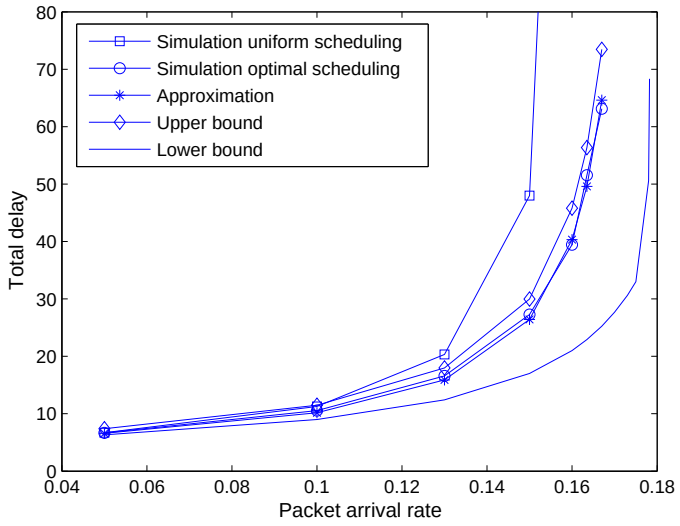


Figure 4.4: Total delay performance comparison for the asymmetric case, $N = 10$ and $n = 2$.

proposed optimization method the expected delay is much lower than that of uniform scheduling. The objective value of (4.13), also plotted in Fig. 4.5(upper bound), is also close to the simulation results.

## 4.6 Conclusions

In this chapter we have analyzed the delay properties of RS in cellular networks by assuming that the BS has MPR capability. For the perfect reception case, we have provided a fundamental lower bound for the delay performance of an arbitrary scheduling policy. For the imperfect reception case, we have proposed a convex optimization problem that can minimize the upper bound of the expected delay of RS by determining the scheduling probability of each independent set of nodes. We have also developed an accurate estimate and a lower bound for the delay of RS for the case in which the BS can support simultaneous transmission of two users. It is worthwhile to note that RS does not require the BS to exchange scheduling information with the

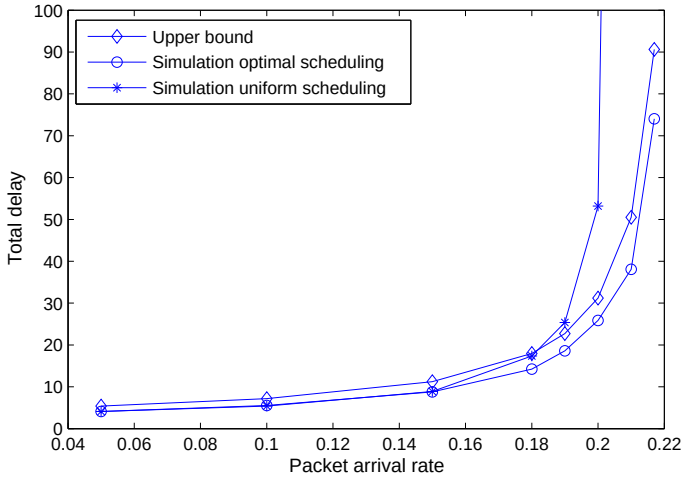


Figure 4.5: Total delay performance comparison for the asymmetric case, $N = 10$, $n = 3$.

mobile nodes, nor does it need global knowledge of the queueing length in the entire network. These properties make RS an ideal scheduling policy for cellular networks.

## 4.7 Appendix IV: Proof of the Proposition 4.1

*Proof*: Because of assumptions **A1**) and **A2**), we have

$$Q_i(t+1) = Q_i(t) - D_i(t) + A_i(t+1) \ . \tag{4.14}$$

Consider the function

$$V\left(\overrightarrow{Q}(t)\right) = \left(\sum_{i=1}^{N} Q_i(t)\right)^2 \ . \tag{4.15}$$

$$
\begin{aligned}
& V\left(\overrightarrow{Q}(t+1)\right) - V\left(\overrightarrow{Q}(t)\right) \\
&= \left(\sum_{i=1}^{N} Q_i(t+1)\right)^2 - \left(\sum_{i=1}^{N} Q_i(t)\right)^2 \\
&= \left(\sum_{i=1}^{N} Q_i(t+1) - \sum_{i=1}^{N} Q_i(t)\right)\left(\sum_{i=1}^{N} Q_i(t+1) + \sum_{i=1}^{N} Q_i(t)\right) \\
&= \left(\sum_{i=1}^{N} A_i(t+1) - \sum_{i=1}^{N} D_i(t)\right) \\
&\quad \left(2\sum_{i=1}^{N} Q_i(t) + \sum_{i=1}^{N} A_i(t+1) - \sum_{i=1}^{N} D_i(t)\right)
\end{aligned} \tag{4.16}
$$

Taking the expectation of both sides we get

$$
E\left\{V\left(\overrightarrow{Q}(t+1)\right) - V\left(\overrightarrow{Q}(t)\right)\right\} = 0\ . \tag{4.17}
$$

Therefore, we have

$$
\begin{aligned}
& E\left\{\left(\sum_{i=1}^{N} D_i(t) - \sum_{i=1}^{N} A_i(t+1)\right)\sum_{i=1}^{N} Q_i(t)\right\} \\
&= \frac{1}{2}E\left\{\left(\sum_{i=1}^{N} A_i(t+1) - \sum_{i=1}^{N} D_i(t)\right)^2\right\}\ .
\end{aligned} \tag{4.18}
$$

Let $E\{A_i(t)\} = r_i$. When the system is stable, the packet arrival rate should be equal to the packet deliver rate, i.e., $E\{D_i(t)\} = E\{A_i(t)\} = r_i$. Because of **A1**), $A_i(t)$ can be either 0 or 1; hence $A_i(t)^2 = A_i(t)$. Due to **A4**), it holds that $E\{A_i(t)A_j(t)\} = r_i r_j$ for $i \neq j$. It is easy to get

$$
E\left\{\left(\sum_{i=1}^{N} A_i(t+1)\right)^2\right\} = \sum_{i=1}^{N} r_i + \sum_{i=1}^{N}\sum_{j=1, j\neq i}^{N} r_i r_j\ . \tag{4.19}
$$

According to Jensen's inequality, we have

$$E\left\{\left(\sum_{i=1}^{N} D_i(t)\right)^2\right\} \geq \left(E\left\{\sum_{i=1}^{N} D_i(t)\right\}\right)^2 = \left(\sum_{i=1}^{N} r_i\right)^2 . \tag{4.20}$$

Since $A_i(t+1)$ is independent of $D_j(t)$ for any $i$ and $j$, it holds that

$$E\left\{\sum_{i=1}^{N} A_i(t+1)\sum_{i=1}^{N} D_i(t)\right\} = \left(\sum_{i=1}^{N} r_i\right)^2 . \tag{4.21}$$

By substituting (4.19), (4.20) and (4.21) into (4.18), we have

$$E\left\{\left(\sum_{i=1}^{N} D_i(t) - \sum_{i=1}^{N} A_i(t+1)\right)\sum_{i=1}^{N} Q_i(t)\right\} \geq \frac{1}{2}\left(\sum_{i=1}^{N} r_i - r_i^2\right). \tag{4.22}$$

Since the packet arrival rate is independent of queueing length, we can get

$$E\left\{\sum_{i=1}^{N} A_i(t+1)\sum_{i=1}^{N} Q_i(t)\right\} = \sum_{i=1}^{N} r_i E\left\{\sum_{i=1}^{N} Q_i(t)\right\} . \tag{4.23}$$

Since in each time slot the BS can at most receive $n$ packets, it is obvious that $\sum_{i=1}^{N} D_i(t) \leq n$.

$$E\left\{\sum_{i=1}^{N} D_i(t)\sum_{i=1}^{N} Q_i(t)\right\} \leq nE\left\{\sum_{i=1}^{N} Q_i(t)\right\} \tag{4.24}$$

By substituting (4.23) and (4.24) into (4.22), we have

$$E\left\{\sum_{i=1}^{N} Q_i(t)\right\} \geq \frac{\sum_{i=1}^{N} r_i - r_i^2}{2\left(n - \sum_{i=1}^{N} r_i\right)} . \tag{4.25}$$

By applying Little's law, the expected delay lower bound of arbitrary policy is

$$D \geq \frac{\sum_{i=1}^{N} r_i - r_i^2}{2\sum_{i=1}^{N} r_i \left(n - \sum_{i=1}^{N} r_i\right)} \ . \tag{4.26}$$

## 4.8 Appendix V

For $N = 2$ by forcing $g_i = 0$ $i = 1, 2$, we have

$$k_1(B_{1,2}P_{1,2}k_2 + B_{1,1}P_{1,2}(1 - k_2) + B_{1,1}P_{1,1}) - r_1 = 0 \ , \tag{4.27a}$$

$$k_2(B_{2,1}P_{1,2}k_1 + B_{2,2}P_{1,2}(1 - k_1) + B_{2,2}P_{2,2}) - r_2 = 0 \ . \tag{4.27b}$$

From (4.27a) we get

$$k_1 = \frac{r_1}{B_{1,2}P_{1,2}k_2 + B_{1,1}P_{1,2}(1 - k_2) + B_{1,1}P_{1,1}} \ . \tag{4.28}$$

Substituting (4.28) into (4.27b) we obtain

$$\begin{aligned}
&(B_{1,2} - B_{1,1})(P_{1,2} + P_{2,2})B_{2,2}P_{1,2}k_2^2 \\
&+ ((B_{1,1}P_{1,2} + B_{1,1}P_{1,1} - r_1)B_{2,2}P_{1,2} \\
&+ (P_{1,2} + P_{1,1})B_{1,1}B_{2,2}P_{2,2} - (B_{1,2} - B_{1,1})P_{1,2}r_2 \\
&+ B_{2,1}P_{1,2}r_1)k_2 - B_{1,1}(P_{1,2} + P_{1,1})r_2 = 0 \ .
\end{aligned} \tag{4.29}$$

By forcing $k_2 = 0$, the left hand side of (4.29) is $-B_{1,1}(P_{1,2} + P_{1,1})r_2 < 0$; by forcing $k_2 = 1$, the left hand side of (4.29) is equal to

$$\begin{aligned}
&\left(\frac{B_{2,1}P_{1,2}r_1}{B_{1,2}P_{1,2} + B_{1,1}P_{1,1}} + B_{2,2}P_{1,2}\left(1 - \frac{r_1}{B_{1,2}P_{1,2} + B_{1,1}P_{1,1}}\right)\right. \\
&\left.+B_{2,2}P_{2,2} - r_2\right)(B_{1,2}P_{1,2} + B_{1,1}P_{1,1}) \ .
\end{aligned} \tag{4.30}$$

The solution of (4.4) satisfies that $B_{1,2}P_{1,2}+B_{1,1}P_{1,1} > r_1$ and $B_{2,1}P_{1,2}+B_{2,2}P_{2,2} > r_2$. Therefor (4.30) is greater than 0. Moreover $(B_{1,2}-B_{1,1})(P_{1,2}+P_{2,2})B_{2,2}P_{1,2} < 0$, hence there is only one solution for $k_1$ and $k_2$ within the range $[0, 1]$.

## 4.9 Appendix VI: Proof of the Proposition 4.2

*Proof*: Let $D$ be the expected delay of RS. We will prove that $D \geq f_1^*$ and $D \geq f_2^*$.

$D \geq f_1^*$:

$\left\|\mathbf{b}_{\{i\}}\right\|_1$ is the success probability of node $i$ when only node $i$ transmits. And the success probability of node $i$ will decrease if node $i$ and $j$ transmit simultaneously. Therefore, $\sum_{i\in S_m} p_m \left\|\mathbf{b}_{\{i\}}\right\|_1$ is the upper bound of the success probability of node $i$. Moreover, (4.10b), (4.10c), (4.10d) and (4.10e) are the necessary conditions for the scheduling probability $p_m$ to maintain the stability of the system. Hence, $f_1^*$ is the lower bound of the expected delay of RS.

$D \geq f_2^*$:

$$
\begin{aligned}
& E\left\{\sum_{i=1}^{N} D_i(t) \sum_{i=1}^{N} Q_i(t)\right\} \\
&= \sum_{\text{for all}\overrightarrow{Q}} E\left\{\sum_{i=1}^{N} D_i(t) \sum_{i=1}^{N} Q_i(t) | \overrightarrow{Q}(t) = \overrightarrow{Q}\right\} P\left\{\overrightarrow{Q}(t) = \overrightarrow{Q}\right\} \\
&= \sum_{\text{for all}\overrightarrow{Q}} E\left\{\sum_{i=1}^{N} D_i(t) | \overrightarrow{Q}(t) = \overrightarrow{Q}\right\} \sum_{i=1}^{N} Q_i P\left\{\overrightarrow{Q}(t) = \overrightarrow{Q}\right\} \qquad (4.31)
\end{aligned}
$$

Because of assumption (**A7**), when we schedule $S_m$ in slot $t$, $E\left\{\sum_{i=1}^{N} D_i(t)\right\} = \|\mathbf{b}_m\|_1$ if all the nodes within $S_m$ transmit simultaneously, otherwise $E\left\{\sum_{i=1}^{N} D_i(t)\right\} < \|\mathbf{b}_m\|_1$. Given the probability of scheduling $S_m$ to be $p_m$, $E\left\{\sum_{i=1}^{N} D_i(t) | \overrightarrow{Q}(t) = \overrightarrow{Q}\right\} \leq \sum_{m=1}^{M} p_m \|\mathbf{b}_m\|_1$. Moreover, (4.12b), (4.12c), (4.12d) and (4.12e) are the necessary

conditions for the scheduling probability $p_m$ to maintain the stability of the system. Therefore,

$$E\left\{\sum_{i=1}^{N} D_i(t)|\overrightarrow{Q}(t)=\overrightarrow{Q}\right\} \leq U^* \ , \tag{4.32}$$

where $U^*$ is the optimal value of the problem (4.12). Substituting (4.32) into (4.31) we have

$$E\left\{\sum_{i=1}^{N} D_i(t)\sum_{i=1}^{N} Q_i(t)\right\} \leq U^* E\left\{\sum_{i=1}^{N} Q_i(t)\right\} \ . \tag{4.33}$$

By substituting (4.23) and (4.33) into (4.22), we can prove $D \geq f_2^*$.

# 5. Summary and Suggested Future Research

## 5.1 Summary

In this dissertation we have studied collision resolution approaches in wireless networks, i.e., a cross layer design for packet collision recovery, an optimal pulse shape design that can facilitate collision resolution, and packet delay analysis in a cellular wireless network under the assumption that the BS has collision resolution capability.

In the first part of this dissertation a novel cross-layer design namely ALOHA-CR has been proposed. This scheme can resolve second order collisions in wireless networks without requiring retransmissions. We have described in detail the physical and MAC layers of the proposed scheme and have derived analytical expressions to predict its performance. Further, the proposed scheme has been implemented on a 5 node SDR system and its measured performance has shown very good agreement with the analytically derived results. The conducted measurements have demonstrated that ALOHA-CR can achieve more than twice the throughput of conventional slotted ALOHA, while maintaining stability for a much wider range of arrival rates and contention probabilities. This indicates that ALOHA-CR might be an excellent option for system deployments that can afford some extra complexity at the access point, while requiring low transmitter complexity (compared to other collision resolution schemes) to meet power or pricing requirements.

In the second part of this dissertation we have focused on the optimal pulse shape design to improve the performance of the multi-user separation algorithm proposed in chapter 2. The optimally designed pulse shape waveform results in low correlation between the columns of the system matrix, while it exploits all available bandwidth

as dictated by a spectral mask. Simulation results for the $K = 2$ case have confirmed that the proposed pulse design leads to better SER performance than that of conventional pulse shape waveforms. Moreover, we have introduced an intentional half-symbol delay between the two users and have used successive interference cancelation in combination with blind source separation to further improve the separation performance. The intentional half-symbol delay means that the users still overlap significantly during their transmissions. The use of intentional delay is necessitated by the fact that, although small user delay and CFO differences help preserve the identifiability of the problem, in practice, they may not suffice to separate the users. Also, although the proposed approach can work for any number of users, as the number of users increases, the CFO and delay differences become smaller, which makes the separation more difficult. Based on our experiments, small CFO differences didn't affect performance. Although introducing large intentional CFO differences among users could help, that would increase the effective bandwidth.

Finally, we have analyzed the delay properties of RS in cellular networks by assuming that the BS has MPR capability. For the perfect reception case, we have provided a fundamental lower bound on the delay performance of an arbitrary scheduling policy. For the imperfect reception case, we have proposed a convex optimization problem that can minimize the upper bound of the expected delay of RS by determining the scheduling probability of each independent set of nodes. We have also developed an accurate estimate and a lower bound for the delay of RS for the case in which the BS can support simultaneous transmission of two users. It is worthwhile to note that RS does not require the BS to exchange scheduling information with the mobile nodes, nor does it need global knowledge of the queueing length in the entire network. These properties make RS an ideal scheduling policy for cellular networks.

## 5.2 Suggested Future Research

### 5.2.1 Physical layer issues

In chapter 2, we have proposed a multi-user separation algorithm that can support the simultaneous transmission of two users. We assumed that the wireless channel between wireless nodes and BS undergos flat fading. However in some cases, such as in an outdoor environment, where the delay spread is very high, the channel between wireless nodes and BS would be frequency selective [23]. Adjusting the proposed algorithm to accommodate frequency selective fading is still an open problem.

### 5.2.2 Delay analysis

In chapter 4, by assuming the BS can support the simultaneous transmissions of two users, we have developed an approximation and a lower bound for the expected delay of RS. We have shown that there is only one solution for the approximated active probability by forcing $g_i$ in equation (4.6) to be 0. Obtaining an approximation for the cases in which the BS can support simultaneous transmissions of more than two users is still unknown, because in that case, the solution to equation (4.6) will not be unique. Moreover, finding a lower bound on the expected delay of RS for this case is also worth investigating.

## Bibliography

[1] S. Wisniewski, "Wireless And Cellular Networks" *Pearson Prentice Hall,* 2005.

[2] M. Ferguson, "On the Control, Stability, and Waiting Time in a Slotted ALOHA Random-Access System," *IEEE Transactions on Communications,* vol.23, no.11, pp. 1306- 1311, Nov. 1975.

[3] I. Gitman, "On the Capacity of Slotted ALOHA Networks and Some Design Problems," *IEEE Transactions on Communications,* vol.23, no.3, pp. 305- 317, Mar 1975.

[4] M. Garetto, T. Salonidis, and E. W. Knightly, "Modeling per-flow throughput and capturing starvation in CSMA multi-hop wireless networkss," *IEEE/ACM Transactions on Networking,* vol. 16, no. 4, pp. 864C877, 2008.

[5] J.H. Kim, and J.K. Lee, "Capture effects of wireless CSMA/CA protocols in Rayleigh and shadow fading channels," *IEEE Transactions on Vehicular Technology,* vol.48, no.4, pp.1277-1286, Jul. 1999.

[6] W.Y. Choi, and S.K. Lee, "A real-time updating algorithm of RTS-CTS threshold to enhance EDCA MAC performance in IEEE 802.11e wireless LANs," *VTC2004-Fall,* vol.7, no., pp. 4801- 4804 Vol. 7, 26-29 Sept. 2004.

[7] T. Sekimoto, and J. Puente, "A Satellite Time-Division Multiple-Access Experiment," *IEEE Transactions on Communication Technology,* vol.16, no.4, pp.581-588, Aug. 1968.

[8] I. Rubin, "Message Delays in FDMA and TDMA Communication Channels," *IEEE Transactions on Communications,* vol.27, no.5, pp. 769- 777, May 1979.

[9] H. Li, and H. Liu, "An Analysis of Uplink OFDMA Optimality," *IEEE Transactions on Wireless Communications,* vol.6, no.8, pp.2972-2983, Aug. 2007.

[10] W. Choi, J.G. Andrews, and R.W. Heath, "Multiuser Antenna Partitioning for Cellular MIMOCCDMA Systems," *IEEE Transactions on Vehicular Technology,* vol. 56, no.5, pp.2448-2456, Sept. 2007.

[11] "IEEE standard 802.11," *http://www.ieee802.org/11/.*

[12] G. Dimic, N.D. Sidiropoulos, and R. Zhang, "Medium access control - physical cross layer design," *IEEE Signal Processing Magazine*, September 2004.

[13] L. Kleinrock and F. A. Tobagi, "Packet switching in radio channels: Part I - carrier sense multiple-access modes and their throughput-delay characteristics," *IIEEE Transactions on Communications*, vol. 23, no. 12, pp. 1400–1416, 1975.

[14] R. Zhang and M.K. Tsatsanis, "Network-assisted diversity multiple access in dispersive channels," *IEEE Transactions on Communications*, vol. 50, no. 4, pp. 623–632, April 2002.

[15] G. Dimic, N.D. Sidiropoulos, and L. Tassiulas, "Wireless networks with retransmission diversity access mechanisms: stable throughput and delay properties," *IEEE Transactions on Signal Processing,* vol.51, no.8, pp. 2019- 2030, Aug. 2003.

[16] R. Lin and A.P. Petropulu, "A new wireless network medium access protocol based on cooperation," *IEEE Transactions on Signal Processing*, vol. 53, no. 12, pp. 4675–4684, December 2005.

[17] L. Dong and A.P. Petropulu, "Multichannel ALLIANCES: A Cooperative Cross-Layer Scheme for Wireless Networks," *IEEE Transactions on Signal Processing,* vol.56, no.2, pp.771-784, Feb. 2008.

[18] H. Yang, A.P. Petropulu, X. Yang, and T. Camp, "A novel location relay selection scheme for ALLIANCES," *IEEE Transactions on Vehicular Technology*, vol. 57, no. 2, pp. 1272–1284, March 2008.

[19] S. Gollakota and D. Katabi, "ZigZag decoding: Combating hidden terminals in wireless networks," *SIGCOMM08*, pp. 159–170, August 2008.

[20] D. Tse and P. Viswanath, Fundamentals of wireless communication, *Cambridge University Press,* 2005.

[21] J. Proakis, "Digital communications," *McGraw-Hill Science Engineering* 2007.

[22] A. Hyvarinen, and E. Oja, "Independent Component Analysis: Algorithms and Applications," *Neural Networks,* 13(4-5):411-430,2000.

[23] T.s. Rappaport, *Wireless communications Principles and Practice*, Publishing House of Electroincs Industry, 2004.

[24] A.P. Petropulu, M. Olivieri, Y. Yu, L. Dong, and A. Lackpour, "Pulse-shaping for blind multi-user separation in distributed MISO configurations," *IEEE International Conference on Acoustics, Speech and Signal Processing (ICASSP 2008)*, pp. 2741–2744, April 2008.

[25] X. Liu, S. Oymak, A. P. Petropulu, and K. R. Dandekar, "Collision resolution based on pulse shape diversity," *IEEE International Workshop on Signal Processing Advances for Wireless Communications*, Perugia, Italy, Jun. 2009, pp. 409–413.

[26] X. Liu, A.P. Petropulu, V. Poor, and V. Koivunen, "Blind Separation Of Two Users Based on User Delays and Optimal Pulse Shape Design," *EURASIP Journal on wireless communications and networking*, vol. 2010, Article ID 939340, 12 pages, 2010, doi:10.1155/2010/939340.

[27] "WARP - wireless open-access research platform," *http://warp.rice.edu/*.

[28] M. Brandt-Pearce, "Signal separation using fractional sampling in multiuser communications," *IEEE Transactions on Communications*, vol. 48, no. 2, pp. 242–251, February 2000.

[29] S. Ghez, S. Verdu, and S.C. Schwartz, "Stability properties of slotted ALOHA with multipacket recption capability," *IEEE Transactions on Automatic Control*, vol. 33, no. 7, pp. 640–649, June 1988.

[30] S. Ghez, S. Verdu, and S.C. Schwartz, "Optimal decentralized control in the random access multipacket channel," *IEEE Transactions on Automatic Control*, vol. 34, no. 11, pp. 1153–1163, November 1989.

[31] V. Naware, G. Mergen, and L. Tong, "Stability and delay of finite-user slotted ALOHA with multipacket reception," *IEEE Transactions on Information Theory*, vol. 51, no. 7, pp. 2636–2656, July 2005.

[32] V. Naware, G. Mergen, and L. Tong, "Stability and delay of finite-user slotted ALOHA with multipacket reception," Tech. Rep. ACSP-TR-08-04-01, Cornell University, Ithaca, NY, 2004.

[33] S. Weber, A. Kini, and A. Petropulu, "A new approximation for slotted buffered Aloha," *42nd Annual Conference on Information Sciences and Systems, 2008. CISS 2008.*, pp. 1143–1148, March 2008.

[34] B. Le Floch, M. Alard, and C. Berrou, "Coded orthogonal frequency division multiplex [TV broadcasting]," *Proceedings of the IEEE*, vol. 83, no. 6, pp. 982–996, June 1995.

[35] J.F. Cardoso and A. Souloumiac, "Blind beamforming for non-Gaussian signals," *IEE Proceedings of Radar and Signal Processing*, vol. 140, no. 6, pp. 362–370, Dec 1993.

[36] F. Zeng , "Investigation of a family of M-sequences," The 9th Asia-Pacific Conference on Communications 2003, APCC 2003. , vol.2, no., pp. 685- 688 Vol.2, 21-24 Sept. 2003.

[37] P.S. Harish, and S. Karthik, "Root raised cosine filter for a WCDMA receiver using distributed arithmetic for power optimization and enhanced speed," *In Proceedings of 2004 International Symposium on Intelligent Signal Processing and Communication Systems 2004. ISPACS 2004.* , vol., no., pp. 512- 515, 18-19 Nov. 2004

[38] Y. Wang, P. Ciblat, E. Serpedin, and P. Loubaton, "Performance analysis of a class of nondata-aided frequency offset and symbol timing estimators for flat-fading channels," *IEEE Transactions on Signal Processing*, vol. 50, no. 9, pp. 2295–2305, Sep. 2002.

[39] T. Roman, S. Visuri, and V. Koivunen, "Blind frequency synchronization in OFDM via diagonality criterion," *IEEE Transactions on Signal Processing*, vol. 54, no. 8, pp. 3125–3135, Aug. 2006.

[40] Dan H. Wolaver, *Phase-locked loop circuit design*, Englewood Cliffs, N.J. : Prentice Hall, 1991.

[41] B. Sklar, *Digital Communications Fundamentals and Applicatons*, Prentice Hall, 2001.

[42] I. Keslassy, "EE 048866: Packet Switch Architectures, Review #2: Queuing Theory," Available online: `http://www.ee.technion.ac.il/people/isaac/048866/7.pdf`.

[43] K. Amiri, Y. Sun, P. Murphy, C. Hunter, J.R. Cavallaro, and A. Sabharwal, "WARP, a unified wireless network testbed for education and research," *IEEE International Conference on Microelectronic Systems Education, 2007. MSE '07.*, pp. 53–54, June 2007.

[44] M. Ghogho, A. Swami and T. Durrani, "On blind carrier recovery in time-selective fading channels," *in Proc. 33rd Asilomar Conf. Signals,. Systems, Computers*, Vol. 1, pp. 243-247, Pacific Grove, CA, Oct. 1999,

[45] F. Gini and G. B. Giannakis, "Frequency offset and symbol timing recovery in flat-fading channels: A cyclostationary approach," *IEEE Trans. Commun.,* Vol. 46, No. 3, pp. 400 - 411, Mar. 1998.

[46] Y. Onozato, J. Liu, and S. Noguchi, "Stability of a slotted ALOHA system with capture effect," *IEEE Transactions on Vehicular Technology*, vol. 38, no. 1, pp. 31–36, Feb. 1989.

[47] Y. Zhang and S.A. Kassam, "Blind separation and equalization using fractional sampling of digital communications signals," *Signal Processing*, vol. 81, no. 12, pp. 2591–2608, Dec. 2001.

[48] X. Liu, J. Kountouriotis, A.P. Petropulu, and K.R. Dandekar, "ALOHA with collision resolution (ALOHA-CR): Theory and software defined radio implementation," *IEEE Transactions on Signal Processing*, vol.58, no.8, pp.4396-4410, Aug. 2010.

[49] E.M. Malkamaki, "Comparison of spectrum efficiencies of 4- and 16-QAM in mobile cellular environment," Third IEE Conference on Telecommunications, 1991. pp.35-40, 17-20 Mar. 1991.

[50] S. Mneina, and G.O. Martens, "Analysis of timing sensitivity and Nyquist pulse design," *Canadian Conference on Electrical and Computer Engineering, 2002. IEEE CCECE 2002.* , vol.2, no., pp. 1059- 1063 vol.2, 2002.

[51] P. Ciblat, P. Loubaton, E. Serpedin, and G.B. Giannakis, "Performance analysis of blind carrier frequency offset estimators for noncircular transmissions through frequency-selective channels," *IEEE Transactions on Signal Processing*, vol. 50, no. 1, pp. 130–140, Jan. 2002.

[52] K.E. Scott and E.B. Olasz, "Simultaneous clock phase and frequency offset estimation," *IEEE Transactions on Communications*, vol. 43, no. 7, pp. 2263–2270, Jul. 1995.

[53] S. Wu, S. Boyd, and L. Vandenberghe, "FIR filter design via spectral factorization and convex optimization," in *Applied and Computational Control, Signals and Circuits*, Biswa Datta, Ed., pp. 215–245, Birkhauser, 1998.

[54] N.D. Sidiropoulos, T.N. Davidson, and Zhi-Quan Luo "Transmit beamforming for physical-layer multicasting," *IEEE Transactions on Signal Processing*, vol. 54, no. 6, pp. 2239–2251, Jun. 2006.

[55] A.V. Oppenheim, and R.W. Schafer, "Discrete-Time Signal Processing," *Prentice Hall Signal Processing*, 2010.

[56] A. Papoulis, and S.U. Pillai, "Probability, random variables, and stochastic processes," *McGraw-Hill*, 2002.

[57] L.N. Trefethen, and B. David, "Numerical linear algebra," *Society for Industrial and Applied Mathematics*, 1997.

[58] N.D. Sidiropoulos, G.B. Giannakis, and R. Bro, "Blind PARAFAC receivers for DS-CDMA systems," *IEEE Transactions on Signal Processing*, vol. 48, no. 3, pp. 810–823, Mar. 2000.

[59] K. Kar, L. Xiang, and S. Sarkar, "Delay Guarantees for Throughput-Optimal Wireless Link Scheduling," *In Proc. IEEE INFOCOM 2009*, Rio de Janeiro, Brazil, pp.2331-2339, Apr. 19-25 2009.

[60] L. Tassiulas, and A. Ephremides, "Stability properties of constrained queueing systems and scheduling policies for maximum throughput in multihop radio networks," *IEEE Transactions on Automatic Control*, vol.37, no.12, pp.1936-1948, Dec. 1992.

[61] G.R. Gupta, and N.B. Shroff, "Delay Analysis for Wireless Networks With Single Hop Traffic and General Interference Constraints," *IEEE/ACM Transactions on Networking*, vol.18, no.2, pp.393-405, April 2010.

[62] D. Shah, and M. Kopikare, "Delay bounds for approximate maximum weight matching algorithms for input queued switches,"

[63] G. Mergen, and L. Tong, "Stability and capacity of regular wireless networks," *IEEE Transactions on Information Theory*, vol.51, no.6, pp. 1938- 1953, Jun. 2005

[64] G. Mergen, and L. Tong, "Stability and capacity of wireless Networks with Probabilistic Reception," Cornell Univresity, Adaptive Communications and Signal Processing Lab., Ithaca, NY, Tech. Rep. ACSP TR-01-03-01, Jan. 2003

[65] A.R. Conn, N.I.M. Gould and P.L. Toint, "Trust-region methods," *MPS/SIAM*, 2000.

[66] R. Rozovsky, and P. R. Kumar, "SEED-EX: A MAC protocol for Ad Hoc networks," *In Proc. ACM Symposium on Mobile Ad Hoc Networking and computing, MobiHoc 2001*, Long Beach, Oct. 4-5, 2001, pp. 67-75

[67] S. Tan, and D. Zheng, and J. Zhang and J. Zeidler, "Distributed Opportunistic Scheduling for Ad-Hoc Communications Under Delay Constraints," *In Proc. IEEE INFOCOM 2010* , Las Vegas, Nevada, USA, pp.1-9, Mar. 14-19, 2010

# Appendix A. Abbreviations

- ALOHA-CR: ALOHA with Collision Resolution
- API: Application Programming Interface
- BER: Bit Error Rate
- BPSK: Binary Phase Shift Keying
- BS: Base Station
- CDMA: Code Division Multiple Access
- CFO: carrier frequency offsets
- CSMA: Carrier Sensing Multiple Access
- CSMA/CA: Carrier Sensing Multiple Access with Collision Avoidance
- DQPSK: Differential quadrature phase shift keying
- FDMA: Frequency-Division Multiple Access
- FPGA: field-programmable gate array
- i.i.d.: Independent and Identically Distributed
- IOTA: Isotropic Orthogonal Transform Algorithm
- ISI: Inter-Symbol Interference
- LS: Least-Squares
- MAC: Medium Access Control

- MIMO: Multiple-Input Multiple-Output
- MPR: Multi-Packet Reception
- MWS: Maximum Weigh Scheduling
- NDMA: Network-assisted Diversity Multiple Access
- OFDMA: Orthogonal Frequency Division Multiple Access
- pdf: Probability Density Function
- PLL: Phase Lock Loop
- QAM: Quadrature Amplitude Modulation
- QoS: Quality of Service
- PSD: power spectral density
- RFIC: Radio Frequency Integrated Circuit
- RRC: raised root cosine
- RS: Random Scheduling
- RTS/CTS: Request-To-Send/Clear-To-Send
- SDR: Software Defined Radio
- SEP: Symbol Error RATE
- SIC: Successive Interference Cancelation
- SINR: Signal-to-Interference-plus-Noise Ratio
- SNR: Signal-to-Noise Ratio

- TDMA: Time-Division Multiple Access
- WARP: Wireless Open Access Research Platform
- WiFi: Wireless Fidelity

## Vita

**General** Xin Liu was born in Chongqing, China, in 1980.

**Education**

Drexel University, Philadelphia, PA, USA
Ph.D. in Electrical Engineering, April 2011 (GPA: 3.99/4.0)

University of Science and Technology of China, Chengdu, China
M.S. in Electrical Engineering, July 2005

University of Science and Technology of China, Chengdu, China
B.S. in Electrical Engineering, July 2002

**Awards**

⋆ Drexel University Conference Travel Subsidy Award, 2009
⋆ University of Science and Technology of China Excellent Graduat Student Scholarship, 2002-2005

**Publications**

[1] **X. Liu**, J. Kountouriotis, A. Petropulu and K. Dandekar, "ALOHA with collision resolution (ALOHA-CR): theory and software defined radio implementation", *IEEE Trans. on Signal Processing*, vol.58, no.8, pp.4396-4410, Aug. 2010.
[2] **X. Liu**, A.P. Petropulu, V. Poor and V. Koivunen, "Blind Separation of Two Users Based on User Delays and Optimal Pulse-Shape Design", *IEURASIP Journal on Wireless Communications and Networking*, vol. 2010, Article ID 939340, 12 pages, 2010.
[3] **X. Liu**, A.B. Premkumar and A.S. Madhukumar, "Multichannel ALLIANCES: a cross-layer cooperative scheme for wireless networks," *IEEE Transactions on Wireless Communications*, vvol 7, no 5, pp.1512 - 1516, May, 2008.
[4] **X. Liu**, J. Kountouriotis, A. Petropulu and K. Dandekar, "ALOHA with collision resolution: physical layer description and software defined radio implementation ," in *Proc. IEEE Intern. Conf. on Acoustics Speech and Signal Processing (ICASSP)*, Dallas TX, Apr. 2010.
[5] **X. Liu**, S. Oymak, A. P. Petropulu and K. R. Dandekar, "Collision Resolution Based On Pulse Shape Diversity", in *Proc. IEEE Signal process advances in wireless communication (SPAWC)*, pp.409-413, Jul. 2009.